SYSTEMATIC STUDIES OF SIGNAL PATHWAYS IN AXONAL INJURY AND REGENERATION

By

ZHIQUN ZHANG

A DISSERTATION PRESENTED TO THE GRADUATE SCHOOL
OF THE UNIVERSITY OF FLORIDA IN PARTIAL FULFILLMENT
OF THE REQUIREMENTS FOR THE DEGREE OF
DOCTOR OF PHILOSOPHY

UNIVERSITY OF FLORIDA

2007

To my father Daxin Zhang, to my mother Xijun Li for their support, encouragement and blessings during my academic journey

ACKNOWLEDGMENTS

First I would like to thank my parents and sisters for their love, support and patience that I needed during my academic career to achieve this doctoral degree. I would like to thank my advisor, Dr. Kevin K. W. Wang, whose support, patience and guidance have allowed me to finish this academic challenge. It is due to Dr. Wang's enlightened vision in research that we pursued areas in calmodulin and system biology that allowed me to reach frontiers of knowledge in ways that neither one of us could have expected when I began this journey.

I would also like to thank the members of my committee, Professors Andrew K. Ottens, Dena Howland and Lungji Chang for their precious time, effort and guidance. I acknowledge Dr. Stephen Larner for his tutorials and help in preparing this document and many other publications. I am grateful to the people in the Departments of Psychiatry and Neuroscience, in particular Professor Susan Semple-Rowland, Dr. Mark Good and B.J. Streetman for their efforts in taking care of things that made my life so simple. I am gracious to my dearest friend and colleague Dr. Firas Kobeissy for his unequalled assistance in the laboratory. Also, I would like to thank all the members of Dr. Wang's laboratory for their assistance and friendship throughout my 5 years pursuing my Ph.D. I would like to especially thank Dr. Ming Cheng Liu and his wonderful wife Dr. Wenrong Zheng, Dr. Stanislav Svetlov, Dr. Ronald Hayes, Mr. Shankar Sadasivan and Mrs. Barbara Osteen, for their effort and support. Very special thanks go to my hushand, Jianghui Chao, who has patiently stood by me and supported me for more than a decade and my son, Ryan Baichuan Chao who has been given me lots of happiness.

TABLE OF CONTENTS

page

LIST OF TABLES

LIST OF FIGURES

Abstract of Dissertation Presented to the Graduate School
of the University of Florida in Partial Fulfillment of the
Requirements for the Degree of Doctor of Philosophy

SYSTEMATIC STUDIES OF SIGNAL PATHWAYS IN AXONAL/NEURONA INJURY AND REGENERATION

By

Zhiqun Zhang

December 2007

Chair: Kevin K W. Wang
Major: Medical Sciences--Neuroscience

It is well known that axons fail to regenerate in the adult central nervous system (CNS) after injury. Both inhibitory and permissive pathways converge at the Rho/ROCK (Rho-associated kinase) pathway. A systems biology approach to decipher Rho/ROCK inhibition induced neuritogenesis signaling transduction pathways would help significantly in understanding the mechanisms of axonal regeneration. To achieve this goal, first we utilized a pharmacological agent Y-27632 (ROCK inhibitor), which has demonstrated the ability to promote neuritogenesis in various model systems. We found that the ROCK inhibitor can induce robust neurite outgrowth in PC-12 cells and it initiated neurites through dephosphorylation of cofilin. Besides the cofilin change, differential gene transcriptome and protein expression influenced by ROCK inhibition were identified by affymetrix Microarray and proteomic studies. More than 200 genes and 20 proteins, many of which are known to be associated with neuritogenesis or cell growth, are potentially involved in ROCK inhibition-induced neurite outgrowth in PC-12 cells. As one of the down-stream targets of ROCK, brain enriched collapsin response mediator protein-2 (CRMP-2) is of most intereste for further study. CRMP-2 plays a crucial role in neurite outgrowth and axon formation. This is the first time calpain mediated degradation of CRMP-2 after *in vivo* TBI and in vitro glutamate excitotoxicitic injury has been

demonstrated. Moreover, proteolytic CRMP-2 appears to correlate well with neuronal cell injury and neurite damage. Our subsequent data showed that calmodulin binds to CRMP-2 in a calcium dependent manner, and thereby significantly retards proteolysis of CRMP-2 both *in vivo* and *in vitro*.

Taken together, data from our studies provide clues regarding the changing factors that are important in the axonal injury/regeneration. The results of these studies lay the foundation for future experiments aimed at finding potential biomarkers and therapeutic targets following axon injury.

CHAPTER 1
INTRODUCTION

Traumatic Axonal Injury: A General Overview

Traumatic axonal injury (TAI) is one of the most common and important pathologic features associated with traumatic brain injury (TBI) (Thienpont et al., 2005). Data from Centers of Disease Control and Prevention and other research groups inferred that there were 26,000 trauma deaths per year due to TAI, with another 20,000 to 45,000 patients suffering with long-term disabilities. Moreover, TAI clinically links to coma and onset of low Glasgow Coma Scale (GCS) scores. Therefore, TAI has recently been recognized as a key predictor of outcome in head and spinal cord trauma (Medana and Esiri, 2003).

TAI was initially described by a pathologist as being with microscopic changes due to wallerian-type axonal degeneration. The axonal segments in the white matter display elongated varicose swelling and axonal bulbs at the terminal stumps of the disconnected axons. These swelling and bulbs are filled with mitochondria, neurofilaments, and other organelles that have been transported to the axon tip. TAI was used to discribe diffuse axonal injury. However, it is not a diffuse injury to the whole brain. Rather it commonly occurs in corticomedullary junctions, located in frontal and temporal regions as well as the corpus callosum (CC), brainstem, and deep gray matter (Farkas and Povlishock, 2007).

Although damages to axon are universally found in cases of severe, moderate and mild head trauma, the ability to diagnosis of TAI is a big challenge for neurosurgeons. The changes in the axon due to injury as noted on conventional brain images scan, such as computed tomography (CT) or standard standard magnetic resonance imaging (MRI) are almost invisible. Fortunately, with the continued development in image technology, the diffusion tensor imaging (DTI), the MRI of diffusion weighted imaging, and magnetization transfer imaging techniques

showed promise in revealing TAI by taking advantage of the molecular disarrangement of the white matter tracts with diffuse axonal pathology (Hergan et al., 2002; Gallagher et al., 2007; Newcombe et al., 2007). However, it is still difficult to detect mild to moderate degree of TAI, even though structural damages to axons that can be seen under microscopy. Furthermore, due to the hostile environment surrounding CNS lesions and the decrease of intrinsic regeneration ability, axons rarely regenerate after injury in the adult central nervous system (CNS). The clinical challenge is to promote compensatory sprouting of the remaining intact axons or the re-growth of several axons across the injury site (Geddes et al., 2000). Usually, TAI is associated with a broad pattern of secondary damage cascades that occur in the neuron cell body. Therefore, a systematic approach to deciphering the signaling transduction pathways involved in axonal injury would help significantly assess and develop therapeutic strategies to traumatic axonal injury.

In the remaining portion of this chapter, I will focus on discussing TAI and recent progress that has been made in the understanding the mechanisms underlying TAI and the development of therapies to promote axon regeneration. Specific topics will include pathology and calmodulin mediated pathways in TAI, inability of axons to regenerate in the adult CNS, and the therapeutic target offered by the Rho-ROCK pathway to enhance axonal regeneration.

Pathology and Calmodulin Mediated Pathways in Traumatic Axonal Injury

Due to intensive research in both the clinical settings and with experimental animal models of TAI, it is now believed that TAI is a progressive event gradually evolving from focal axonal alteration to delayed axonal disconnection.

Typically, mechanical forces induce direct axon disconnection (primary axotomy). This is a relatively low occurrence with the exception of tissue tearing in the white matter in severe brain injury. The most common cause of white matter loss is secondary biochemical events that

may ultimately result in axon disconnection with the significant pathologic feature of a bulb formation at the terminal end of the axon (Smith et al., 2003; Buki and Povlishock, 2006).

In most of cases the injury process happens not only in the neuron cell bodies, axons and dendrites but also in glial cells. However, axons often extend for long distances from their cell bodies, and therefore are more vulnerable to injury even without related somatic or dendritic alterations. Regardless of injury sites, TAI is associated with a broadly similar pattern of secondary deleterious cascades in the neuron cell bodies, including disruption of sodium and calcium channel actvities, abnormal myelination, disturbed mitochondrion functions, excitotoxicity, ischemia, oxidative stress and neuroinfalmmation responses (Povlishock et al., 1999; Farkas and Povlishock, 2007).

Physical damages have been thought to be due to direct cause of changes in the activity of Na^+ channels leading to pathological influx of axonal sodium ion with resultant swelling. This, together with activation of voltage sensitive Ca^{2+} channels and activation of Na^+/ Ca^{2+} exchangers, has been demonstrated to lead to increased intracellular Ca^{2+}. As a Ca^{2+} sensor, calmodulin binds to a diverse group of calmodulin binding proteins including enzymes, cytoskeletal proteins, receptors and ion channels, and thereby regulates neuronal/axonal response upon stimulus. Calmoldin binding to the pore forming subunit of voltage-gated calcium channel induces a rapid inactivation of Ca^{2+} channels which limits the amount of Ca^{2+} influx in response to injury (Peterson et al., 1999).

Furthermore, studies have demonstrated that calmodulin binding to N-Methyl-D-Aspartate Receptor (NMDA) subunit 1 facilitates calcium-dependent inactivation of NMDA receptor, which in turn serves as a negative feedback to fine tune Ca^{2+} influx after injury (Zhang et al., 1998).

As noted, there is immediate microscopic axonal damage after trauma with reduced spacing or compaction of neurofilaments (NFC) within 6 hours. It has been demonstrated that this compaction is coming from the loss or collapse of neurofilament sidearms, which may mediated by proteolytic or phosphorylation modification of the neurofilament (NF) after calcium influx. Different aspects showed that calmodulin also mediates the pathology of NFC. It is well established that calmodulin activates and binds to calcineurin upon Ca^{2+} influx, altering NF phosphorylation, thereby modifying the repelling forces of the side-arms, leading to formation of NFC (Hashimoto et al., 2000). Recent studies reported that a group of GMC family proteins including the cytoplasmic protein GAP43, MARCKS and cytoskeleton-associated protein 23 kDa (CAP23) has been found to modulate the formation of filopodia and microspikes, as well as neurite outgrowth in the spinal cord regeneration model by regulating actin polymerization, origination and disassemble. These GMC proteins bind to acid phospholipids PI-(4,5)-P2, calmodulin, protein kinase C and actin filaments in a mutually exclusive manner, modifing the raft-recruitment of signaling molecules, such as src, and in turn are involved in the dynamic interactions that occur between cell surface and the cytoskeleton core molecules of the growing axon during axon regeneration. Additionally, calmodulin binding to these GMC proteins with or without Ca^{2+} may contribute an important link in translating receptor-mediated calcium fluxes into signals that may be guiding growth cones. This may be done by modifing Ca^{2+} homeostasis (Gerendasy, 1999; Krucker et al., 2002; van Dalen et al., 2003). The calmodilin involvement in traumatic axonal injury is summarized in Figure 1-1. Excessive calcium influx can cause growth cone collapse. However, with the fall of initial high level intracellular calcium level, growth cone formation is allowed after axonal injury.

Given the importance of calmodulin involvement in gene regulation, protein synthesis, axonal transportation and cell motility, it is imparative to study the calmodulin signal pathway in a systematic manner after traumatic injury.

At the same time excess Ca^{2+} influx results in the activation of the non-lysosomal cysteine protease, such as μ-calpain (calpain-1) and m-calpain (calpain-2). The result of the activation of calpains is an irreversible cytoskeletal structural and functional proteolysis that invariably leads to cell death (Hayes et al., 1998; Pike et al., 1998; Yamashima, 2004). Ca^{2+} overloading may also open the mitochondrial membrane permeability transition (MPT) pore, and subsequently leads to mitochondrial swelling and ultimaely mitochondrial rupture. In turn, cytochrome C release from those abnormal/ruptured mitochondria, with concomitant caspase activation in the axon (Buki et al., 2000). The activation of calpain and caspases continue to devastate intra-axonal cytoskeletal and organelles leading to the ultimate demise of the axons with a signature pathologic feature of disconnection. To data, no systematic calmodulin binding proteins pathways study after traumatic brain/axonal injury has taken place. Therefore, one of our goals is to profile all the calmodulin binding proteins and their changes in the brain under pathological injury perturbations, and further explore calmodulin involved mechanisms underlying the traumatic neuronal/axonal injury.

Axons Rarely Regenerate after Injury in the Adult CNS

It is well known that axons rarely regenerate after injury in the adult central nervous system. This is the main reason why permanent functional damages, such as paralysis and loss of sensation exist in traumatic brain injury or spinal cord injury patients. During the last two decades, numerous studies showed multiple concurrent factors contribute to restrict the growth potential of maturing neurons by acting at different levels. Among those factors, the best

characterized are the intrinsic regeneration ability's of the neurons and the hostile environment surrounding CNS lesions (Tang, 2003; Hata et al., 2006).

The poor axonal growth outcome of injured mature CNS neurons was first observed by Cajal in the 1927. Subsequently, breakthrough experiments conducted by Aguayo and his colleagues demonstrated that injured neurons in the adult spinal cord can regenerate over long distances when the peripheral nervous system (PNS) grafts were introduced into the lesion site (Aguayo et al., 1981). However, neurons stopped extending their axons when they were exposed to the CNS environment immediately after leaving the PNS graft. This indicated that the hostile environment around the CNS lesion restricts the axonal regeneration after injury. A series of subsequent experiments identified some of the environmental inhibitors released from CNS myelin and astroglial scar, which are responsible for the restrictions of CNS axonal plasticity and regeneration. The characterized inhibitors include Nogo, myelin-associated glycoprotein (MAG), oligodendrocyte-myelin glycoprotein (OMgp), ephrinB3, and chondroitin sulphate proteoglycans (CSPGs) (Smith et al., 2003; Xie and Zheng, 2007).

Schwab and their colleagues developed a monoclonal antibody that when it targets Nogo it can neutralize its inhibitory properties in vitro. Furthermore, in vivo application of the antibody strikingly enhances the axonal regeneration and is associated with functional performance improvement in the adult CNS after spinal cord injury. Three different isoforms of Nogo have been found and are due to alternative transcription of the Nogo genes. Nogo-A is highly expressed by oligodendrocytes, while Nogo-B and Nogo-C are widely present within and outside the CNS. Nogo-A has two domains with inhibitory activity on neurite outgrowth. One is extracellular loop of sixty-six amino acids (Nogo-66), which also exists in two other isoforms. The other is Nogo-A with a unique domain, located in the N-terminal region. Unfortunately, the

actual inhibitory determinant has not yet defined. Fortunately, the identification of a receptor for the Nogo-66 (NgR) delineates which residues of Nogo-66 are specifically responsible for the inhibitory activity (Walmsley and Mir, 2007).

It is interesting that the application of an antagonist of Nogo-A effectively promotes axonal regeneration, however the effect is incomplete. Independent studies on myelin-associated inhibition discovered other inhibitors, such as MAG and OMgp. MAG is an immunoglobulin superfamily protein and expressed by both CNS and PNS glial cells. One interest feature of MAG is the developmentally regulated function. It is initially promote neurite outgrowth and only becomes inhibitory beyond a specific developmental time point. Since the MAG protein remains unaltered during development, its expression level does not correlate with axon growth. Furthermore, the distribution of MAG in both CNS and PNS suggests that it may not be as potent as Nogo-A.

OMgp is a 120 kDa glycosylphosphotidylinositol (GPI)-anchored protein. This protein is present in the membrane surrounding the Nodes of Ranvier made by oligodendrocyte. Recent in vitro studies suggested the roles for this protein include growth cone collapse and inhibition of neurite outgrowth. Furthermore, OMgp kock ut mice show elevated collateral sprouting from the CNS nodes of Ranvier, suggesting a potent role for OMgp in restricting axonal sprouting under development and physiology condictions. However, the precise role for OMgp in adult CNS axon regeneration after injury is yet to be determined in vivo.

Quite remarkably, all three myelin-associated inhibitors, Nogo-A, MAG and OMgp, exert their inhibitory effects by binding the GPI-linked neuronal Nogo-66 receptor (NgR) despite lack of sequence similarity (Yamashita et al., 2005). NgR does not have an intracellular signaling domain; therefore, it needs the transmembrane co-receptors LINGO and p75NTR or TROY (also

known as TAJ) to transduce neurite outgrowth inhibitory signals. Owing to the observation that NgR can bind to multiple myelin proteins, the design of the specific receptor targets can lead to interventions that can overcome the failure of CNS regeneration.

At the site of the CNS injury, a complex cellular reaction referred as the"glila scar" forms through the activation of astrocytes, microglial cells, macrophages and fibroblasts. CSPGs, a group of extracellular matrix inhibitors, are deposited in the dense complicated glial scar structure. Recent studies have identified the inhibitory role of CSPGs play on axon growth/regeneration both *in vitro* and *in vivo*. Furthermore, enzymatic degradation of CSPGs by chondroitinase ABC both enhanced axon elongation and played a part in significant behavioral improvements after spinal cord injury. Although a great deal attention has been placed on CSPGs, no definitive CSPG receptors have been identified. It has been shown that CSPGs interacts with growth factors, sequestering them away from their receptors (Del Rio and Soriano, 2007). Protein kinase C and the Rho-Rho kinase (ROCK) pathway may also been involved in the barrier effect of CSPGs on neurite outgrowth (Monnier et al., 2003b). And aside from CSPGs, several other putative axonal growth/regeneration inhibitors have been ascribed to the glial scar, such as tenascin, NG2, neurocan and semaphorin 3. However, the relevant potential of these molecules as inhibitors in axonal growth need to be further verified.

Although the hostile extracellular environment around the lesion in the CNS has been thought of as being a dominant inhibitory factor on axon regeneration, the intrinsic growth capacity of the injured neurons is also critical. It is not surprising that embryonic CNS neurons are able to extend long axons in the adult CNS environment. Moreover, isolated adult PNS neurons can grow long axons in the white matter tracts of the adult CNS (Davies et al., 1997; Davies and Silver, 1998). Compared to the embryonic CNS or PNS neurons, this response

suggests that mature CNS neurons have significantly reduced intrinsic capacity for axonal regeneration after injury. In addition, neutralization of environment inhibition is not significant enough per se to induce robust axon regeneration. Axons still regenerate poorly in the knockout mice that lack all three isoforms of Nogo or the NgR that mediates the effects of all three myelin-associated inhibitors, Nogo-A, MAG and OMgp (Zheng et al., 2003; Zheng et al., 2006).

In order to initiate and sustain axon regeneration a neuron requires the upregulation of specific transcription factors, cytoskeletal elements, growth cone components, and mediators of signal transduction. Comparing the mature axon to developing axon, some notable changes have been observed: 1) the ability to activate growth genes, such as GAP43 and CAP23, and form growth cones declines in adult; 2) age-dependent cAMP decreases; 3) sensitivity to the neurotrophic growth factors, such as BDNF, NGF and GDNF decreases; and 4) the capacity for sustained extensive structural remodeling is also reduced. Numerous observations have reported that induction of neuronal growth genes such as GAP43, allows neuritic elongation overriding myelin-derived inhibition. However, overexpression of GAP43 or CAP23 in transgenetic mice induces spontaneous sprouting but not regeneration.

There are a number of factors that switch effects. For example the decline of cAMP during development switches the response of retinal axons to netrin-1 from attraction to repulsion (Shewan et al., 2002), and the effect of MAG on cerebellar neurons switchs from growth-promoting to growth inhibitory (Cai et al., 2002). There is also evidence showing that the injection of disbuteryl cAMP into DRG neurons promotes regeneration. Cyclic AMP regulates the transcription of growth related genes through CREB, thereby resulting in the upregulation of genes such as arginase 1, IL-6 and polyamine synthesis, which directly promote axon regeneration. Although sensitivity to the neurotrophic factors decreases, there is some evidence

to suggest that locally or dynamically applying NGF or BDNF can partially restore the axonal damage. Moreover, priming neurons with neurotrophic factor is yet another means of stimulating cAMP production to overcome inhibition of myelin. The term priming is used to describe experiments where neurons are treated overnight with neurotrophic factors and are, subsequently, transferred to an inhibitory substrate (Cai et al., 1999).

Even though selective strategies targeting a single factor yields some effects, concomitant interventions that enhance intrinsic growth capability coupled with block of environmental inhibition might produce more significant regeneration.

Molecular Approach to Promote Axonal Regeneration Converge at Rho-ROCK Pathway

Several critical signals of convergence within the developing and regenerating axon for targeting axon outgrowth have been identified. One of such critical convergence point is the Rho-ROCK pathway. RhoA, one of the best characterized of the small GTPases, exists in two states: a biochemically inactive GDP-bound state and an active GTP-bound state. Rho kinase (ROCK) was the first identified RhoA downstream effecter. Two isoforms of ROCK have been described: ROCK I and ROCK II. ROCK II is highly expressed in the muscel and brain, while ROCK I is more ubiquitously distributed in all tissues. So far, no funcational difference has been found between these two isoforms. Activated RhoA GTPase binds to ROCK and thereby regulates cell motility, neuronal morphogenesis, axon guidance and outgrowth, dendrite development, and synapse formation (Ng and Luo, 2004; Mueller et al., 2005).

With regard to the numerous inhibitors that have been identified as potential obstacles to axonal regeneration, there is accumulating evidence that their intracellular signaling converge by means of Rho. It has been demonstrated that MAG, NogoA and Omgp can bind to NgR, Lingo and p75 or TROY to form a trimeric receptors complex, and thus activate the Rho-ROCK pathway thereby exhibiting an inhibitory effect on axon renegeration (Wang et al., 2002;

Yamashita et al., 2002; Lingor et al., 2007; Zhao et al., 2007). Furthermore, other environmental inhibitors around lesion, such as CSPG, repulsive guidance molecule (RGM) and members of the semaphorin and ephrin families also stimulate the RhoA–ROCK pathway (Lingor et al., 2007). Several laboratories have reported that by blocking RhoA activity with either the dominant-negative RhoA or bacterial toxin Clostridium botulinum exoenzyme C3 transferase (C3), or by inhibiting ROCK with Y27632, promotes axonal elongation, overcoming the inhibitory effects of myelin, as well as CSPG, semaphorin 3A and EhpA receptor signaling *in vitro* (Wahl et al., 2000; Monnier et al., 2003a; Yukawa et al., 2005).

Most importantly, there is associated other evidence indicates there is a TBI or spinal cord injury (SPI) induced activation of RhoA and RhoB at the lesion site in human brains (Brabeck et al., 2003; Brabeck et al., 2004) and of ROCKI and ROCKII in rat, respectively (Aimone et al., 2004). Intriguingly, the observed of upregulation of RhoA and RhoB was still detectable months after TBI in human (Brabeck et al., 2004) or over a period of 4 weeks after spinal cord injury (SCI) in rats (Conrad et al., 2005). Moreover, the persistent of the activation of Rho-ROCK pathway around the lesion site makes Rho-ROCK inhibition an attractive therapy not only for acute and sub-acute treatment, but also for delayed intervention after CNS injury.

While the intrinsic capabilities of neurons to regenerate axons in the mature CNS decrease, there has been renewed interest in improving the neuron's intrinsic ability to promote axon regeneration. Cyclic AMP activates transcript factor CREB, and this in turn leads to growth gene expression. As an interesting adjunct to the role of cAMP signaling in promoting axonal regeneration, RhoA activity was inactivated by elevated cAMP by PKA phosphorylation. Separate studies also point to the crosstalk that occurs between cAMP and Rho/ROCK by integrating MAG signaling events. A direct correlation between neuronal cAMP levels and axon

outgrowth mediated by overcoming the inhibition of MAG was found in DRG, cerebellar, cortical and hippocampal neurons. MAG binding to the NgR and p75NTR complex, with subsequent activation of Rho, executes inhibition of axonal outgrowth (Christensen et al., 2003; Hannila and Filbin, 2007).

Locally or dynamically applying neurotrophic factors such as NGF, BDNF and NT3, or priming neurons with neurotrophic factors enhances axonal regeneration both *in vitro* and *in vivo* (Blesch et al., 1998; Blesch and Tuszynski, 2007). It was reported that neurotrophin binding to the p75 low affinity neurotrophin receptor abolishes Rho activity, as well as increases cAMP level (Yamashita et al., 2002). Thus, boosting intrinsic growth capability of neurotrophin or cAMP may be mediated, at least in part by inhibition of Rho/ROCK pathway.

Since both inhibitory and permissive pathways point to the Rho/ROCK pathway, it makes this pathway an attractive target for the application of an Rho/ROCK inhibitor in order to enhance the regeneration of injured CNS axons (Figure 1-2). Fortunately, a number of specific Rho/ROCK inhibitor compounds have been developed, including analogues BA-210, fasudi, HA-1077, Y-27632 (Davies et al., 2000) and wf-536 (Nakajima et al., 2003). Among them, fasudi has already been used in patients with cerebral vasospsm after aneurismal subarachnoid hemorrhage.

Remarkably, the local application of C3 exoenzyme or Y-27632 improved functional recovery in mice and rats with transection spinal-cord injuries in different studies. In these studies, ROCK inhibition not only enhanced axonal growth beyond the lesion site, but also decreased tissue damage and cavity formation (Lehmann et al., 1999; Dergham et al., 2002; Chan et al., 2005).

However, the complete mechanism of ROCK-mediated axonal suppression is still unclear. What has been well established is that Rho-ROCK pathway played a central role in cytoskeletal dynamic rearrangement. ROCKs, when activated by the small GTPase RhoA, phosphorylate various actin associated proteins, such as myosin light chain (MLC), myosin light chain phosphatase (MLCP), LIM kinases, calponin, MARCKs, ERM (ezrin/radixin/moesin), adducin, and profilin IIa. These in turn stimulate actin polymerization, which seems lead to cell contraction, stress fiber assembly and growth cone collapse (Amano et al., 2000; Ohashi et al., 2000; Fournier et al., 2003; Riento and Ridley, 2003).

Additionally, ROCKs also phosphorylate a group of intermediate filament proteins, such as vimentin, glial fibrillary acidic protein (GFAP) and neurofilament L (Kosako et al., 1997; Goto et al., 1998; Hashimoto et al., 1998; Matsuzawa et al., 1998). Although recent observation suggest it might contribute to the cytokinesis, the exact phosphorylation induced regulation step is not clear.

Other downstream targets of ROCKs include microtubule associated protein 2 (MAP2), tau and collapsing response mediator protein 2 (CRMP-2) (Arimura et al., 2000; Amano et al., 2003). These proteins are either especially expressed or highly enriched in the brain and spinal cord to regulate microtubule dynamics. Most interestingly, CRMP-2, whose activity is regulated by phosphorylation, is known to interact with tubulin and Numb and promote microtubule assembly and Numb mediated endocytosis (Mimura et al., 2006). Phosphorylated CRMP-2 by ROCK decreases its functions and in turn contributes to growth cone collapse and MAG-mediated neurite retraction (Yamashita et al., 2002; Arimura et al., 2005).

Therefore, Rho-ROCK pathway seems to be an integration point for various signaling pathways restricting axon growth, particularly those regulating cytoskeletal rearrangements

(Figure 1-2). From the standpoint of understanding axon growth/regeneration at the system level, it is very important to identify all components in the ROCK-protein pathways linked to axon growth/regeneration.

The rat pheochromocytoma cell line, PC-12, has been widely used as an important model system for axon growth. An important feature of PC-12 cells is that they differentiate into a neuronal phenotype in response to various neurotrophins. For instance, nerve growth factor (NGF) treated PC-12 cells exhibit proliferation arrest, neuritogenesis and electrical excitability (Greene and Tischler, 1976). Moreover, PC-12 cells elicit neuritogenesis via Rho inhibition by Clostridium C-3 exoenzyme treatment (Lehmann et al., 1999; Sebok et al., 1999; Fournier et al., 2003), making it an invaluable model system for studying Rho-ROCK transduction pathways in neuritogenesis.

As mentioned previously, one major objective of my dissertation research is to explore signal transduction pathways involved in the axon injury. In order to perform that research the following steps were undertaken.

First, the calmodulin signal pathways were examined at a systematic level after traumatic injury. A novel CaM-affinity capture coupled reversed liquid chromatography tandem mass spectrometry (PRLC-MS/MS) method needed to be developed to identify the CaM binding proteome and its vulnerability to calpain and caspase proteolysis. CRMP-2, a putative CaM binding protein, was further characterized.

Next, a systems biology approach was established to decipher the Rho/ROCK signal pathways in neuritogenesis. Systems biology is a latest domain in biology that aims at system-level understanding of complex biological processes. The scope of systems biology combines multiple advanced research areas, such as biosciences, data mining, control theory and other

engineering fields. A therapeutic approach by ROCK inhibitor was applied to PC-12 cells to induce neuritogenesis. Differential gene transcriptome and protein expression influenced by ROCK inhibition were identified by Affymetrix mciroarray and proteomic studies.

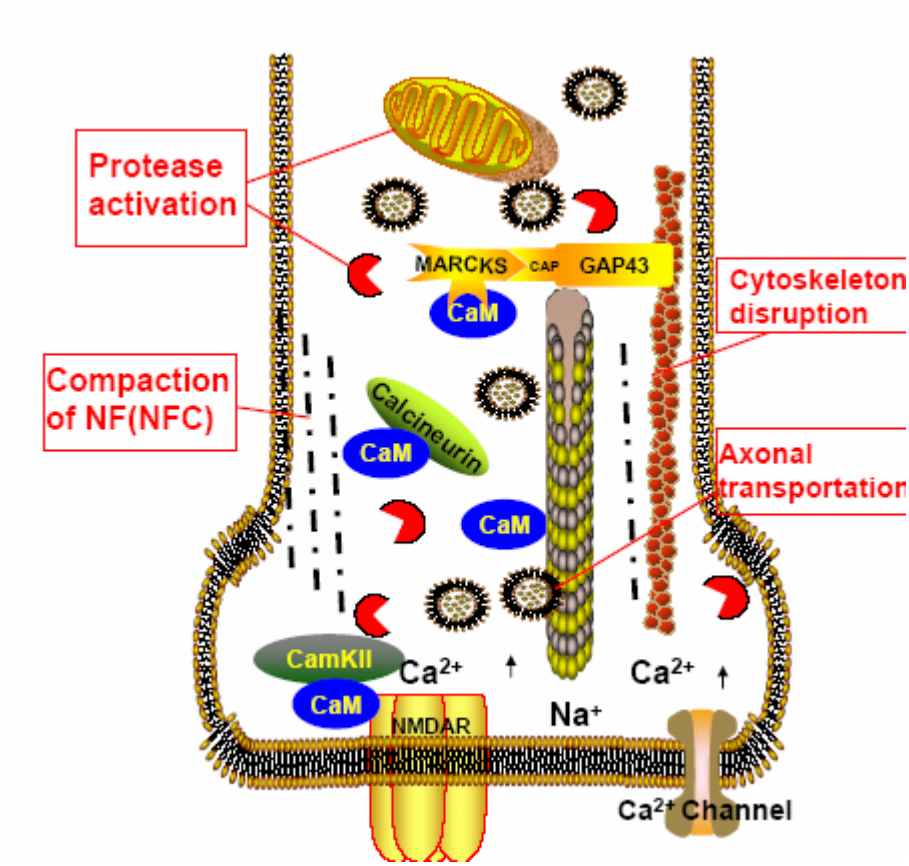

Figure 1-1. Ca^{2+}/Calmodulin involved traumatic axonal injury.

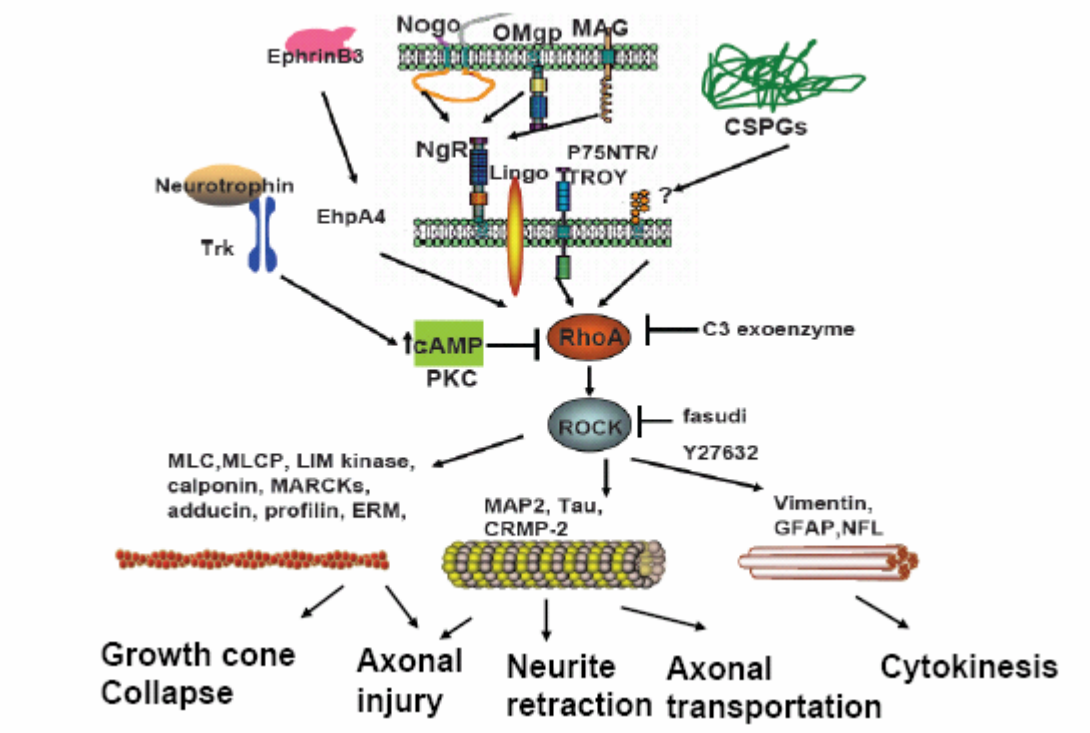

Figure 1-2. Pathways involved in axonal injury/regeneration converge at Rho-ROCK pathway.

CHAPTER 2
USING CALMODULIN-AFFINITY CAPTURE TO STUDY THE RAT BRAIN CALMODULIN BINDING PROTEOME AND ITS VULNERABILITY TO CALPAIN AND CASPASE PROTEOLYSIS

Introduction

Calmodulin (CaM) is one of major calcium (Ca^{2+}) sensors that are central in regulating multiple intracellular events. CaM exerts its regulatory functions through the modulation of a diverse number of CaM-binding proteins (CaMBPs) in a Ca^{2+} dependent manner (Benaim and Villalobo, 2002; Haeseleer and Palczewski, 2002; Bouche et al., 2004). With the extraordinarily high concentration of CaM (10 to 100 μM) found in neuron of the central nervous system (CNS) (Xia and Storm, 2005), there is significant interest in the downstream pathways involving CaM regulation. Several CaMBPs have already been characterized including adenyl cylases (AC1 and AC8), calcineurin A, CaM-dependent protein kinase I, II, IV, neuronal nitric oxide synthase, and various calcium-ion channels. Known CaMBPs are involved in synaptic plasticity, learning, memory (Xia et al., 1993; Xia and Storm, 2005); however; it is necessary to identify all unknown CaMBPs in order to fully construct a calcium-CaM mediated protein network in the brain.

In traumatic brain injury (TBI), increased calcium influx leads to a rapid rise in cytosolic calcium levels and activation of the cysteine proteases calpain and caspase (Wang, 2000b; Pineda et al., 2004). As a result, activated calpains and caspases produce irreversible proteolysis, and ultimately leading to necrotic and apoptotic cell death (Pike et al., 2001; Pineda et al., 2004). Recently, disruption of calcium signaling was also recognized as the underlying cause of neuronal dysfunction and associated apoptosis in stroke and Alzheimer's disease (AD)(O'Day and Myre, 2004). Previous studies showed that CaMBPs as a group are potential substrates for calpains and caspases, and are vulnerable to brain injury induced proteolysis and deregulation (Wang et al., 1989b; Barnes and Gomes, 1995; McGinnis et al., 1998; Mukerjee et al., 2000;

Mukerjee et al., 2001). For example, non-erythroid αII-spectrin, an identified Ca^{2+} dependent CaMBP, is degraded to 150, 145 and 120 kDa fragments in TBI. Further studies showed that calpain-2 mediated αII-spectrin proteolysis produces a 150 and a 145 kDa fragment (SBDP150 and SBDP145) that are present in neuronal necrosis and apoptosis, whereas the caspase-3 proteolysis produces a sub-150 kDa and a 120 kDa fragment (SBDP150i and SBDP120) that appear exclusively in neuronal apoptosis. Therefore, specific spectrin fragments can be used as markers for the activation of necrosis and apoptosis (Wang, 2000b). The vulnerability of αII-spectrin to proteolysis in both necrosis and apoptosis may be just one example of common proteolytic and functional changes occurring among CaMBPs after brain injury and in neurodegenerative disease. Therefore, the global identification and characterization of CaMBPs and their vulnerability to calpain and caspase proteolysis may improve our understanding of the pathophysiological mechanisms associated with neuronal injury.

In the past, traditional molecular biology techniques, such as the calmodulin overlay technique (CaMBOT), have been used to isolate and identify individual CaMBPs (O'Day, 2003). A genetic and proteomic approach to screen protein-protein interaction based expression libraries with CaM has proven to be a powerful way in identifying novel CaMBPs in Arabidopsis and yeast (Zhu et al., 2001; Reddy et al., 2002). Those techniques have provided remarkable results; however, there are notable limitations. The laborious procedures of radioisotope labeling, isolation and sequencing of cDNA encoding for CaMBPs, and complicated proteome chip preparation hindered use of those techniques to profile CaMBPs in animals. More recently, a novel mRNA display method was introduced to identify and characterize human CaMBPs in a comprehensive manner (Shen et al., 2005). The mRNA display method provides a powerful way to read and amplify CaMBPs selected from a large human proteome library. This technique

offered improved ability to analyze the low-abundance proteins. Furthermore, binding CaM-motifs are easily mapped by locating overlapping regions of selected fragments of the parent protein of interest. However, as an in vitro amplification process this technique requires efficiency and specificity of many steps (transcription, translation, fusion, etc), thus limits the effective coverage of the CaM-bindng proteome. Moreover, this method is a labor intensive process with hundreds of in vitro translation, library amplification, cloning and sequencing steps (Gold, 2001; Takahashi et al., 2003; Shen et al., 2005).

Recent developments in mass spectrometry technology, coupled to advances in the fields of bioinformatics, have allowed us to investigate CaMBPs in a high throughput manner. In this study we have exploited Ca2+-dependent CaMBP interaction with CaM agarose and the subsequent contrary calcium-chelating dissociation of CaMBPs from the resin to purify a CaM binding sub-proteome. Following resolution by one dimension sodium dodecyl sulfate-polyacrylamide gel electrophoresis (1D-SDS-PAGE), the purified CaMBPs and their calpain-2 and caspase-3 proteolytic products were profiled by RPLC-MSMS analysis.

Materials and Methods

Brain Tissue Collection and Protein Extraction

Animal surgery procedures were conducted in compliance with the Animal Welfare Act and the University of Florida Institutional Animal Care and Use Committee and the National Institutes of Health guidelines detailed in the Guide for the Care and use of Laboratory Animals. As described previously (Pike et al., 2001), adult male (280–300g) Sprague-Dawley rats (Harlan; Indianapolis, IN) were initially anesthetized with 4% isoflurane in a carrier gas of 1:1 O_2/N_2O (4 minutes) followed by maintenance anesthesia of 2.5% isoflurane in the same carrier gas until the animals were sacrificed by decapitation. Naïve cortex tissue was removed, rinsed with ice-cold PBS, and halved. Brain tissues were rapidly dissected, rinsed in ice-cold PBS, snap-frozen in

liquid nitrogen, and stored at -80ºC until used. The brain samples were pulverized with a small mortar and pestle set over dry ice to a fine powder. The pulverized brain tissue powder was then lysed for 90 minutes at 4ºC with 50 mM Tris-HCl (pH 7.4), 5 mM EDTA, 5 mM EGTA, 1% Triton X-100, and 1 mM DTT (added fresh). Brain cortex lysates were then centrifuged at 100,000 g for 10 minutes at 4ºC. The supernatant was retained and a DC protein assay (Bio-Rad; Hercules, CA) was performed to determine protein concentration.

In Vitro Calpain-2 and Caspase-3 Digestion of Brain Lysate

Naïve cortex lysate was prepared as above. In vitro digestion of rat lysate (5 mg) with the purified proteases, porcine calpain-2 (Calbiochem, San Diego, CA) and recombinant human caspase-3 (Chemicon, Temecula, CA) was performed in a buffer containing 100 mM Tris-HCl (pH 7.4) and 20 mM DTT. For calpain-2, 2 mM CaCl2 was also added, and then incubated at room temperature for 30 minutes. For caspase-3, sample was incubated at 37ºC for 4 hours. The protease reaction was stopped by the addition of 30 μM calpain inhibitor (MDL 28170) (Calbiochem, San Diego, CA) or 100 μM pan-caspase inhibitor (Z-D-DCB) (Calbiochem, San Diego, CA) and a protease inhibitor cocktail solution (Roche Biochemicals, Indianapolis, IN).

CaM Affinity Capture and Elution

Naïve brain (control) and digested lysates (900 μg each) were premixed with 600 μL (50% slurry) CaM-Sepharose (CaM-agarose) (Sigma, St. Louis, MO) in 20 mM Tris-HCl (pH 7.4) and 150 mM NaCl (TBS). EDTA (5 mM) was added to the calpain-2 digest prior to mixing with CaM-agarose. A negative control was also prepared using plain lysis buffer with CaM-agarose. After premixing the lysate with CaM-agarose, 10 mM CaCl2 was added and the reacting mixture was continuously incubated for 90 minutes at room temperature to ensure efficient binding. The CaM-agarose bound CaMBPs were collected by centrifugation, were washed eight times with 1.5 mL TBS with 1 mM CaCl2, and eluted from the resin in 300 μL TBS containing 15 mM

EDTA. Purified CaMBPs were concentrated via a Millipore YM-10 filter unit (Millopore, Bellerica, MA), suspended in 2x sample buffer (Invitrogen, Carlsbad, CA), and resolved by 10-20% sodium dodecyl sulfate-polyacrylamide gel electrophoresis (SDS-PAGE) visualized by Coomassie blue (Bio-Rad R250) staining.

In Gel Digestion

Visible bands were excised, cut into four 1 mm cubes, and washed with HPLC water followed by 50% 100 mM ammonium bicarbonate/ 50% acetonitrile. Pieces were dehydrated with 100% acetonitrile followed by speed vacuum. Cubes were re-hydrated with 10 mM dithiothreitol for 30 minutes at 56 °C. Proteins were alkylated with 55 mM iodoacetamide in 50 mM ammonium bicarbonate for 30 minutes in the dark at room temperature. Gel cubes were then washed with water and dehydrated with 100% acetonitrile. To each tube was added 15 µL of a 12.5 ng/µL trypsin solution for 30 minutes at 4 °C. Then 20 µL of 50 mM ammonium bicarbonate was added and the gel cubes were incubated overnight at 37 °C. Peptides were extracted first in water then in 50% water/50% acetonitrile sequentially. Extracted peptides were dried by speed vacuum and re-suspended in mobile phase solution for capillary RPLC-MSMS.

Capillary RPLC-MSMS Based Protein Identification

Capillary reversed phase liquid chromatography tandem mass spectrometry protein identification was performed as described previously (Ottens et al., 2005). Briefly, sample digests (2 µL) were loaded via an autosampler onto a 100-µm x 5-cm c-18 reversed phase capillary column at 1.5 µL/min. Peptide elution was performed by linear gradient: 5% to 60% methanol in 0.4% acetic acid over 30 minutes at 200 nL/min. Tandem mass spectra were collected in data-dependant mode (3-most intense peaks) on a Thermo Electron LCQ Deca XP plus ion trap mass spectrometer. Tandem mass spectra were searched against an NCBI rat indexed RefSeq protein database using Sequest. Filtering and sorting was performed with

DTAselect software by peptide number and Sequest cross correlation values (Xcorr values of 1.8, 2.5, 3.5 for +1, +2, +3 charge states) (Tabb et al., 2002). Peptides filtered and sorted by DTAselect were assigned to specific protein accession numbers (National Center for Biotechnology Information [NCBI]).

Immunoblot Analysis

Purified calmodulin binding proteins and control samples were separated by SDS-PAGE gel, and transferred to a polyvinylidene difluoride (PVDF) membrane by the semi-dry method. Membranes were blotted either with anti-αII spectrin (Biomol Affinity, Exeter, UK), anti-calcineurin A (BD-transduction, San Jose, CA), anti-βII spectrin (BD-transduction, San Jose, CA), anti-dynamin (BD-transduction, San Jose, CA) or anti-calmodulin (upstate, Charlottesville, VA) antibodies, and developed with biotin and avidin-conjugated alkaline phosphatase. Blots were developed using nitroblue tetrazolium and 5-bromo-4chloro-3-indolyl phosphate.

Results

Calmodulin Binding Proteomic Profiling by Calmodulin-affinity Capture

To explore the rat brain calmodulin binding proteome, we employed a calmodulin-affinity capture method combined with RPLC-MSMS based proteomics. The specificity of the proteome methodology (Figure 1A) is derived from the Ca2+ dependent CaM-CaMBPs interaction. It is also important to note that the presence of endogenous CaM in samples reduces the efficiency of affinity capture brain CaMBPs to CaM agarose. To allow efficient CaM-agarose binding, endogenous CaM-CaMBP complexes were first dissociated in the presence of EDTA (5 mM). The lysate was then mixed with excess amount of CaM-agarose followed by the additional excess CaCl2 (10 mM) to allow association of CaMBPs to CaM-agarose. The optimal excess amount of CaM-agarose for CaM-affinity capture appears to be 100 μg CaM immobilized agarose per 300 μg rat brain protein lysate (data not shown). The majority of CaMBPs bound to

the CaM-agarose were specifically released in the presence of excess EDTA producing an enriched CaMBP sub-proteome.

To assess the vulnerability of those purified CaMBPs to proteolysis, we performed in vitro calpain-2 and caspase-3 digestions on the same amount of naïve brain protein lysate prior to applying the CaM-affinity capture described above. In all cases, rat brain CaMBPs (and fragments) were selectively eluted from CaM-agarose resin with an EDTA-containing buffer (Figure 2-1A). The naïve control CaM binding proteome is shown next to the calpain-2 or caspase-3 digested CaM binding proteome in Figure 2-1B by Coomassie blue staining. Sepharose-4B was used as a control to rule out non-specific binding to the resin alone. No detectable proteins were eluted from Sepharose-4B group compared with the CaM-agarose group (Figure 1C).

Identification of CaM Binding Proteome and Calpain/caspase Mediated Breakdown Products by RPLC-MSMS Based Proteomics

As shown in Tables 2-1 and 2-2, a total of 69 proteins were identified between the three samples separated on the gel in Figure 2-1B. After checking the CaMBPs database (http://calcium.uhnres.utoronto.ca/ctdb (Yap et al., 2000)) and Medline data mining, we summarized 26 identified known CaMBPs in Table 2-1 with hyperlinked accession number in the NCBI (National Center for Biotechnology Information) Database and their respective molecular mass and approximate molecular mass on gel, as well as the number of peptides identified and the associated protein sequence coverage found by RPLC-MSMS in naïve, calpain and caspase digested samples. Table 2-2 lists 43 putatively novel CaMBPs which include the brain abundant proteins collapsin response mediator protein 2 (CRMP2), GTPase dynamin 1 and creatine kinase. In analyzing data from Tables 2-1 and 2-2, an apparent reduction in protein mass on gel in relation to the native protein mass was indicative of proteolysis in the calpain and

caspase digests. This was exemplified by the identification of αII-spectrin (natively 280 kDa) at 150 kDa on-gel after calpain-2 and caspase-3 digestion, the mass of known αII-spectrin breakdown products (Pike et al., 2004). Myelin basic protein was also shown vulnerable to calpain-2 digestion while calmodulin dependent phosphodiesterase 1A was found vulnerable to caspase-3 digestion (Table 2-1). Of 43 putative CaMBPs (Table 2-2), pyruvate kinase-3, glutamate oxaloacetate transaminase-1, enolase, albumin precursor protein, peptidylprolyl isomerase A, brain myelin proteolipid protein and alpha H+/K+ transport ATPase were all shown vulnerable to calpain-2 proteolysis. βII-spectrin, pyruvate kinase-3, glutamate oxaloacetate transaminase-1 and glutamate oxaloacetate transaminase-2 were all shown vulnerable to caspase-3. The proteins αII-spectrin, pyruvate kinase-3 and glutamate oxaloacetate transaminase-1 were found sensitive to calpain and caspase digestion in our CaM-binding sub-proteome.

Functional Analysis of Putatively Novel CaM-Binding Proteins

In total, we identified 43 putatively novel CaMBPs implicated in a wide range of cellular activities, while only a few of these proteins are potential background proteins (marked in Tables 2-1 and 2-2 by *). All putative CaMBPs were searched against the Gene Ontology Consortium (http://www.geneontology.org (Harris et al., 2004)) and the Human protein Reference Database (http://www.hprd.org (Peri et al., 2003)) public databases, and grouped into categories that define their biological and molecular functions, as indicated in Table 2-3. The largest group of putative CaMBPs is involved in metabolism and energy pathways (60%). In the cellular communication and signal transduction category, we identified nine putative CaMBPs (21%), which include four 14-3-3 isoforms, GTPase dynamin-1, CRMP2 and the G-protein coupled receptor P2Y4. There was also a significant number of CaMBPs implicated in cell growth and maintenance (14%), such as two cytoskeletal associated protein and four structural proteins.

Interestingly, we found four mitochondrial proteins that seldom appear in the literature, three of which were susceptible to calpain/caspase digestion. Thus, the presented methodology may be useful in the study of mitochondrial CaMBPs and their role in cell death.

Immunoblot Analysis of Select CaMBPs Identified by RPLC-MSMS Following CaM-Affinity Purification

Traditional immunoblots were performed on αII-spectrin and calcineurin (Figure 2-2) to validate their proteolytic fragments identified by RPLC-MSMS. Figures 2-2A and 2-2B showed immunoblots from crude brain lysate before and after CaM-affinity purification. Figure 2-2A confirmed the extent of proteolysis of samples in caplain-2 digestion produced SBDP150 and SBDP145 while caspase-3 digestion produced SBDP150i and SBDP120 (Wang, 2000b) (Wang, 2000b). Data in Figure 2-2B correlated with RPLC-MSMS data (Table 2-1) to show intact αII-spectrin and the 150 kDa breakdown products after CaM-affinity binding, an indication that the CaM-binding domain is retained in this fragment. Figure 2-2B also shows that calcineurin was proteolysis to 55 and 49 kDa fragments upon calpain-2 digestion, and that both retained the CaM-binding domain. In contrast, caspase-3 proteolysis of calcineurin produced a 45 kDa fragment that did not contain a CaM binding domain. The putatively novel CaMBP dynamin was examined by Immunoblot in Figure 2-3A. Interestingly, dynamin was digested by calpain-2 into fragments at 65 and 40 kDa, and by caspase-3 into 42, 40 and 32 kDa, none of which were observed by RPLC-MSMS. This is because only the 65 kDa fragment appeared to retain the CaM-binding domain, which was likely missed due to its low abundance. Figure 2-3D illustrates that intact and caspase-3 digested βII-spectrin were also found to elute from the CaM-agarose, validating the RPLC-MSMS data in Table 2. βII-spectrin has a putative CaM binding domain (Boivin and Galand, 1984; Bignone and Baines, 2003) supporting the observation that βII-spectrin elutes from CaM-agarose; however, the possible protein-protein interaction with αII-

spectrin (Boivin and Galand, 1984; Bignone and Baines, 2003) can also explain the presence of βII-spectrin, as will be discussed later.

Unexpectedly, calmodulin (17 kDa) was observed in the CaMBP elution fraction. Dissociation of CaM from a protein complex, such as with delta subunit of phosphorylase kinase (Dasgupta et al., 1989), was one possibility, or that CaM could be an artifact as leaking from the CaM-agarose resin. To verify the source of the CaM, we used plain lysis buffer (without protein) as a negative control. Figure 2-4 demonstrates that the CaM was also detected in the negative control, which indicates that small amount CaM was leaking from the CaM-agarose resin during the CaM-affinity purification procedure. This is likely due to disruption of non-covalently bound CaM to the agarose beads. To avoid this in the future, the CaM-agarose should be extensively pre-washed with a concentrated EDTA solution.

Discussion

To date, this is the first proteomic study of the CaM binding proteome and its vulnerability to calpain and caspase proteolysis in the rat brain. Most of the known CaMBPs were previously identified by the CaM overlay coupled genome encoding technique, which is a low throughput method due to the limitations associated with radioisotope labeling and DNA sequencing (O'Day, 2003). We present a simple, easy to scale up, high-throughput method for discovery and study CaMBPs which we used to identify 69 known and putative CaMBPs in a single experiment. Of the 26 known CaMBPs (Table 2-1), including αII-spectrin, calcineurin, synapsin 1, α-synuclein, CaM kinase II, myelin basic protein and synaptotagmin-1 among others, most are cytoplasmic proteins; however, of the 43 putative CaMBPs identified (Table 2-2), a large number were proteins normally localized in mitochondria, such as ubiquinol cytochrome c reductase core protein 2, mitochondrial creatine kinase, mitochondrial glutamate oxaloacetate transaminase 2, and mitochondrial malate dehydrogenase (Table 2-3). Interestingly, only

mitochondrial malate dehydrogenase was found at naïve conditions, while the other mitochondrial proteins were found in the calpain-2 or caspase-3 digests. Mitochondria have been established as a Ca2+ "sink" during cytosolic Ca2+ overload that precedes apoptic and necrotic cell death (Carafoli, 2003; Saris and Carafoli, 2005). Prior studies suggested that CaM can be found in mitochondria (Ruben et al., 1980; Itano et al., 1986; Babcock et al., 1997); however, this is the first study to demonstrate the presence of mitochondrial associated CaMBPs in rat brain that are potentially involved in CaM regulated Ca2+ signaling cascades during apoptosis or necrosis.

Within 12 substrates found in CaMBPs, nine of them are vulnerable to calpain-2. This is consistent with our previous observation that many CaMBPs are vulnerable to calpain proteolysis (Wang et al., 1989b). Furthermore, the immunoblot analyses in Figure 3 demonstrate that the CaM-affinity / RPLC-MSMS method can efficiently capture and enrich CaMBPs along with their proteolyzed fragments that still contain calmodulin binding sites. In addition, our calcineurin results were consistent with a previous calcineurin proteolytic degradation study (Lakshmikuttyamma et al., 2004). Dynamin 1, one of the GTPase proteins, is generally considered essential for intracellular membrane trafficking events such as synaptic vesicle endocytosis in nerve terminals (Takei et al., 2005; Verma and Hong, 2005). Recent reports indicated the involvement of calcium in dynamin mediated synaptic vesicle endocytosis; however, this is the first report to show that dynamin interacts with CaM (Cousin, 2000; Smillie and Cousin, 2005), providing the basis for investigating possible dynamin-CaM modulation of vesicle endocytosis.

Previous studies showed that βII-spectrin can be eluted from the CaM-column with very weak affinity (Boivin and Galand, 1984; Berglund et al., 1986), whereas another study indicated

that βII-spectrin passed through the CaM-affinity column (Glenney and Weber, 1985). In our study, immunoblot analysis demonstrated that βII-spectrin and its proteolyzed fragments were captured by the CaM-affinity resin. Since αII-spectrin and βII-spectrin form a high affinity tetramer, βII-spectrin and its proteolyzed fragments elute possibly due to protein-protein interactions with αII-spectrin (Bignone and Baines, 2003). In a similar fashion, clathrin heavy chain subunits also bind to a light chain subunit(Ybe et al., 1999) that is a known CaMBP. Additionally, using a yeast two-hybrid screen and in vitro CaM overlay assay, human adaptor protein 14-3-3 epsilon protein was found to interact with human calmodulin (Luk et al., 1999). Whereas, seven 14-3-3 isoforms, including zeta, eta, gamma, were also shown to interact with each other through direct or indirect association (Jin et al., 2004). More stringent conditions might be needed to rule out some indirect interactions. Taken together, these would suggest that some putative CaMBPs listed in Table 2-2 may bind to CaM through similar protein-protein interactions, presenting the possibility of a complex CaM binding network that can be elucidated from the presented results.

Though CaM-affinity purification is an efficient method to enrich Ca2+ dependent CaMBPs, some highly abundant brain proteins might be non-selectively retained by the CaM resin, such as M2 pyruvate kinas, pyruvate kinase-3, glyceraldehyde-3-phosphate dehydrogenase, phosphoglycerate mutase 1,α and β-actin (Shevchenko et al., 2002). In the future, proteins that non-specific bind could be minimized by incubating the samples first with plain agarose beads and then applying the supernatant for CaM-agarose purification. To address these issues, the putative CaMBPs we identified need to be further confirmed by an independent method such as biotinylated CaM overlay technique (O'Day, 2003).

In conclusion, the combined CaM-affinity capture / RPLC-MSMS method is a simple and efficient way to explore the CaM-binding proteome and its vulnerability to proteolysis. The putative CaMBPs and their calpain/caspase substrates identified in this study will be helpful in constructing a protein-protein interaction map that may help to explain how brain cells respond in terms of initiating proteases to Ca2+ stimuli. This approach can easily be applied to other biological samples and may provide promising potential in finding novel biomarkers and therapeutic targets in TBI, stroke and other neurodegenerative disease which involve calcium "dyshomeostasis"(Lopez-Otin and Overall, 2002; O'Day, 2003; O'Day and Myre, 2004; Kurz et al., 2005; Liu et al., 2005).

Table 2-1. Known CaMBPs and potential breakdown products identified by CaM affinity capture/RPLC-MSMS.

			Naïve			Calpain-2			Caspase-3		
Protein Name	Accession no.	MW of Protein(kDa)	MW from gel(kDa)	Matched peptides	Sequence Coverage(%)	MW from gel(kDa)	Matched peptides	Sequence Coverage(%)	MW from gel(kDa)	Matched peptides	Sequence Coverage(%)
[#] Alpha-II spectrin	P16086	272	280	3	1.2				280	30	17
						150	6	2.9	150	5	2.9
Clathrin, light polypeptide	NP_446287								30	2	9.8
Plasma membrane calcium ATPase 4	NP_001005871	129	140	3	3.4						
Heat shock protein 90	AAT99569	83.3	90	2	3	90	4	6.5			
Synapsin 1	NP_062006	74.1							75	2	2.3
Heat shock protein 8	NP_077327	70.8	70	5	6.3	70	2	4.5	70	2	4.5
Heat shock protein 70	CAA54424	70	70	7	8.7	70	5	6.9	70	1	2.5
Calcineurin, catalytic Subunit, alpha isoform	NP_058737	58.7	55	4	10.7	55	3	6.7	55	4	6.7
CaM kinase II beta subunit	S68470	72.7				55	1	2	55	1	2
CaM kinase II gamma Subunit	S43845	56				55	1	2	55	1	2
CaM-kinase II delta chain	NP_036651	56.4	200	1	2.4				50	2	4.6
CaM-kinase II alpha chain	NP_037052	55.3	200	1	2.7	50	1	2.7	50	3	8
			50	1	2.7						
[#] Phosphodiesterase 1A, calmodulin-dependent	NP_110498	62.3							55	1	1.7
Synaptotagmin 1	S09595	47.4				55	3	8.1			
Tubulin, alpha 1	NP_071634	49.9	50	12	24.2	50	20	26.7	52	1	4
Tubulin, beta 5	NP_775125	49.9	50	1	2.2						
Tubulin, beta2-like	NP_954525	49.9	50	14	41	52	4	14.2			
Neuron-specific class III beta-tubulin	AAM28438	49.9	50	5	15	50	4	12.4	52	1	2.2

Table 2-1 (continued)

Myristoylated alanine rich Protein kinase C substrate	A39773	30							75	1	4.9
Neuronal axonal membrane protein Nap-22	Q05175	21.8							22	2	18.6
Sirtuin 2	AAH86545	43.3	34	2	10						
Guanine nucleotide-binding protein, beta-2	NP_112299	37							32	2	6.2
Guanine nucleotide-binding protein, beta-3	NP_068630	37							32	1	2.9
Guanine nucleotide-binding protein, beta 1	AAH78809	37	32	2	5.9						
Synuclein, alpha	NP_062042	14.5	17	2	18.6	17	2	19.3			
[#] Myelin basic protein	NP_058722	17	17	6	23	13	3	14.4			
Synaptobrevin 2	NP_036795	12.6				13	1	14.7			

[#] undergoing proteolysis; * potential background proteins (Shevchenko et al., 2002).

Table 2-2. Putative CaMBPs identified by CaM-affinity capture/ RPLC-MSMS.

			Naïve			Calpain-2			Caspase-3		
Protein Name	Accession no.	MW of protein(kDa)	MW from gel (kDa)	Matched peptides	Sequence Coverage (%)	MW from gel(kDa)	Matched peptides	Sequence Coverage (%)	MW from gel(kDa)	Matched peptides	Sequence Coverage (%)
# Spectrin beta 2 isoform 1	NP_001013148	274	280	3	1.4						
									180	9	3.8
Clathrin, heavy polypeptide	NP_062172.	192	200	5	4.1	200	2	1.6	200	2	1.4
Collapsin response mediator protein 2	P47942.	62.3	180	2	4.7	180	1	2.8			
						62	2	3.7	62	3	6.1
Na+/K+ -ATPase alpha 3 subunit	NP_036638	116	100	4	6.3	100	5	7.1			
Na,K-ATPase alpha-1	AAA41671	112	100	4	6.3	100	6	8.7	100	1	1.8
Na,K-ATPase alpha-2	NP_036637	112							100	1	1.8
Dynamin 1	NP_542420	97				95	1	1.2			
Microtubule-associated protein 6	NP_058900	86.5							150	4	6.4
Aconitase 2, mitochondrial	NP_077374	85.5				85	3	6.7			
Syntaxin binding protein 1	NP_037170	67.7				65	6	9.4	65	5	9.4
* M2 pyruvate kinase	AAB93667	57.8	55	5	13						
* Pyruvate kinase-3	NP_445749	57.8				55	5	13.8	55	1	3.4
			50	1	2.7						
ATPase, H+ transporting, V1 subunit B, isoform 2	AAH85714	56.6	50	2	5.1						
ATP synthase alpha chain	P15999	59.8	50	2	4.7	52	2	4.7			
ATP synthase beta subunit	AAB02288	56.3	50	5	14	50	5	11.5			
#* Enolase	NP_036686	47.2							46	5	19.1
						33	1	3			
G-protein coupled receptor P2Y4	CAA75007	46	44	1	4.2				44	2	18.6

Table 2-2 (continued)

Glucose phosphate isomerase	NP_997475	62.8	50	1	3						
Glutamine synthase	AAH87131	42				38	1	2.1	40	1	2.1
Glutamate dehydrogenase 1	NP_036702										
2',3'-cyclic nucleotide 3'-Phosphodiesterase	AAA64429	47.3	45	2	5.5	45	4	10.7	45	3	8.5
Creatine kinase, mitochondrial 1	AAH91335	47.5				43	1	3.8			
Creatine kinase, brain	NP_036661	42.7	100	4	16	100	2	4.2	100	5	15.7
			43	3	13	43	2	9.7	43	6	21.5
* Alpha 2 actin	P62738	42	40	3	9.8	40	3	9			
* Cytoplasmic beta-actin	AAH63166	41.7				40	2	7.5	40	2	13.2
Ubiquinol cytochrome c reductase Core protein 2	AAH83610	48.2				40	1	3.5			
#Glutamate oxaloacetate Transaminase 1	AAH61877	46.3				38	3	11	38	4	4.4
Similar to Transcriptional activator Protein PUR-alpha	XP_226016	34.9				34	1	2.8			
* Glyceraldehyde-3-phosphate Dehydrogenase	AAH87743	33	34	5	23	34	3	13			
# Glutamate oxaloacetate Transaminase 2	NP_037309	47.4							38	3	4.4
Malate dehydrogenase 1, NAD (soluble)	NP_150238	36.4	34	6	21	34	1	3	34	3	10.5
Malate dehydrogenase, mitochondrial	NP_112413	35.5	32	8	20				32	7	25.7
# Albumin precursor, PRO0883 Protein	ABRTS	69.4				33	1	2.5			
Lactate dehydrogenase A	NP_058721	36.7	32	2	6.7				32	2	3
Lactate dehydrogenase B	NP_036727	36.7							32	1	4.8

Table 2-2 (continued)

L4-3-3, zeta	NP_037143	28	28	4	19	28	2	10.6
L4-3-3, eta	NP_037184	28	28	3	17	28	1	5.7
L4-3-3, gamma	NP_062249	28	28	2	9.7			
L4-3-3, theta	NP_037185	28	28	2	9	28	1	3.3
* Phosphoglycerate mutase 1	JC1132	28.9	28	2	8.3			
Calmodulin	AAH58485	17	17	1	6	17	2	7.4
# Peptidylprolyl isomerase A; cyclophilin A	NP_058797	18				13	2	20.2
# Myelin proteolipid protein	AAA41898	30.1				25	4	16.2
# H+/K+-ATPase, alpha	AAB93902	115				10	1	1.4

undergoing proteolysis; * potential background proteins (Shevchenko et al., 2002).

Table 2-3. Functional grouping of putative novel CaMBPs

Cellular communication of Signal transduction (21%)	
Adaptor Molecules	Notes
L4-3-3, zeta	expressed in golgi and cytoplasm involved in complex scaffold activity
L4-3-3, eta	expressed in golgi and cytoplasm involved in complex scaffold activity
L4-3-3, gamma	expressed in golgi and cytoplasm involved in complex scaffold activity
L4-3-3, theta	expressed in golgi and cytoplasm involved in complex scaffold activity
Transport/cargo protein	
Syntaxin binding protein 1	
ATPase, H+/K+ transport., alpha	
Cytoskeletal associated protein	
Collapsin response mediator protein 2	
GTPase	
Dynamin 1	primary function a GTPase activity involved in vesicle endocytosis
G protein coupled receptor	
G-protein coupled receptor P2Y4	
Cell growth and/or maintenance (14%)	
Cytoskeletal associated protein	
Spectrin beta 2 isoform 1	
Microtubule-associated protein 6	
Structural protein	
Clathrin, heavy polypeptide	
Alpha 2 actin	
Cytoplasmic beta-actin	
Brain myelin proteolipid protein	

Table 2-3 (continued)

Metabolism and Energy pathways (60%)	
Transport/cargo protein	
Na+/K+ -ATPase alpha 3 subunit	
Na,K-ATPase alpha-1	
Na,K-ATPase alpha-2	
ATPase, H+ transporting, V1 subunit B Isoform 2	
ATP synthase alpha chain	
ATP synthase beta subunit	
Enzyme	
Aconitase 2, mitochondrial	Hydratase
Enolase	Hydrolase
2',3'-cyclic nucleotide 3'-phosphodiesterase	Phosphodiesterase
* Ubiquinol cytochrome c reductase core Protein 2	Reductase
Glutamate oxaloacetate transaminase 1	aminotransaminase
* Glutamate oxaloacetate transaminase 2	aminotransaminase
* Creatine kinase, mitochondrial 1	phosphotransferase
Creatine kinase, brain	phosphotransferase
Phosphoglycerate mutase 1	Mutase
Peptidylprolyl isomerase A; cyclophilin A	Isomerase
Glucose phosphate isomerase	Isomerase
Malate dehydrogenase 1, NAD (soluble)	Dehydrogenase
* Malate dehydrogenase, mitochondrial	Dehydrogenase
Glutamate dehydrogenase 1	Dehydrogenase
Glyceraldehyde-3-phosphate Dehydrogenase	Dehydrogenase
Lactate dehydrogenase A	Dehydrogenase
Lactate dehydrogenase B	Dehydrogenase
Glutamine synthase	Dehydrogenase
M2 pyruvate kinase	phosphtransferase
Pyruvate kinase-3	phosphtransferase

Table 2-3 (continued)

Unclassified (5%)
Similar to Transcriptional activator protein PUR-alpha
Albumin precursor, PRO0883 protein

*proteins localized in mitochondria

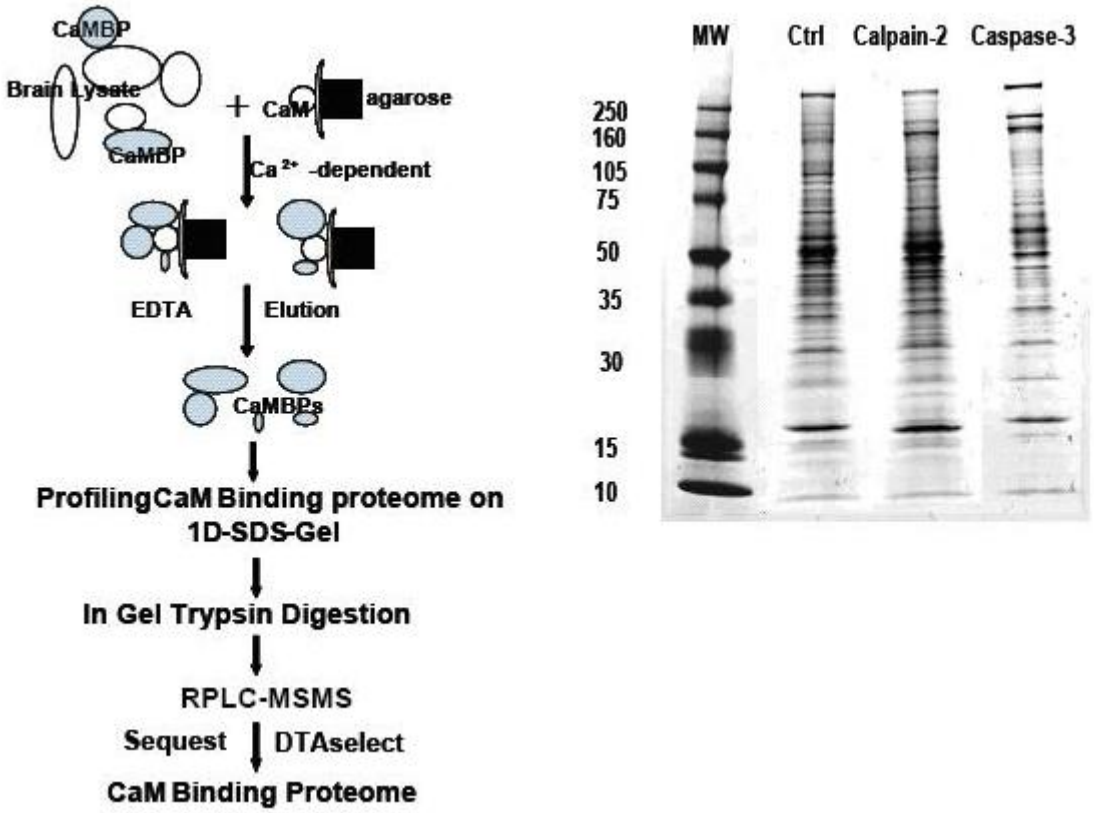

(A) (B)

Figure 2-1. Calmodulin binding proteome studies. A) Schematic diagram of novel calmodulin-affinity purification RPLC-MSMS methodology to study the rat brain calmodulin binding proteome. B) The intact and calpain-2/caspase-3 digested CaM binding proteome visualized by Coomassie blue staining. Each visible band was excised, in-gel digestion and analyzed by RPLC-MSMS. C) Naïve brain lysate was incubated with Sepharose-4B as a control. Sepharose-4B eluent was compared to the CaM-agarose eluent

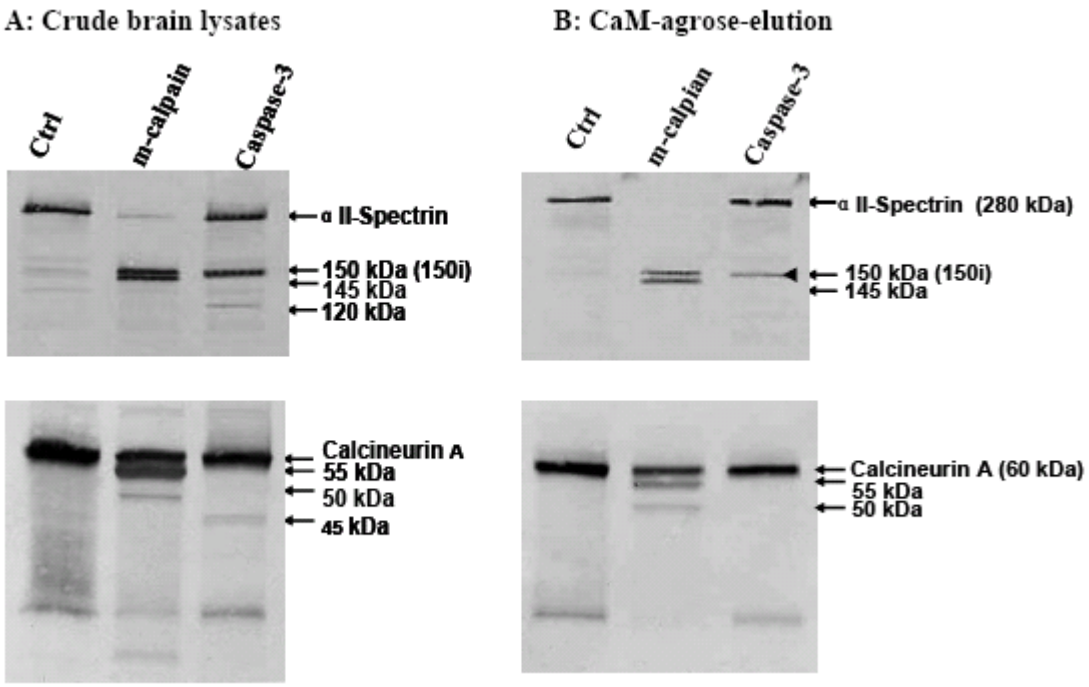

Figure 2-2. Confirmation of CaM-affinity capture for 2 known CaM binding proteins (αII-spectrin and calcineurin). A) and their breakdown products. (A) Control samples from naïve and degraded brain lysates before CaM-agarose purification. (B) CaMBPs from CaM-agarose-elution in the presence of 15 mM EDTA were separated by SDS-PAGE and analyzed by immunoblot for αII- spectrin and calcineurin A. Arrow head indicates αII-spectrin breakdown product 150i.

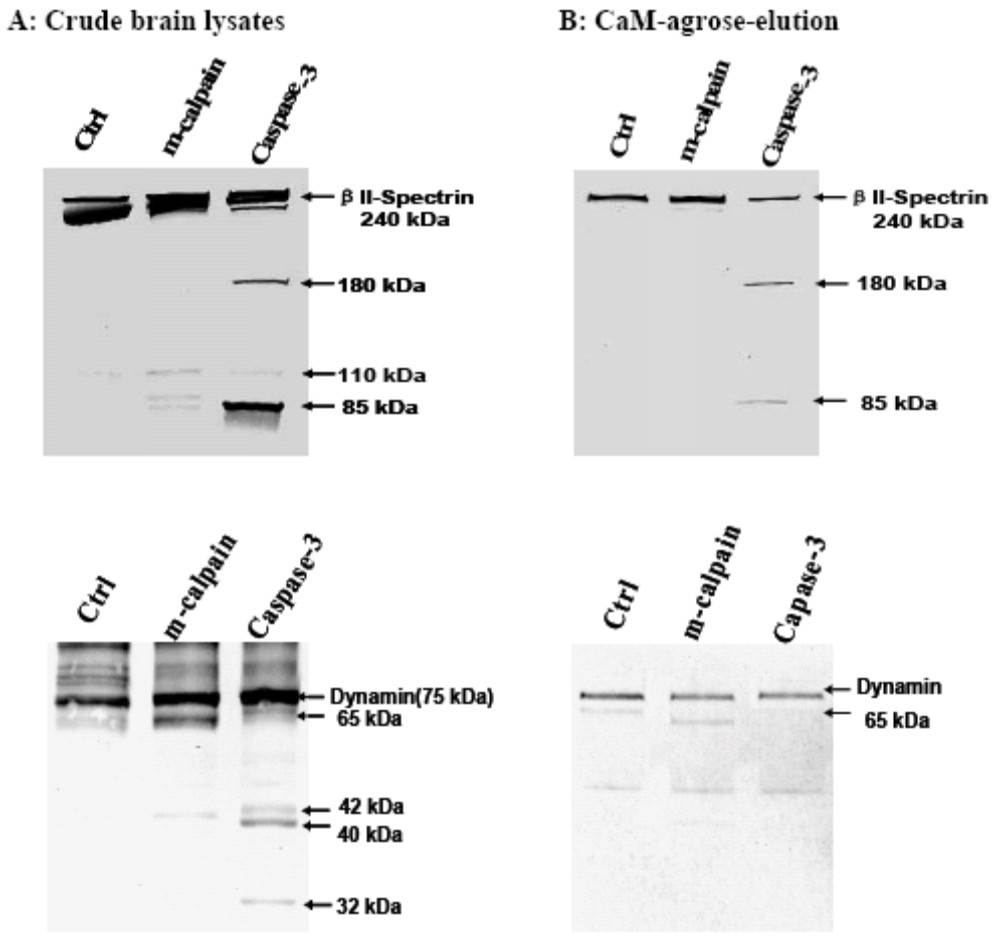

Figure 2-3. Immuoblot of dynamin, betaII-spectrin as examples of putative CaMBP proteins and their breakdown products. (A, C) dynamin and βII-spectrin were found degraded *in vitro* by calpain-2 and caspase-3 in rat cortex (crude brain lysate). (B, D) intact dynamin and βII-spectrin and their calpain-2/caspase-3 breakdown products were found to have putative calmodulin binding domains (CaM-agarose elution)

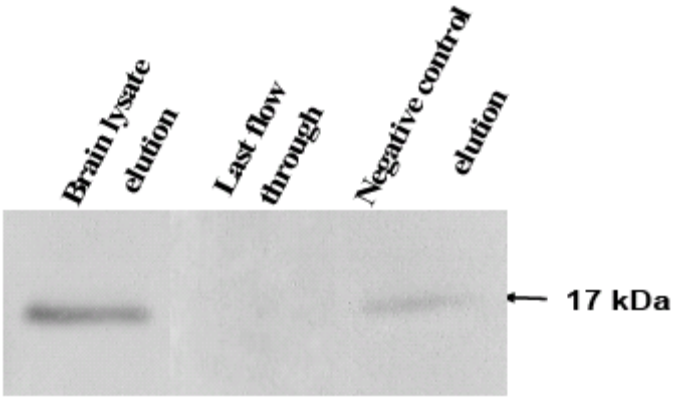

Figure 2-4. Quality control CaM-affinity purification immunoblot. Plain lysis buffer was incubated with CaM-agarose as a negative control, and compared with naïve brain lysate that was CaM-affinity purified.

CHAPTER 3
CALPAIN-MEDIATED COLLAPSIN RESPONSE MEDIATOR PROTEIN-1, 2 AND 4 PROTEOLYSIS FOLLOWING NEUROTOXIC AND TRAUMATIC BRAIN INJURY

Introduction

Collapsin response mediator proteins (CRMPs) are a family of cytosolic proteins that are highly expressed in the brain (Wang and Strittmatter, 1996). They have been shown to be involved in different aspects of axonal outgrowth, neuronal morphogenesis and cell death (Charrier et al., 2003). CRMP-1, 2 and 5 play an essential role in growth cone collapse in response to repelling guidance cues, such as semaphorin 3A or lysophosphatidic acid (Arimura et al., 2004; Bretin et al., 2005). CMRP-4 is highly expressed in post-mitotic neurons in the early embryonic brain and appears to be involved in brain development. Further, CRMP-4 is also found in brain regions that retain the capability of neurogenesis or axonal outgrowth and/or synaptic rearrangement during adulthood (Liu et al., 2003).

CRMP-2, the first CRMP discovered, is found concentrated in growing axons, dendrites, and the cytoplasm of differentiating neurons. Specifically, CRMP-2 is important in the determination of neuronal polarity and axonal elongation (Inagaki et al., 2001; Fukata et al., 2002a). Additionally, when CRMP-2 is highly phosphorylated it may play a role in neurodegeneration, as observed in neurofibrillary tangles in Alzheimer's diseased brains (Yoshida et al., 1998; Gu et al., 2000; Butterfield et al., 2003; Uchida et al., 2005). A growing body of evidence suggests that CRMP-2 may also participate in the pathophysiology of other neurological disorders. Decreased expression of CRMP-2 has been reported in fetal brains with Down's syndrome (Weitzdoerfer et al., 2001), patients with mesial temporal lobe epilepsy (Czech et al., 2004), focal rat brain ischemia (Chung et al., 2005) and in the frontal cortex of patients who suffer from psychiatric disorders (schizophrenia, bipolar, or major depression disorders) (Johnston-Wilson et al., 2000). In contrast, an increase in CRMP-2 has been observed

after chronic anti-depressant treatment in the rat hippocampus (Khawaja et al., 2004). CRMP-2 has also been reported to mediate axonal damage and neuronal death via a semaphorine-CRMP pathway (Barzilai et al., 2000; Gu and Ihara, 2000). Although the pathophysiology of neuronal injury varies among neurological disorders (e.g. TBI, stroke, epilepsy, and Alzheimer's disease), evidence points to CRMP-2's involvement in excitotoxic mechanisms of neuronal damage (Arundine and Tymianski, 2003).

Recently, CRMP-3 was found truncated in response to excitotoxicity in vitro and cerebral ischemia in vivo by activated calpain. Calpain-cleaved CRMP-3 was observed to translocate into the nucleus evoking neuronal cell death (Hou et al., 2006). We suspected that the other CRMPs might also have an association with excitotoxic neuronal cell injury, since the sequence homology is high among CRMP family members (50-75%) (Schweitzer et al., 2005). Therefore, in this study, we examined the integrity of CRMP-1, 2, 4 and 5 following in vitro neurotoxin treatments and in vivo traumatic brain injury (TBI) in rats.

Materials and Methods

Primary Cortical Neuron Culture

Primary cortical neurons from post-natal day one Sprague–Dawley rat brains were plated on poly-L-lysine coated culture plates (Erie Scientific, Portsmouth, NH, U.S.A.). In detail, cells were dissociated with trypsin and DNase I, resuspended in 10% plasma-derived horse serum (PDHS) in Dulbecco's modified Eagle's medium (DMEM), and plated on poly-L-lysine treated 35 mm (density: 3.0 × 106 cells per well) plates. Cells were allowed to grow in an atmosphere of 10% CO2 at 37°C for three days and then treated with 1 μM 4-amino-6-hydrazino-7-ß-D-ribofuranosyl-7H-pyrrolo (2,3-d)-pyrimidine-5-carboxamide (ARC) for two days. The ARC was removed and fresh 10% PDHS in DMEM was added after which the cells were grown for an additional 10–14 days. All animal studies conform to guidelines outlined in the Guide for the

Care and Use of Laboratory Animals from the National Institutes of Health and are approved by the University of Florida.

Neurotoxic Challenges and Pharmacologic Intervention

In addition to untreated controls, the following conditions were used: maitotoxin (MTX) (3 nM; WAKO Chemical USA Inc., Richmond, VA) as a calpain-dominated challenge for three hours; apoptotic inducer staurosporine (STS) (0.5 μM; Sigma, St. Louis, MO) for 24 hours; the Ca2+ chelator ethylene diamine tetra-acetic acid (EDTA) (5 mM; Sigma) for 24 hours as a caspase-dominated challenge (Waterhouse et al., 1996; Chiesa et al., 1998; Mizuno et al., 1998; McGinnis et al., 1999); and NMDA (200 μM; Sigma) for 3 to 24 hours as an excitotoxic challenge. For pharmacologic intervention, cultures were pretreated one hour before the MTX, EDTA or NMDA challenge with either the calpain inhibitor SJA6017 (Senju Pharmaceuticals, Kobe, Japan) (Fukiage et al., 1997; Kupina et al., 2001), or the pan-caspase inhibitor Z-VAD (OMe)-FMK (R&D, Minneapolis, MN).

Lactate Dehydrogenase Release Assay of Cell Death

A lactate dehydrogenase (LDH) release assay (CytoTox One Reagent, Promega, Madison, WI) was performed to assess cell death. Primary cortical neurons were seeded at 3.0 x 106 cells per well in 6-well plates, cultured for two weeks as described above, and then pretreated for one hour before introducing NMDA (200 μ M) with or without calpain inhibitor SJA6017 (30 μM) or caspase inhibitor Z-VAD (20 μM) in DMEM (Glucose 50 mM). Culture media were collected at three-hour intervals and assayed for LDH release by following the manufacture's instructions. Three replicates for each time point were assayed.

Cell Lysate Collection and Preparation

Primary neuronal cells were collected and lysed for 90 min at 4°C with a lysis buffer containing 50 mM Tris (pH 7.4), 5 mM EDTA, 1% (v/v) Triton X-100, 1 mM DTT, and a Mini-Complete protease inhibitor cocktail tablet (Roche Biochemicals, Indianapolis, IN). The lysates were centrifuged at 10,000 g for 5 minutes at 4ºC to remove insoluble debris, and then were snap-frozen and stored at -80°C until use.

Immunocytochemistry

Primary cortical neurons were fixed with 4% paraformaldehyde (PFA) in PBS for 10 minutes, washed with PBS and permeabilized with 0.1% triton X-100 in PBS for 5 minutes. Immunocytochemistry staining was performed following a one-hour blocking step in 10% goat serum at room temperature. The neurons were incubated overnight at 4ºC with monoclonal mouse-anti-CRMP-2 (C4G, IBL, Aramachi, Takasaki-shi, Gunma, Japan) at a dilution of 1:500. Alexa 488-conjugated goat-anti-mouse secondary antibody (Molecular Probes, Eugene, OR) was added at a dilution of 1:1000, followed by washing with PBS. The cells were mounted using medium containing 4, 6-diamidine-2-phenylindole (DAPI) (Vector Laboratories, Burlingame, CA). Fluorescence images were captured with a 20x objective on the Zeiss Axiovert 200 Fluorescence Microscope with a CCD camera, and merged using SPOT imaging software (Diagnostic Instruments, Sterling Heights, MI).

Rat TBI Model

A controlled cortical impact (CCI) device was used to model TBI (Dixon et al., 1991; Pike et al., 1998). Adult male (280-300 g) Sprague-Dawley rats (Harlan: Indianapolis, IN) were anesthetized with 4% isoflurane in a carrier gas of oxygen (4 min.) followed by maintenance anesthesia of 2.5% isoflurane in the same carrier gas. Core body temperature was monitored continuously by a rectal thermistor probe and was maintained at 37±1°C by placing an

adjustable temperature controlled heating pad beneath the rats. Animals were mounted in a stereotactic frame in a prone position and secured by ear and incisor bars. A midline cranial incision was made and a unilateral (ipsilateral) craniotomy (7 mm diameter) was performed adjacent to the central suture, midway between bregma and lambda. The dura mater was kept intact over the cortex. Brain trauma was produced by impacting the right cortex (ipsilateral cortex) with a 5 mm diameter aluminum impactor tip (housed in a pneumatic cylinder) at a velocity of 3.5 m/s with a 1.6 mm compression and 150 ms dwell time (compression duration). Sham-injured control animals underwent identical surgical procedures, but did not receive an impact injury. Appropriate pre- and post-injury management was maintained to ensure compliance with guidelines set forth by the University of Florida Institutional Animal Care and Use Committee and the National Institutes of Health guidelines detailed in the Guide for the Care and Use of Laboratory Animals.

Brain Tissue Collection and Preparation

At the 8 post-CCI time points (2, 6, 24 hours and 2, 3, 5, 7, 14 days), animals were anesthetized and sacrificed by decapitation. Brains were immediately removed, rinsed with ice cold PBS and halved. Two different brain regions (cortex and hippocampus) were removed from the right and left hemispheres, rinsed in ice cold PBS, snap-frozen in liquid nitrogen, and stored at –80°C until use. For Western blot analysis, the brain samples were pulverized to a fine powder with a small mortar and pastel set over dry ice. The pulverized brain tissue was then lysed for 90 minutes at 4ºC with lysis buffer containing 50 mM Tris-HCl (pH 7.4), 5 mM EDTA, 5 mM EGTA, 1 % Triton X-100, and 1 mM DTT (added fresh). Brain cortex lysates were then centrifuged at 10,000 g for 10 minutes at 4ºC. The supernatant was retained and a DC protein assay (Bio-Rad, Hercules, CA) was performed to determine protein concentration. Naïve cortex lysate was prepared as above.

In Vitro Calpain-2 and Caspase-3 Digestion of Brain Lysate

In vitro digestion of rat lysate (5 mg) was performed with the purified proteases human erythrocyte caplain-1, rat recombinant calpain-2 (Calbiochem, San Diego, CA) and recombinant human caspase-3 (Chemicon, Temecula, CA) in a buffer containing 100 mM Tris-HCl (pH 7.4) and 20 mM DTT. For the calpains 2 mM CaCl2 was also added to the lysate and then incubated at room temperature for 30 minutes. For caspase-3, samples were incubated at 37ºC for four hours. Protease reactions were stopped by the addition of either calpain inhibitor SJA6017 to a concentration of 30 μM (Senju Pharmaceuticals, Kobe, Japan) or the pan-caspase inhibitor Z-VAD to a concentration of 20 μM and a protease inhibitor cocktail solution.

SDS-PAGE Electrotransfer and Immunoblot Analysis

Protein concentrations of cell or tissue lysates were determined via Bio-Rad DC Protein Assay (Bio-Rad, Hercules, CA). Protein balanced samples were prepared for sodium dodecyl sulfate-polyacrylamide gel electrophoresis (SDS-PAGE) in a two-fold loading buffer containing 0.25 M Tris (pH 6.8), 0.2 M DTT, 8% SDS, 0.02% bromophenol blue, and 20% glycerol in distilled water. Samples were heated for 90 seconds at 90ºC, then centrifuged for 2 minutes. Samples were routinely resolved by SDS-PAGE on Tris-glycine gels for 2 hours at 130V. Following electrophoresis, separated proteins were laterally transferred to polyvinylidene fluoride (PVDF) membranes by the semi-dry method. Rat CRMP-5 antibody (targeting residues 369 –564, Chemicon, Temecula, CA), dialyzed with PBS using Slide-A-Lyzer MINI Dialysis Units, (Pierce, 3.5MWCO, 69550, Rockford, IL), was then biotinylated using EZ-link, sulfo-NHS-LC-LC-biotin following the manufacture's instructions. Membranes were incubated with either anti-CRMP-1, or -4 (targeting residues 499-511, Chemicon), biotinylated-anti-CRMP-5 antibodies or anti-CRMP-2 (C4G) (IBL) or a C-terminal anti-CRMP-2 antibody made at the University of Florida (raised against a synthetic peptides of residues 551-559), and then

developed with biotin (except for CRMP-5) and avidin-conjugated alkaline phosphatase and nitroblue tetrazolium and 5-bromo-4-chloro-3-indolyl phosphate. Quantitative evaluation of protein levels was performed via computer-assisted densitometric scanning (NIH ImageJ version 1.6 software) (Zhang et al., 2006b).

Statistical Analysis

All experiments described were performed at least in triplicate. Densitometric values represent the mean ± S.E.M. Statistical significance was determined using a one-way ANOVA test, with a significance level of $p < 0.01$.

Results

Proteolysis of CRMP-2 Following NMDA and MTX Induction in Primary Cortical Neurons

In our previous studies, the ionotrophic glutamate receptor agonists N-methyl-D-aspartate (NMDA) and Ca2+ channel opener maitotoxin (MTX) were used to model acute neuronal injury in primary cortical neurons (Wang et al., 1996; Nath et al., 2000a; Dutta et al., 2002). With this method, the integrity of CRMP-2 following neurotoxin induction was examined. In this study, a marked reduction in the intact CRMP-2 (66 kDa and 62 kDa) was noticed along with the appearance of a 55 kDa band after excitotoxic injury (200 μM NMDA) in rat primary cortical neuron cultures (Fig. 3-1A). Similar results were observed after MTX treatment (Fig. 3-1A). Two anti-phospho-CRMP-2 specific antibodies (3F4 and C-terminal Phospho-CRMP-2) were used to rule out the possibility that the 55 kDa band was due to de-phosphorylation. The altered profile of the 66 kDa and 62 kDa CRMP-2 was not observed after NMDA and MTX treatment (data not shown). It appears the 55 kDa fragment is a likely breakdown product of CRMP-2. Suspecting that a similar proteolytic event may occur with other members of the CRMP family, we examined the integrity of CRMP-1, 4 and 5 under identical conditions (Fig. 3-1B). Decrease

in intact CRMP-1 and CRMP-4 were observed, as well as the increase of a 58 kDa CRMP-4 BDP. However, CRMP-5 levels remained unchanged following neurotoxic treatment. We further explored CRMP-2 dynamics following NMDA (200 μM) induction using a time course analysis. The 55 kDa CRMP-2 BDP appeared by 3 hours and became prominent within 24 hours (Fig. 3-1C). Importantly, the densitometric analysis showed that the reduction of intact CRMP-2 was paralleled by the increased 55 kDa BDP over time (Fig. 3-1D).

Calpain Inhibition Blocked the Proteolysis of CRMP-2

To rule out non-specific CRMP-2 proteolysis during protein extraction, we looked for matching CRMP-2 degradation in cortical cultures pretreated with either the specific calpain inhibitor SJA6017 or the pan-caspase inhibitor Z-VAD prior to neurotoxin treatment. The results show that the formation of the 55 kDa fragment was blocked by SJA6017, but not by Z-VAD (Fig. 3-2). Therefore, calpain appears to be responsible for proteolysis of the intact 62 kDa CRMP-2 protein into the 55 kDa breakdown product (BDP). Interestingly, despite preservation of the intact 62 kDa CRMP-2 by SJA6017, the 66 kDa CRMP-2 levels declined as explained in the Discussion section (Fig. 3-2).

Next, the apoptosis inducer staurosporine (STS, 0.5 μM), a calpain and caspase activator challenge, and the calcium chelator EDTA (5 mM), a caspase-dominant challenge, were used on primary cortical neurons (McGinnis et al., 1999; Nath et al., 2000b; Wang, 2000a). The results show that the intact 62 kDa CRMP-2 was rapidly degraded into the 55 kDa BDP upon STS treatment, but not upon the caspase-activated EDTA treatment. STS-mediated generation of the 55 kDa CRMP-2 BDP was also effectively blocked by SJA6017 while Z-VAD offered no protection (Fig. 3-2, upper panel). The production of the 55 kDa CRMP-2 BDP strikingly paralleled the production of the 150 and 145 kDa αII-spectrin breakdown products, which were

monitored as markers for calpain activity in NMDA and STS treatment (Nath et al., 2000b) (Fig. 3-2, lower panel).

Calpain Inhibition Attenuates NMDA Induced Neuronal Cell Injury and Neurite Damage and Prevents CRMP-2 Redistribution Following NMDA Treatment

LDH release assays were performed to investigate the role of calpain and caspase activation of NMDA induced neuronal cell injury and CRMP-2 degradation. The release of LDH, normally present in the cytoplasm of neurons, into the cell culture media can be used as a measure of dying cells (Riss and Moravec, 2004). The results showed that NMDA treatment induced CRMP-2 proteolysis in a time-dependent manner (Figs. 3-1C, D). NMDA treatment induced significant neuron death after 3 hours,, peaking at 24 hours, which is consistent with the production of the 55 kDa CRMP-2 BDP. Moreover, the calpain inhibitor (SJA6017) provided significant protection for about 6 hours, while the caspase inhibitor (Z-VAD) offered no protection from NMDA treatment (Fig. 3-3A).

We next examined the levels of CRMP-2 following 6 hours of NMDA treatment with and without the calpain and caspase inhibitors to further explore the association of CRMP-2 with NMDA induced neurite damage (Fig. 3-3B). Figure 3-3B shows neurons with healthy, long neurites (control, upper panel). Under higher magnification, CRMP-2 is more prominently observed in neurites than in the cell body (arrow, control, lower panel). After six hours of NMDA challenge, neurites significantly retracted (NMDA, upper panel). Under higher magnification, CRMP-2 redistribution to the cell body (arrow, lower panel) was observed. In contrast, neurites in most neurons appeared to be preserved with the calpain inhibitor pretreatment (N+SJA, upper panel). The redistribution of CRMP-2 to the cell body was prevented (N+SJA, lower panel). On the other hand, Z-VAD offered no protection and was unable to prevent CRMP-2 redistribution (N+VAD, Fig 3-3B). Taken together, these data further

suggest that proteolysis of CRMP-2 may contribute to calpain-mediated neurite degeneration and cell death after NMDA challenge.

CRMP-2 Integrity After TBI

Next, we examined whether the CRMPs were proteolyzed in vivo following traumatic brain injury. We examined the contralateral and ipsilateral cortex and hippocampus tissues harvested 48 hours post-TBI since this is when calpain activation is most significant (Pike et al., 1998). A notable decrease in intact CRMP-1, 2 and 4 were observed in the ipsilateral cortex and hippocampus while at the same time the 55 kDa CRMP-2 BDP and 58 kDa CRMP-4 BDP were found to increase (Fig. 3-4A). However, there was no significant change in the intact CRMP-5 after TBI. Examination of the contralateral tissue showed no noticeable decrease in the intact CRMPs and no production of BDPs. Tissue examination also verified that CRMP degradation only appeared following TBI, and not in sham (craniotomy only) animals (Fig. 3-4B). Together, these results suggest that CRMP-2 proteolysis occurred following TBI in our animal model and it is probable that the same occurred with CRMP-1 and CRMP-4.

Post-CCI cortical and hippocampal rat brain tissue was used to assess the temporal dynamics of CRMP-2 following TBI. The amount of intact 62 kDa CRMP-2 decreased from 6 hours to 3 days with a corresponding increase of the 55 kDa BDP (Fig. 3-5). The change was significant for both the intact and the 55 kDa CRMP-2 BDP at 24 and 48 hours for the ipsilateral cortex (Figs. 3-5A, B). Significant changes in the hippocampus were, also, observed between 24 hours and 3 days (Figs. 3-5C, D). Interestingly, the level of intact and cleaved CRMP-2 seems to return to control levels by day 5 after TBI both in the cortex and hippocampus based upon Western blot analyses. Spectrin proteolysis was used to correlate CRMP-2 degradation with calpain and caspase activity (Fig. 3-5). We found that the formation of the SBDP150/145 calpain product paralleled the formation of the 55 kDa CRMP-2 BDP demonstrating that CRMP-2

proteolysis correlated well with the calpain activity over time after TBI. CRMP-2 fragmentation patterns are similar between TBI and brain lysate digestion.

We previously identified calpain involvement in CRMP-2 proteolysis following TBI, just as we had in cell culture after neurotoxin treatment (Figs. 3-1 and 3-3). To further test this as shown in Fig. 3-6, in vitro calpain-2 treatment of naïve brain lysate resulted in the same fragmentation pattern observed after TBI in vivo. The 62 kDa and 66 kDa intact CRMP-2 bands disappeared. Pretreatment of the naïve lysate with the calpain inhibitor (SJA6017) blocked formation of the 55 kDa CRMP-2 BDP and preserved the 62 kDa CRMP-2 bands. In contrast caspase-3 treatment did not produce the 55 kDa BDP, although the 66 kDa intact CRMP-2 band did fade even after applying the caspase inhibitor Z-VAD (see Discussion). We confirmed the complete inhibition of calpain and caspase activity by parallel monitoring of calpain and caspase associated □II-spectrin degradation (Fig. 3-6). We then verified, using Phoretix 1D-gel imaging software, that the molecular weight of the calpain mediated CRMP-2 proteolytic product matched that of the 55 kDa BDP observed post-TBI. Therefore, this suggests that calpain was involved in the cleavage of the 55 kDa CRMP-2 BDP, while caspase-3 was not. Taken together, these data suggest that CRMP-2 proteolysis is due to calpain activation following TBI.

Discussion

In this work we demonstrated for the first time the degradation of CRMP-1, 2, and 4 after acute neuronal injuries by in vivo TBI and in vitro glutamate excitotoxicity (Figs. 3-1 and 3-4) and that the proteolytic enzyme involved was calpain-2. As the current manuscript was under review, Bretin and colleagues also reported that CRMP-1, 2, 4 are proteolyzed by NMDA treatment in cortical neurons (Bretin et al., 2006). Chung et al. (Chung et al., 2005) also recently reported proteolysis of CRMP-2 in focal ischemic rat brain, however, the responsible protease was not identified. In agreement with those findings, our study demonstrates that CRMP-1, 2 and

4 are proteolyzed after neurotoxic injury and TBI. Moreover, we have confirmed that the decrease of intact CRMP-2 occurs with a concurrent increase of a 55 kDa CRMP-2 fragment due to calpain-2 proteolysis, in vitro and in vivo, and that the calpain-mediated CRMP-2 proteolysis appears to be associated with neuronal cell injury and neurite damage.

The data demonstrate CRMP-2 was proteolyzed into a 55 kDa BDP under two calpain-dominant challenges (MTX and NMDA) and with the apoptotic inducer STS in cortical neurons (Figs. 3-1A and 3-2). Interestingly, the decrease of the intact CRMP-2 and increase of CRMP-2 55 kDa BDP following NMDA treatment (Figs. 3-1C, D) noticeably paralleled NMDA induced neuronal cell death over time (Fig. 3-3A). In addition to attenuating cell death induced by NMDA treatment for about 6 hours (Fig. 3-3A), pretreatment of primary cortical culture with the cell-permeable calpain-inhibitor SJA6017, and not the caspase inhibitor Z-VAD, prevented the formation of the 55 kDa CRMP-2 BDP, preserving the intact 62 kDa CRMP-2 protein (Fig. 3-2). Furthermore, calpain inhibition prevented redistribution of CRMP-2 from neurites to the cell body, and preserved the architecture of neurites (Fig. 3-3B). These data suggested CRMP-2 proteolysis may be linked to calpain mediated neurite degeneration. Any further relationship between calpain-mediated truncation of CRMPs and neurite damage that may exist has yet to be determined. In addition to LDH assay, other methods such as 3-(4, 5-dimethylthiazol-2-yl)2,5-diphenyl-tetrazolium bromide (MTT) assay, TUNEL assay , Hoechst and propidium iodide (PI) staining may be used to concordantly assess and confirm neuronal cell injury or death. Consistent with other therapeutic approaches using other calpain inhibitors in vitro (Adamec et al., 1998; Araujo et al., 2004; Lopez-Picon et al., 2006) and in vivo (Markgraf et al., 1998; Kupina et al., 2001), preincubating with the calpain inhibitor (SJA6017) did not effectively protect neurons from excitoxic injury after 12 hours. This suggests, in addition to the calpains,

other pathways, such as calmodulin (Pohorecki et al., 1990), phospholipase , protein kinase A and so forth (Adamec et al., 1998; Llansola et al., 2000), may also contribute to the excitotoxic neuron death. It was also noticed that proteolysis of CRMP-2 was only exhibited in the injured brain regions where there was the formation of the CRMP-2 55 kDa BDP which appears to correlate with calpain activation over time following TBI (Figs. 3-4 and 3-5). The apparent rebound of CRMP-2 by day 5 after TBI may be due to necrotic tissue loss thereby leaving the remaining more intact and/or recovering tissue for sampling (Sahuquillo et al., 2001; Liu et al., 2006). Finally, treatment of naïve brain lysate with purified and activated calpain-2, but not caspase-3, resulted in the 55 kDa cleavage product identical to that observed after TBI (Fig. 3-6). Taken together, these data demonstrate that calpain mediated CRMP-2 proteolysis occurred and that it appears to be linked to neuronal cell injury and neurite damage after excitotoxic injury.

Interestingly, both calpain and caspase treatment resulted in the disappearance of the 66 kDa CRMP-2 band, whereas only calpain treatment induced formation of the 55 kDa CRMP-2 BDP (Fig. 3-6). Previous studies showed that the 66 kDa CRMP-2 is a phosphorylated form of CRMP-2 while the 62 kDa form was unphosphorylated. Work by Gu et al. demonstrated that following incubation of brain lysate with EGTA, the 66 kDa CRMP-2 was dephosphorylated to the 62 kDa CRMP-2 form (Gu et al., 2000). Our caspase digestion buffer contained EGTA and EDTA the disappearance of the 66 kDa CRMP-2 band following caspase-3 treatment was probably due to dephosphorylation, but this was not preventable by the pan-caspase inhibitor (Fig. 3-6).

CRMP-2 has two domains, a dihydropyrimidinase (DHPase) domain (residues 64-413), and a C2 domain (residues 486-533), illustrated in Fig. 3-7A following SBASE analysis (http://hydra.icgeb.trieste.it/sbase). Even though CRMP-2 has high sequence similarity to

DHPase, it has no known enzyme activity (hydrotoinase or dihydrophrimidinase) (Wang and Strittmatter, 1997). Important phosphorylation sites are located within the C2 domain (Gu et al., 2000; Cole et al., 2004; Yoshimura et al., 2005). Sequence analyses also suggest there are multiple putative calpain cleavage sites within the C-terminus region of CRMP-2 (Fig. 7) with the preferred residues Leu, Thr and Val in position P2, and Lys, Tyr and Arg in position P1 (Tompa et al., 2004). Along with the C4G antibody, whose epitope is found in the large boxed sequence in Fig. 3-7 (residue 486 to 528) (Gu et al., 2000), another C terminal antibody was used (epitope residue 551-559) to narrow down the possible cleavage sites involved in forming the 55 kDa CRMP-2 BDP (Arimura et al., 2005) (Fig. 7). With the latter antibody, the intact CRMP-2 was shown to decrease following excitotoxic treatment and TBI, but the 55kDa BDP was not observed (data not shown). This suggests that the cleavage site is located between residue 486 and 551. There are also two PEST regions (residues 496-511 and 535-552) located on the C-terminal end of CRMP-2 (residues 486-559) as identified by PESTfind analysis (http://www.at.embnet.org/embnet/ tools/bio/PESTfind). PEST regions tend to depict regions of rapid degradation in proteins. A previous correlation between the presence of a PEST site and calpain susceptibility provided evidence that calpain was the enzyme that degraded PEST region-containing proteins (Wang et al., 1989a). The first PEST region RGLYDGPVCEVSVTPK (residues 496-511) contains preferred calpain cleavage site Leu498-Tyr499-Asp. Furthermore, cleavage at residue 499 will result in a truncated CRMP-2 with a theoretical mass 54.7 kDa matching the experimental mass of 55 kDa for the CRMP-2 BDP. The other putative calpain-cleavage sites highlighted in Fig. 3-7 may also meet the criteria of the calpain digestion, but their theoretical fragment mass would be larger than the observed 55 kDa BDP. Thus, after analyzing the sequence and based upon our experimental data, we propose that the most likely calpain

cleavage is between residues LY499↓D500 in CRMP-2 (Fig. 3-7). N-terminal microsequencing is underway to confirm the exact cleavage site.

The biological significance of calpain-mediated CRMP-2 proteolysis is not yet clear. An important function of CRMP-2 is its involvement in axonal regeneration or elongation. Over-expression of CRMP-2 induces the formation of multiple axons and primary axon elongation. Truncation of 24 amino acids or more from the C-terminus abolishes the ability of CRMP-2 to promote multiple axons (Inagaki et al., 2001). Studies have shown that phosphorylation at Thr514 or Thr509, Ser518 and Ser522 of CRMP-2 by GSK3β and Cdk5 regulates axon outgrowth (Fig. 3-7) (Gu et al., 2000; Cole et al., 2004; Yoshimura et al., 2005). Additionally, recent studies showed that Rho-kinase (ROCK) phosphorylates CRMP-2 at Thr-555 (Arimura et al., 2000) inhibiting the ability of CRMP-2 to bind tubulin and Numb, thereby inducing growth cone collapse (Nishimura et al., 2003; Arimura et al., 2005). Furthermore, CRMP-2 binds to the light chain of kinesin-1 (KLC) at region 440-572, regulating soluble tubulin transport to the distal part of the growing axon (Kimura et al., 2005). Based on these previous studies, it is apparent that calpain truncated CRMP-2, between LY499↓D500, would remove all the phosphorylation sites and disrupt CRMP-2 interactions with KLC or ROCK, thereby deregulating axonogenesis and neuronal polarity (Fig. 3-7). In addition, calpain-cleaved CRMP-2 may also be involved in neuronal cell damage. A recent study showed that over-expression of the CRMP-2 ΔC413 mutant, which lacks the C-terminal residues 413–572, led to CRMP-2 leakage into the nuclear compartment, inducing apoptosis (Tahimic et al., 2006).

In addition to CRMP-2, this report moreover showed that CRMP-1 and CRMP-4 were also degraded after excitotoxic neuronal injury and TBI (Figs. 1, 4). These results are consistent with the recent study on calpain-mediated truncation of CRMP-4 in response to NMDA and

H2O2 toxicity (Kowara et al., 2005). Until now, there has been no report on the degradation of CRMP-1 following neurotoxic injury or TBI. However, it was reported that truncation of 183 amino acids from the C-terminus caused a significant decrease of neurite formation and extension following NT3 treatment of DRG neurons (Quach et al., 2004). CRMP-3 was, also, recently shown to be vulnerable to calpain proteolysis, and that calpain-cleaved CRMP-3 translocated into the nucleus, inducing neuronal cell death (Hou et al., 2006). Although all CRMPs high sequence homology, CRMP-1 and 4 exhibit the closest identity with each other (68-75%), while CRMP-5 has the relatively least identity with the rest of family members (49-50%). As a result, CRMP-5 may best be classified as a member of a different subfamily (Fukada et al., 2000). It is therefore not surprising that CRMP-5 levels were unaffected after TBI. Further studies are being conducted to elucidate the pathophysiological significance of the cleavage of CRMP-2 in the nervous system. This may give us new insights into the mechanism of axon or neuron damage in the central nerve system, such as may occur after spinal cord injury, TBI and stroke.

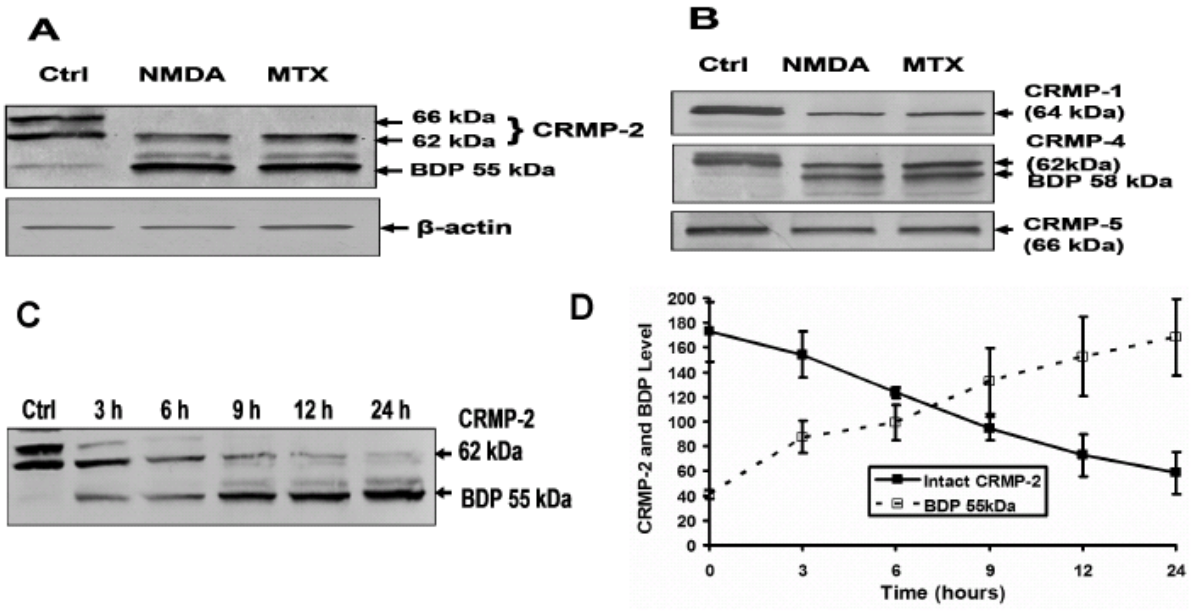

Figure 3-1. Effect of neurotoxins on the integrity of CRMP-1, 2, 4 and 5 in primary cortical neurons. NMDA (200 μM) was used as an excitotoxic challenge and maitotoxin (MTX) (3 nM) was used as calpain-dominant neurotoxin challenge in rat primary cortical neuron culture. (A) Primary cortical neurons were exposed to NMDA (200 μM) for 6 hours or maitotoxin (3 nM) for 3 hours. Total protein extracts were separated by SDS-PAGE and immunoblotted with anti-CRMP-2 (C4G) and β-actin. A marked reduction of intact CRMP-2 was noticed along with the appearance of a 55 kDa band following NMDA and MTX treatment. (B) The same samples were probed with CRMP-1, CRMP-4 and CRMP-5 antibodies. Decrease of CRMP-1 and CRMP-4 with a 58 kDa and 62 kDa doublet was observed following NMDA and MTX treatment; however, no remarkable change in CRMP-5 was detected. Results shown are representatives of three experiments. (C) NMDA induced CRMP-2 proteolysis in a time-dependent manner. Primary cortical neurons were subjected NMDA treatment (200 μM) at different time points. A representative Western blot probed with CRMP-2 is shown. (D) Densitometric analysis of intact CRMP-2 and BDP 55 kDa following NMDA treatment at the various time points. Values were means ± S.E.M. n = 3.

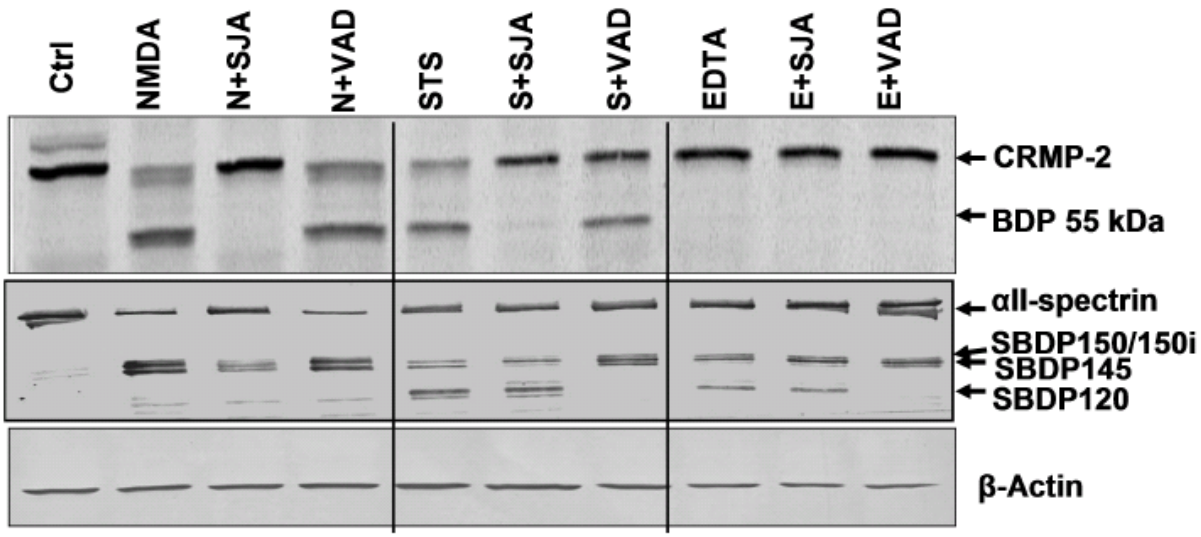

Figure 3-2. Effects of calpain and caspase-3 inhibition on neurotoxin induced proteolysis of CRMP-2 in primary cortical neurons. Primary cortical neurons were pretreated with calpain inhibitor (30 μM SJA6017) and caspase-3 inhibitor (20 μM Z-VAD) for one hour, and then exposed to NMDA (200 μM) for 6 hours, apoptosis inducer STS (0.5 μM) and EDTA (5 mM) for 24 hours. Total proteins in the cell lysates were resolved by SDS-PAGE and immunoblotted with anti-CRMP-2 (C4G) (top). Paralleled αII-spectrin (middle) proteolysis was monitored as a marker of calpain and caspase activity. β-actin (bottom) was used as a loading control. Calpain inhibition preserved the intact CRMP-2, while caspase inhibition did not. Results shown are representatives of three experiments.

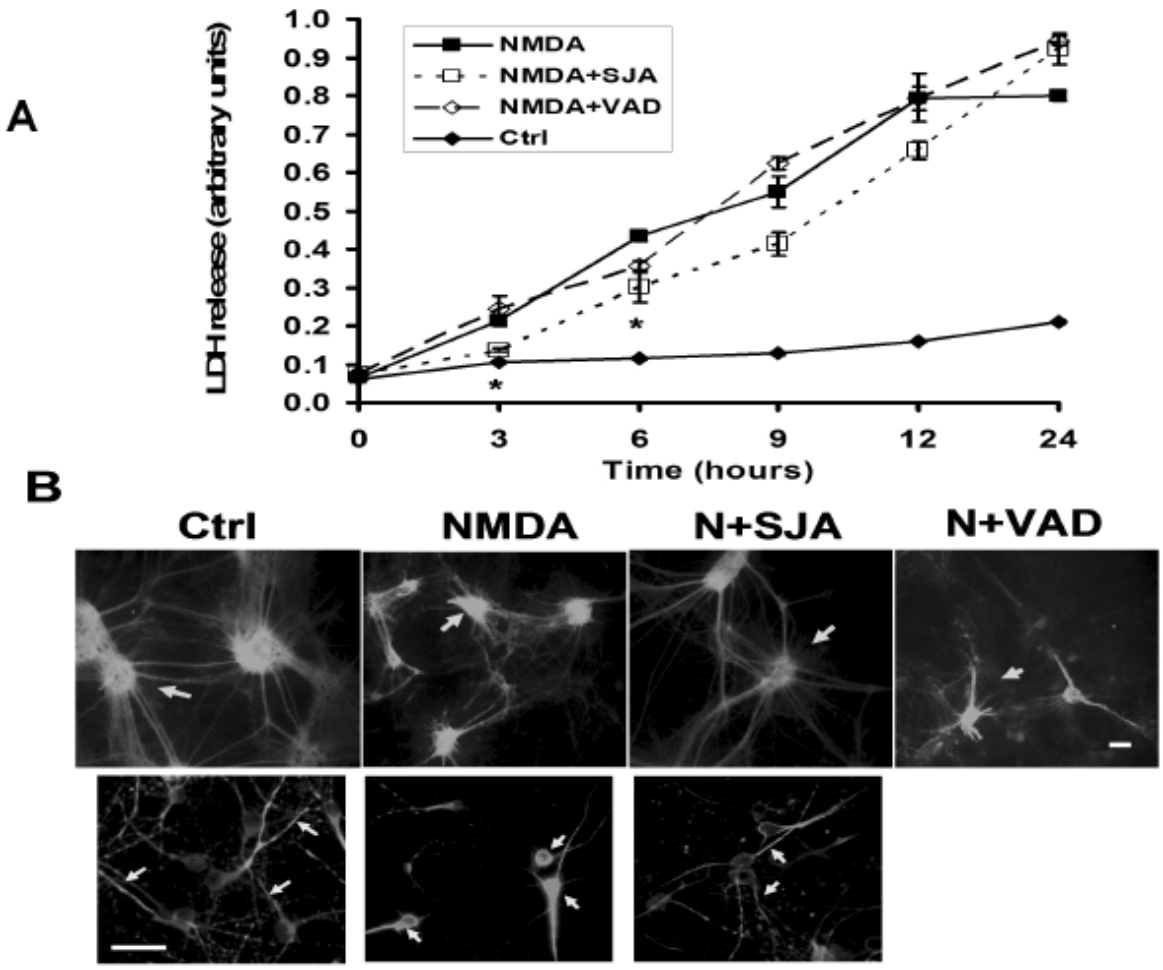

Figure 3-3. Calpain inhibition attenuated NMDA induced neuronal death and prevented CRMP-2 redistribution and neurite damage following NMDA induction. Primary cortical neurons were pretreated with calpain (30 μM SJA6017) and caspase-3 (20 μM Z-VAD) inhibitors for one hour or with serum free medium alone, and then exposed to NMDA (200 μM) for various hours. (A) Time course of LDH release following NMDA treatment. Values represent means ± S.E.M. n = 4. A difference was considered to be statistically significant when the *P* value was less than 0.01 (**P* < 0.01). (B) Immunocytochmistry of CRMP-2 (C4G) following NMDA treatment (6 hours) with or without calpain and caspase inhibition. Arrows indicate the accumulation of CRMP-2. Scale bar=50μm

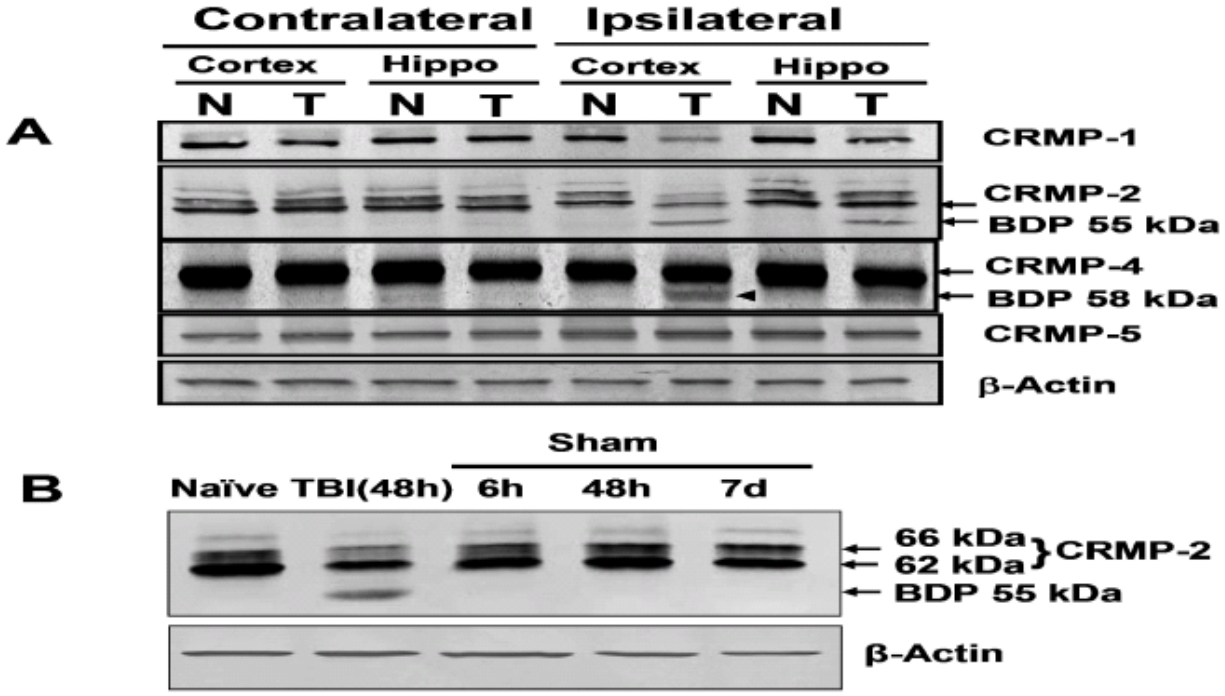

Figure 3-4. Immunoblot analysis of integrity of CRMPs in rat brain after TBI. (A) The integrity of CRMPs (1, 2, 4 and 5) in Naïve (N) and 48 hours post-TBI (T) contralateral, ipsilateral cortex and hippocampus (Hippo). Those tissue lysates were subjected to immunoblotting and probed with CRMPs and β-actin antibodies. (B) Naïve, shams and 48 hours post-TBI ipsilateral cortex lysates were subjected to immunoblotting and probed with CRMP-2 (C4G) (top), and β-actin (bottom) antibodies. A marked decrease in the 62 kDa CRMP-2 was noticed with the appearance of a 55 kDa CRMP-2 band. β-actin was used as a loading control. Results shown are representative of three experiments.

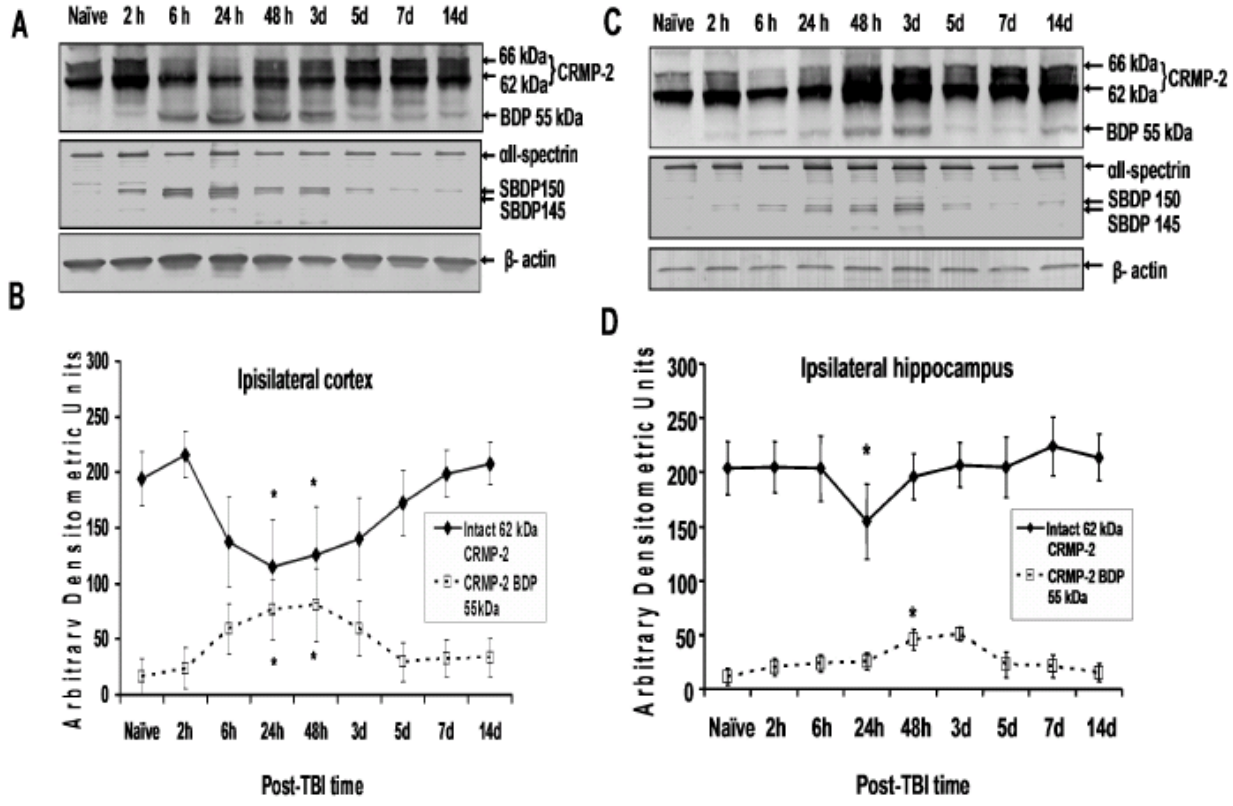

Figure 3-5. Time-course of CRMP-2 proteolysis in rat cortex and hippocampus following TBI. The brain samples were collected from naïve, ipsilateral cortex (A) and ipsilateral hippocampus (B) with TBI (1.6mm impact) 2 hours to 14 days after injury (2h, 6h, 24h, 48h, 3d, 5d, 7d, 14d). Brain lysates were subjected to immunoblotting and probed with CRMP-2 (C4G) (top), αII-spectrin (middle) or β-actin (bottom) antibodies. Quantitative analysis of the intact CRMP-2 (62 kDa) and 55 kDa breakdown product of CRMP-2 in ipsilateral cortex (C) and ipsilateral hippocampus (D) were done by densitometry analysis. Values represent means ± S.E.M. n = 3. *p<0.01 compared with naïve.

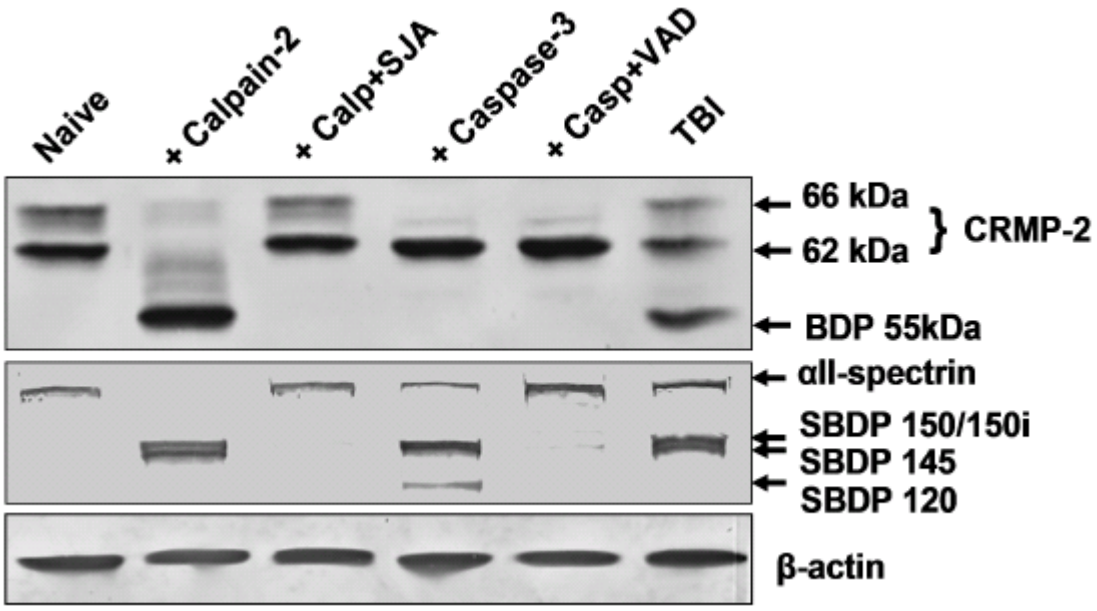

Figure 3-6. Fragmentation patterns of CRMP-2 after TBI matches calpain-2 digested CRMP-2 *in vitro*. Naïve cortex lysate incubated with calpain-2 or caspase-3 in the presence or absence of calpain inhibitor (30 μM SJA6017) or caspase inhibitor (20 μM Z-VAD). The same amount of TBI ipsilateral cortex 48 hours after injury and *in vitro* calpain-2 or caspase-3 treated naïve cortex lysate were analyzed by immunoblots and probed with CRMP-2 (C4G) antibody. Calpain treatment resulted in CRMP-2 proteolysis to 55 kDa BDP that matched fragmentation pattern after TBI *in vivo*. Fragmentation was blocked by calpain inhibitor, but not by caspase-3 inhibitors. αII-spectrin proteolysis was monitored in parallel as a marker of calpain and caspase activity.

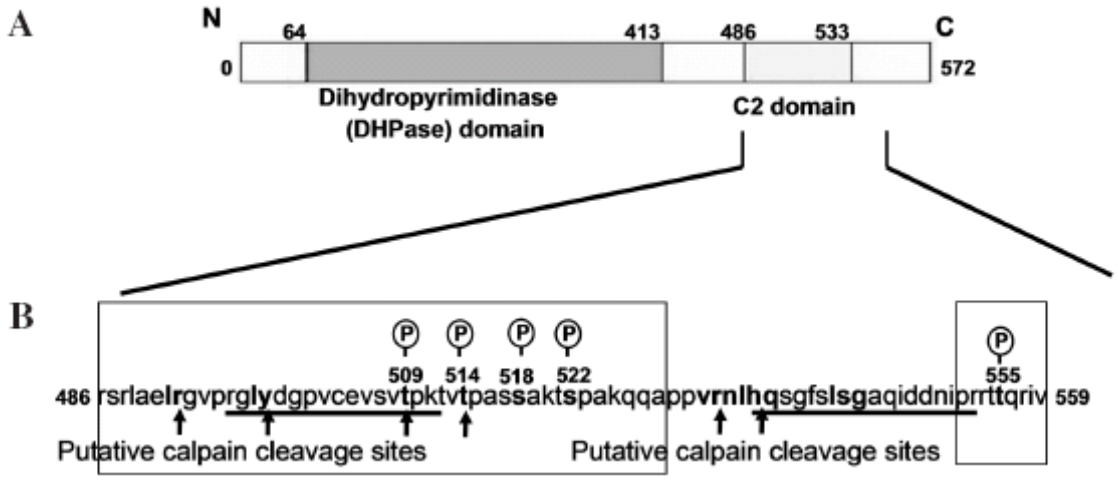

Figure 3-7. Sequence analysis of CRMP-2 and potential calpain cleavage sites assignment. Part A shows the domain architecture of CRMP-2 predicted by SBASE SVM (http://hydra.icgeb.trieste.it/sbase). Part B depicts a schematic representation of residues 486-559 toward the C-terminus of CRMP-2. PEST regions are underlined, while portions used for generating CRMP-2 antibody (C4G) (residue 486-528) and CRMP-2 (c-terminal) antibody (residue 551-559) are boxed. Arrows beyond the box indicate putative calpain cleavage sites.

CHAPTER 4
CRMP-2 IS A NEW CALMODULIN-BINDING PROTEIN

Introduction

CRMP-2, also known as CRMP62, TOAD-64 (turned on after division 64 kDa), Ulip-2 (Unc-33-like phosphoprotein), and DRP2 (dihydropyrimidinase-related phosphoprotein), is one of at least five isoforms (CRMP1-5) in the CRMP family (Wang and Strittmatter, 1996, 1997). CRMP-2 is a developmentally regulated protein and highly expressed in the nervous system. Two splice isoforms of CRMP-2, namely CRMP-2A and 2B, have been identified. CRMP-2A, the long N-terminal isoform is specifically associated with axons of the corpus callosum, the bundles of the striatum, and the mossy fibers of the hippocampus, whereas CRMP-2B is ubiquitously distributed throughout the cell body, in the axons or dendrites (Yuasa-Kawada et al., 2003; Bretin et al., 2005). A growing body of evidence has demonstrated the importance of CRMP-2 and its phosphorylated isoforms in various neuronal functions. CRMP-2 was first identified as an intracellular protein involved in the transduction cascade initiated by semaphorin 3A (Sema 3A). Sema 3A induced neuronal growth-cone collapse which is mediated via the sequential cdk5 and GSK3β phosphorylation of CRMP-2 on Ser522 and Thr509 (Goshima et al., 1995; Ito et al., 2000). In contrast, when lysophosphatidic acid (LPA) induces growth-cone collapse, CRMP-2 is phosphorylated on Thr-555 by Rho-kinase, downstream of RhoA(Arimura et al., 2000). CRMP-2 has also been reported to regulate neuronal polarity and axon elongation. Overexpression of CRMP-2 induces the formation of multiple axons and elongation of the primary axon in hippocampal neurons(Fukata et al., 2002b; Fukata et al., 2002a).

A number of studies have demonstrated that CRMP-2 interacts with a number of proteins, including tubulin, kinesin, Numb, Sra/WAVE and phospholipase D2, to exhibit its functions (Fukata et al., 2002b; Lee et al., 2002; Nishimura et al., 2003; Kawano et al., 2005; Kimura et al.,

2005). CRMP-2 binds to tubulin heterdimers to promote microtubule assembly and regulates polarized Numb-mediated endocytosis of neuronal adhesion molecule L1 in the growth cone. CRMP-2 interacts with Sra-1/WAVE1, a regulator of the actin cytoskeleton, which in turn transports the protein complex to distal part of the growing axon in a kinesin-1 dependent manner and thereby regulating axon outgrowth and formation (Kawano et al., 2005). In addition, our recent CaM affinity capture coupled with reversed-phase liquid chromatography tandem mass spectrometry (RPLC-MSMS) profiling CaM-binding proteome suggests that CRMP-2 may also interact with CaM (Zhang et al., 2006a).

Upon elevation of intracellular Ca^{2+}, CaM undergoes conformational change and binds to different CaM binding proteins, resulting in multiple cellular functions. Many of the downstream targets that CaM binds to and activates are unable to bind calcium themselves; therefore they need CaM as a calcium sensor and signal transducer. With the extraordinarily high concentration of CaM (10 to 100 μM) found in neuron of the central nervous system, CaM binding to enzymes, cytoskeletal proteins, receptors and ion channels, regulates neuronal/axonal response upon stimulus(Wang et al., 1989b; O'Day, 2003; Xia and Storm, 2005). For example, CaM binding to calcinuerin and neurofilament (NF) regulates the proteolysis and phosphorylation of NF, which in turn modifies axonal injury after calcium influx (Johnson et al., 1991). Similarly, CRMP-2 has been reported undergoes proteolysis or phosphorylation modification under different neurobiological disorders, such as epilepsy, stroke, traumatic brain injury and Alzheimer's disease (Gu et al., 2000; Cole et al., 2004; Czech et al., 2004; Chung et al., 2005; Jiang et al., 2007; Zhang et al., 2007). One common feature of these diseases is the alteration of intracellular Ca^{2+} homeostasis which appears to play a central role in the mechanisms of the neuronal/axonal

injury that underlies these diseases (Sola et al., 1999; Smith et al., 2003; Czogalla and Sikorski, 2005; Johnston, 2005).

Given the relevance of the Ca^{2+}/CaM signaling system in the processing of Ca^{2+} signals and taking into account the importance of CRMP-2 in the axon formation and elongation, it is possible to hypothesize that CaM binding may influence the proteolysis or phosphorylation of CRMP-2, thereby modulating CRMP-2 involved cytoskeleton reorganization upon Ca^{2+} influx. To address these questions, we validated the interaction between CaM and CRMP-2 and then further investigated the possible roles that CaM may play in post translational modification of CRMP-2 and CRMP-2 related actin reorganization in response to neuronal or axonal injury.

Materials and Methods

Animal Surgery, Brain Tissue Collection and Protein Extraction

Animal surgery procedures were conducted in compliance with the Animal Welfare Act and the University of Florida Institutional Animal Care and Use Committee and the National Institutes of Health guidelines detailed in the Guide for the Care and use of Laboratory Animals. Adult male (280-300 g) Sprague-Dawley rats (Harlan: Indianapolis, IN) were anesthetized with 4% isoflurane in a carrier gas of oxygen (4 min.) followed by maintenance anesthesia of 2.5% isoflurane in the same carrier gas. Cortex, hippocampus brain tissues were removed, rinsed with ice-cold PBS, and halved. Brain tissues were rapidly dissected, rinsed in ice-cold PBS, snap-frozen in liquid nitrogen, and stored at -80ºC until used. The brain samples were pulverized with a small mortar and pestle set over dry ice to a fine powder. The pulverized brain tissue powder was then lysed for 90 minutes at 4ºC with 50 mM Tris-HCl (pH 7.4), 5 mM EDTA, 5 mM EGTA, 1% Triton X-100, and 1 mM DTT (added fresh). Brain cortex lysates were then centrifuged at 100,000 g for 10 minutes at 4ºC. The supernatant was retained and a DC protein assay (Bio-Rad; Hercules, CA) was performed to determine protein concentration.

Cell Culture

Primary cortical neurons from first post-natal day Sprague–Dawley rat brains were plated on poly-L-lysine coated culture plates (Erie Scientific, Portsmouth, NH, U.S.A.). In detail, cells were dissociated with trypsin and DNase I, re-suspended in 10% plasma-derived horse serum (PDHS) in Dulbecco's modified Eagle's medium (DMEM), and plated on poly-L-lysine treated 35 mm (density: 3.0×10^6 cells per well) plates. Cells were allowed to grow in an atmosphere of 10% CO_2 at 37°C for three days and then treated with 1 μM 4-amino-6-hydrazino-7-ß-D-ribofuranosyl-7H-pyrrolo (2,3-d)-pyrimidine-5-carboxamide (ARC) for two days. The ARC was removed and fresh 10% PDHS was added in DMEM, after which the cells were grown for an additional 10–14 days. All animal studies conform to guidelines outlined in the Guide for the Care and Use of Laboratory Animals from the National Institutes of Health, and are approved by the University of Florida. PC-12 cells were maintained at 37ºC in Dulbeco's modified Eagle's medium (DMEM) supplied with 10% fetal bovine serum (FBS), 5% heat-inactivated horse serum, 100 μg/ml of streptomycin, 100 U/ml of penicillin and 1% Fungizone (Gibco, Rockville, MD) in a humidified 5% CO_2 incubator. HEK293 cells were maintained in DMEM supplied with 10% FBS, 100 μg/ml of streptomycin, 100 U/ml of penicillin and 1% Fungizone.

Plamid Constructs and Transfection

The cDNA of human CRMP-2 was amplified by PCR from IMAGE clone#3870039 using the primers 5'-ACCAGAATTCAGATGTCTTATCAGGGGAAGAAAA-3' and 5'-ATCAGTCGACCTAGCCCAGGCTGGTGATGTT-3'. Primers were purchased from IDT (Coralvile,IA). The PCR products were subcloned into pAcGFPV1 (Clontech). HEK293 cells were transfected with GFP-hCRMP-2 or GFP vector using Lipofectamine 2000 (Invitrogen, Carlsbad, CA, USA). Stable GFP-hCRMP-2 expression HEK293 cells were selected by using media containing 400 ug/ml G418.

Cell Lysate Collection and Preparation

Primary neuronal cells or PC-12 cells were collected and lysed for 90 minutes at 4^{o}C with a lysis buffer containing 50 mM Tris (pH 7.4), 5 mM EDTA, 1% (v/v) Triton X-100, 1 mM DTT, with or without a Mini-Complete protease inhibitor cocktail tablet (Roche Biochemicals, Indianapolis, IN). The lysates were centrifuged at 100,000 g for 5 minutes at 4ºC to remove insoluble debris, and then were snap-frozen and stored at -80^{o}C until use.

Preparation of Biotinylated Calmodulin

Purifed bovine or human brain CaM (Calbiochem, San Diego, CA) was dialyzed with PBS using Slide-A-Lyzer MINI Dialysis Units (Pierce, 3.5MWCO, 69550, Rockford, IL). The concentration of dialyzed CaM was determined by a DC protein assay (Bio-Rad; Hercules, CA). Then CaM was biotinylated using EZ-linkTM, sulfo-NHS-LC-LC-biotin (Pierce, Rockford, IL cat.21338) by following the manual.

Calmodulin Overlay Experiments

The purified CRMP-2 and calcineurin protein was subjected to SDS-PAGE. Proteins were separated by SDS-PAGE electrophoresis and elctrtrotransferred to a PVDF membrane. The PVDF membranes were incubated with 5% (W/V) bovine serum albumin in TBST medium containing either 1mM $CaCl_2$ or 1mM EDTA to prevent nonspecific binding. Biotinlyated bovine or human brain CaM was next added (20 ng/ml) and incubated for another hour. The membrane were then extensively washed in TBST in the presence of 1mM $CaCl_2$ or EDTA and further incubated for 1 h with avidin-conjugated alkaline phosphatase in the presence or absence of Ca^{2+}. Again, Blots were extensively washed, and the positive CaMBP bands were detected using nitroblue tetrazolium and 5-bromo-4chloro-3-indolyl phosphate.

In Vitro Calpain-2 and Caspase-3 Digestion of Cell Lysate or Purified hCRMP-2

PC-12 cell lysate was prepared as above. *In vitro* digestion of rat lysate (5 mg) or purified CRMP2 protein with the purified proteases, human erythrocyte caplain-1, rat recombinant calpain-2 (Calbiochem, San Diego, CA) and recombinant human caspase-3 (Chemicon, Temecula, CA) were performed in a buffer containing 100 mM Tris-HCl (pH 7.4) and 20 mM DTT. For calpain-1 or -2, 1 mM $CaCl_2$ or 5 mM $CaCl_2$ was added respectively with or without 50μM W7, and then incubated at room temperature for 30 minutes. For caspase-3, samples were incubated at 37ºC for 4 hours. The protease reaction was stopped by the addition of 30 μM calpain inhibitor (SJA 1670) or 100 μM pan-caspase inhibitor (Z-D-DCB) (Calbiochem, San Diego, CA) and a protease inhibitor cocktail solution (Roche Biochemicals, Indianapolis, IN).

Neurotoxin Challenges and Pharmacologic Intervention

In addition to untreated controls, the following conditions were used: maitotoxin (MTX, 3 nM; WAKO Chemical, USA Inc) as a calpain-dominated challenge for 3 hour, NMDA (200 μM; Sigma) for 8-24 hours as an excitotoxin challenge. For pharmacologic intervention, cultures will be pretreated 1 hour before MTX and NMDA challenge with calpain, caspase-3 inhibitors.

Immunocytochemistry

Primary cortical neurons were fixed with 4% paraformaldehyde (PFA) in PBS for 10 minutes, washed with PBS and permeabilized with 0.1% triton X-100 in PBS for 5 minutes. CRMP-2 staining was performed following a one-hour blocking step in 10% goat serum at room temperature. Then the neurons were incubated overnight at 4ºC with monoclonal mouse-anti-CRMP-2 (C4G, IBL, Aramachi, Takasaki-shi, Gunma, Japan) at a dilution of 1:500. Alexa 488-conjugated goat-anti-mouse secondary antibody (Molecular Probes, Eugene, OR) was added at a dilution of 1:1000, followed by washing with PBS. F-actin was fluorescently labeled with 5 units/ml Rhodamine-conjugated phalloidin for 30 minutes at room temperature. The cells were

mounted using medium containing 4, 6-diamidine-2-phenylindole (DAPI) (Vector Laboratories, Burlingame, CA). Fluorescence images were captured with a 20x objective on the Zeiss Axiovert 200 Fluorescence Microscope with a CCD camera, and combined using SPOT imaging software (Diagnostic Instruments, Sterling Heights, MI).

Results

Identification of CRMP-2 as a Calmodulin-binding Protein

In our previous studies, we developed a novel CaM-affinity capture coupled with RPLC-MSMS method to enrich and identify proteins or peptides which have CaM binding domains. Data suggested that CRMP-2 might be a putative novel CaM binding protein. CaM binding proteome of rat brain was visualized by Coomassie blue staining (Figure 4-1). CRMP-2 was marked by red rectangle red rectangle. Our mass spectrometry results showed a total of 4 peptides of CRMP-2 that were sequenced by RPLC-MSMS. By comparing those peptides to full length of rat CRMP-2, they corresponded to 238-255, 258-270,440-452, and 470-481 residues, respectively (underline in **Figure 4-1**). The overall sequence coverage of CRMP-2 identified by RPLC-MSMS is 9.6%. Moreover, the peptides 258-270 and 470-481 were found twice. Two putative calmodulin binding domains (CaMBDs) were found by searching CaMBD search program (http://calcium.uhnres.utoronto.ca/ctdb/ctdb/sequence.html)(Yap et al., 2000). One is located between residues 258-275, and the other between residues 475-493. Helical wheel projections of these two putative CaMBDs were shown in **Figure 4-1B**. CaMBD-2 shows an appropriate amphiphilic helix distribution with predominantly hydrophobic face on one side and a positively charged on the other side.

Studies have shown that CRMP-2 can be phosphorylated at Thr514 or Thr509, Ser518 and Ser522 by GSK3β and Cdk5 or Thr-555 by Rho-kinase (Gu et al., 2000; Cole et al., 2004; Yoshimura et al., 2005). Additionally, recent studies have shown that the most likely calpain

cleavage site is between residues 486 and 551. The schematic diagram of CRMP-2 (**Figure 4-1C**) indicates that CaMBD-2 overlaps the c-terminal C2 domain (residues 486-533) which is very close to the calpain cleavage sites and multiple phosphorylation sites. Thus, it suggests that CaM binding might affect proteolysis and/or phosphorylation of CRMP-2.

To confirm that CRMP-2 can be purified by CaM-agarose, we probed the CaM-affinity EDTA elution and Ca^{2+} flow through with CRMP-2 antibody. **Figure 4-2A** shows that CMRP-2 can be pulled down with Ca^{2+} chelator EDTA. However, the detection of CRMP-2 in the CaM-agarose pull down elution with EDTA does not exclude the possibility that CRMP-2 could be isolated because of indirect association with other CaM-binding proteins. Hence, we performed biotinylated CaM overlay experiment with purified GST-CRMP-2 protein in either the presence or absence of Ca^{2+}. In the presence of Ca^{2+}, a strong band was observed and was accompanied by positive control calcineurin after development with streptavidian-peroxidase. However, in the absent of Ca^{2+}, no band observed (**Figure 4-2B**). Therefore, it suggests that CaM directly and specifically binds to CRMP-2 in a Ca^{2+}-dependent manner.

CaM Regulates CRMP-2 Mediated Filopodia Formation

The dynamics of filopodia is necessary for understanding the growth cone formation, thus we investigated the signaling pathways that might involved in cytoskeleton change. Here, rhodamine-phalloidin F-actin immunostaining and monoclonal CRMP-2 immunostaining (green) were performed with DAPI counterstaining (blue) of the nuclear DNA. Consistent with results from other groups, CRMP-2 was found to colocalize with F-actin in PC-12 cells (**Figure 4-3**). Interestingly, before treatment with the CaM antagonist W7, CMRP-2 overlapped with F-actin, and found to uniform lie in parallel with each other within the cell body. After thirty minutes of treatment, organized F-actin structure was lost as was the cytoskeleton structure (**Figure 4-3B**). We were intrigued by the fact that CRMP-2 might interact with F-actin and that CaM was

involved in F-actin dynamics. Therefore, we suspecte that CaM may modulate CRMP-2 mediated filopodia formation. It is well known that over-expressing CRMP-2 in hippocampal neurons induces axon formation (Inagaki et al., 2001). Our data suggests that the over-expression of GFP-CRMP-2 in HEK293 cell induces longer filopodia formation when compared to overexpression of GFP alone. After thirty minutes CaM antagonist W7 challenge, the long filopodia retracted. In contrast, there is no change in the GFP-over-expressing HEK293 cells' filopodia. The change of filopodia is even more dramatic in cells treated with LiCl, a GSK3β inhibitor. GSK3β is implicated in axonal/neurite formation and by inhibiting GSK3β leads to dephosphorylation of CRMP-2, thus resulting in axon elongation. When CRMP-2 over-expressing HEK293 cells are incubated with LiCl for one hour, more cells were found bearing longer filopodia. Application of W7 dramatically reduces the numbers of cells with longer filopodia (**Figure 4-4**). Taken together, our data suggests that CaM may be involved in CRMP-2 mediated filopodia formation.

CaM Binding Retards Calpain-mediated CRMP-2 Proteolysis in Vitro

Our previous studies suggested that calpain mediates CRMP-2 proteolysis (Zhang et al., 2007). In order to assess the effect of CaM binding on CRMP-2 proteolysis by calpain *in vitro*, we compared the cleavage efficiency of the CRMP-2 with or without CaM by calpain in vitro. Purified GST-CRMP-2 protein was treated with calpain-1 or calpain-2 in either the presence or absence of CaM.

The addition of CaM to GST-CRMP-2 significantly retards CRMP-2 proteolysis as noted by the decrease in the level of the CRMP-2 breakdown product (CRMP-2 BDP) in both calpain-1 and calpain-2 treated panels (**Figure 4-5A**). To further examine the effect of endogenous CaM binding on proteolysis of CRMP-2, we treated PC-12 cell lysates with calpain-1 or calpain-2 after applying CaM antagonist W7. The W7 treated panel exhibits higher level of CRMP-2 BDP

compared to the untreated cells **(Figure 4-5B)**. Thus, this indicates that CaM inhibition enhances CRMP-2 proteolysis by calpain-1 or 2 *in vitro*. Altogether, these results demonstrate that CaM binding prevent calpain-mediated CRMP-2 proteolysis *in vitro*.

Post-translation Modification of CRMP-2 Following Ca^{2+}/CaM Binding *ex vivo*

As we have shown that CaM binding retards calpain-mediated CRMP-2 proteolysis *in vitro. N*ext we examined whether Ca^{2+}/CaM modulates CRMP-2 proteolysis ex *vivo*. CRMP-2 BDP was used as a marker for calpain activity after MTX treatment. We treated GFP and GFP-CRMP-2 over-expressing HEK293 cells with different concentrations of W7, from 5 μM to 100 μM, for thirty minutes. Only one band was visible on the immunoblot representing the intact CRMP-2 meaning that the protein was not cleaved into the 55 kDa CRMP-2 BDP (Data not shown). However, when we added W7 to the Ca^{2+} channel opener MTX treated cells, a robust 55 kDa was clearly visible more than MTX treated only cells (**Figure 4-5C**). This indicates that the application of W7 application acts synergistically with MTX to cleave CRMP-2. Therefore, CaM may be involved in the regulation of CRMP-2 proteolysis after intracellular Ca^{2+} elevation ex *vivo*.

It has been reported that two isoforms of CRMP-2 are expressed in primary cortical neurons. Consistent with Bretin's mice data (Bretin et al., 2005), our previous and ongoing studies suggest that CRMP-2A and 2B isoforms do exist in rat primary cortical neurons and human SY5Y cell line as well, but not in cerebellar granule neurons and PC-12 cells (Data not shown). Since the antibody C4G can recognize both phosphorylated and non-phosphorylated CRMP-2 isoforms in primary cortical neurons and since phosphorylation dynamics of CRMP-2 is more important in determinating axon elongation, we examined the effect of CaM binding on CRMP-2 phosphorylation dynamics. We found that elevated intracellular Ca^{2+} concentration due to MTX or NMDA treatment causes CRMP-2 to undergo dephosphorylation and proteolysis

even in the presence of high level of endogenous CaM. Although the calpain inhibitor SJA6017 can protect CRMP-2 from proteolysis, it can not prevent CRMP-2 dephosphorylation in the pathology state (**Figure** 4-6).

Next, we studied the effect of CaM on phosphorylation dynamics of CRMP-2. A GSK3β inhibitor, LiCl, was used to induce CRMP-2 dephosphorylation in primary cortical neurons. As shown in **Figure 4-7A**, there was a significant decrease of the phosphor-CRMP-2B after LiCl treatment, while no change was observed following co-treatment with W7. Quite remarkably, the protein phosphotase PP1 and PP2A inhibitor okadaic acid significantly enhanced the level of phosphor-form of both CRMP-2A and B, while PP2B inhibitor cybermethrin did not **(Figure 4-7C)**. CaM antagonist W7 produces no dramatic effect on the phosphorylation dynamics of CRMP-2 induced by okadaic acid and cybermethrin. Thus, this indicates that phosphotases PP1 and PP2A were responsible for the dephosphorylation of CRMP-2 *in vivo* and CaM does not affect the phosphorylation dynamics.

Discussion

The RPLC-MSMS based CaM-pull down proteomic data and the CaM overlay experiment with recombinant CRMP-2 indicated that CRMP-2 binds to CaM in a Ca^{2+}-dependent manner **(Figure 4-1)**. There are two CaMBDs for CRMP-2 as predicated by the CaMBD predication program. CaMBD2 (residues 475-493) has been shown to form a helix in a recent crystal structure study of CRMP-2 (Stenmark et al., 2007). Furthermore, this region is rich in basic and hydrophobic residues. The helical wheel projection of CaMBD2 shows this region could form an appropriate amphiphilic helix with characteristic hydrophobic amino acid residues, namely Phe475, Ala 484, Leu488 and Leu491, on one face and on the other face with a cluster of charged amino acid residues. This is in agreement with the results of previous studies showing that CaM binding sequence potentially forms a basic amphiphilic a-helix (Wang, 2000b). Thus,

CaM more likely binds to CRMP-2 through the CaMBD2. A further deletion mutation study or synthesized peptides of CRMP-2 is needed to further identify the exact CaMBD.

Next, the schematic diagram of CRMP-2 indicates that CaMBD-2 overlaps its c-terminal C2 domain which is very close to the calpain cleavage sites and the multiple phosphorylation sites. Thus, this suggests that CaM binding might affect proteolysis or phosphorylation of CRMP-2. In agreement with previous studies, different phosphor-forms of CRMP-2 exist in cortical neurons in its physiological state (Figure **4-6 to 4-7**). Intact CRMP-2 may bind to F-actin constitutively to stabilize axon and growth cone structure. However, under pathological condition with the elevated cytosolic Ca^{2+}, CRMP-2 may be undergoing different post-translational modification in response to the stimulus with or without CaM regulation (**Figure 4-5 to 4-8**). Initially, activation of calpains and protein phosphatases PP1 and PP2A followed by Ca^{2+} influx results in CaM independent CRMP-2 dephosphorylation (**Figure 4-5 to 4-7**). With the sustained Ca^{2+} influx and calpains activation, CRMP-2 undergoes CaM independent proteolysis, which may contribute to growth cone collapse and axonal injury (**Figure 4-6**). Concurrently, neurons need to activate profound intrinsic repair signaling pathways to prevent axonal/neuronal injury and boost axonal recovery in response to Ca^{2+} influx. In our proposed model, with the Ca^{2+} influx, CaM undergoes conformational change, binds to CRMP-2 and protects CRMP-2 from calpain-mediated cleavage (**Figure 4-5**). In addition, CaM binding to CRMP-2 appears to play a role in F-actin bundling (**Figure 4-3**), thereby maintaining a stable structure or enhancing axonal regeneration (**Figure 4-4**).

It is well established that actual extension of axons occurs at its distal tip, the growth cone. The peripheral and central domains of the growth cone are composed of by two F-actin based structures, filopodia and lamellipodia. These actin-rich structures contribute to the force

necessary for the forward extension of the growth cone. It is therefore important to understand of how actin dynamics are regulated and this could provide key insights into how axonal regeneration may be promoted (Dent and Gertler, 2003). There have not been any systematic studies of the interaction CRMP-2 with actin, however, there is some evidence suggesting that CRMP-2 may interact with F-actin (Gungabissoon and Bamburg, 2003; Arimura et al., 2005; Kawano et al., 2005). CRMP-2 merged with actin at growth cone. Our data suggests that CRMP-2 co-localizes with F-actin and that the CaM antagonist W7 disputes this F-actin based structure in PC-12 cells. Furthermore, W7 reduced the number and length of filopodia induced by CRMP-2 over-expression. Therefore, our study of CaM affects on filopodia formation may have application on the growth cone dynamics of axon regeneration. Further studies of how CaM modulates CRMP-2 involvement in the actin dynamics in the growth cone of neuron are needed.

In our studies, this is the first time that CaM was found to protect CRMP-2 from the cleavage by calpain. We interpret this effect as a consequence of direct CaM binding to the corresponding domain of the CRMP-2 CaMBD2 (residues 475-493), which is adjacent to the cleavage site. As a Ca^{2+} sensor, CaM binds to numerous different CaMBPs resulting in the specific intracellular response to the Ca^{2+} signal. For example, CaM binding to the plasma membrane Ca^{2+} ATPase, GAP-43 leads to inhibition of calpain-mediated cleavage at several sites located within the CaMBD. In other cases, CaM either accelerated the proteolysis (brain spectrin, calponin and calcineurin) by calpain or changed the pattern of cleavage (myosin, myosin light chain kinase) (Kosaki et al., 1983; Harris et al., 1989; Tsunekawa et al., 1989; Croall et al., 1996). Furthermore, studies have demonstrated that CaM binding to N-Methyl-D-Aspartate Receptor (NMDA) subunit 1 facilitates calcium-dependent inactivation of NMDA Receptor, which in turn serves as a negative feedback to fine tune Ca2+ influx after injury(Zhang

et al., 1998; van Dalen et al., 2003). Previous studies have also showen that the proteolysis of CRMP-2 also occurs in ischemia and TBI (Zhang et al., 2007). Similarly, it is possible that CaM binding to CRMP-2 also in turn prevents its degradation and stabilizes growth cone structure in a negative feedback loop to fine tune the response to injury *in vivo*.

Phosphorylation of CRMP-2 is important in determining the function of CRMP-2 in axon elongation and growth cone collapse (Arimura et al., 2005; Yoshimura et al., 2005). Gu et al suggested that PP1 and PP2A may be involved in the dephosphorylation of CRMP-2 *in vitro* (Gu et al., 2000). A recent proteomic study also found that CRMP-2 is phosphorlated upon okadaic acid treatment (Hill et al., 2006). Given the fact that NMDA or MTX induction induces CRMP-2 dephosphorylation and PP1 and PP2 inhibitor enhanced CRMP-2 when co-treated with calpain inhibitor, we proposed PP1 and PP2A were responsible for CRMP-2 dephosphorylation both in vitro and in vivo. Different from other cytoskeletonal proteins, such as NF, tau and MAP2 (Yamamoto et al., 1985; Hashimoto et al., 2000),our data shows that CaM binding does not influence the phosphorylation of CRMP-2. This may be due to high concentration of endogenous CaM or highly dynamics of temporal and spatial phosphorylation modifications that occur *in vivo*.

In summary, our study indicates that CRMP-2 is a new calmodulin binding protein and CaM binding may retard proteolysis of CRMP-2, but not phosphorylation, thereby modulating CRMP-2 involvement with F-actin dynamics in response to certain pathological states. Understanding the signaling mechanisms of Ca^{2+}/CaM and CRMP-2 in cytoskeleton dynamics may open up the possibility of developing novel strategies to alleviate cell death and promote axon regeneration *in vivo*.

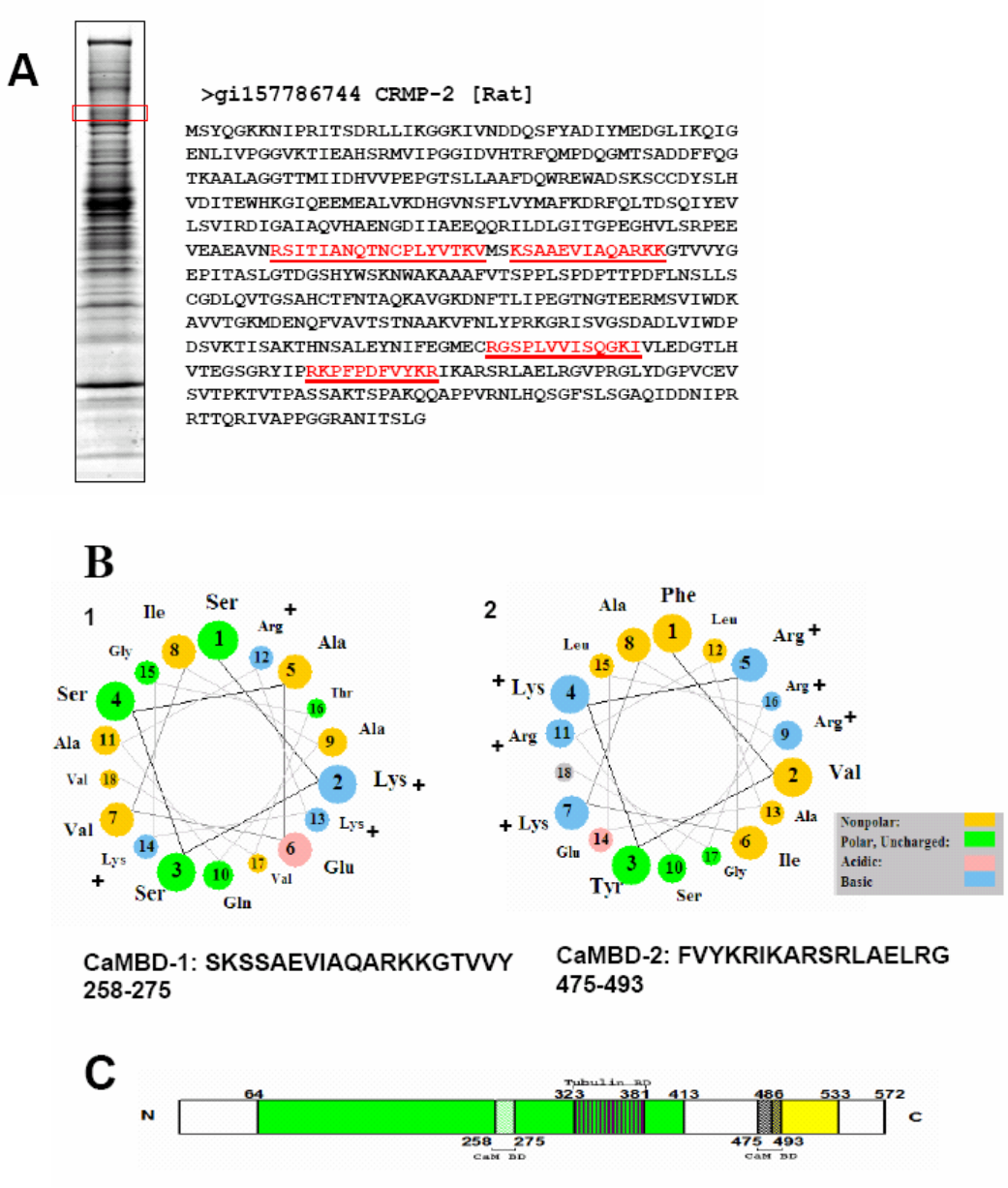

Figure 4-1. CRMP-2 is a putative CaM binding protein. (A) Identification of CRMP-2 as a putative calmodulin binding protein by mass spectrometry. The rat brain CaM binding proteome was visualized by Coomassie blue staining. Each visible band was excised, in-gel digested and analyzed by RPLC-MSMS. CRMP-2 band was boxed as indicated. (B) Putative CaM-binding domains (CaMBD) of CRMP-2 analysis. Putative CaMBDs were searched by using CaMBD search program (http://calcium.uhnres.utoronto.ca/ctdb/ctdb/sequence.html). Helical wheel projections of amino acids from putative CaMBDs were present as B1 and B2 (http://cti.itc.virginia.edu/~cmg/Demo/wheel/wheelApp.html). Positively charged residues are marked with a plus sign, whereas hydrophobic residues are marked as yellow. (C) Schematic diagram of localization of potential CaMBDs in CRMP-2.

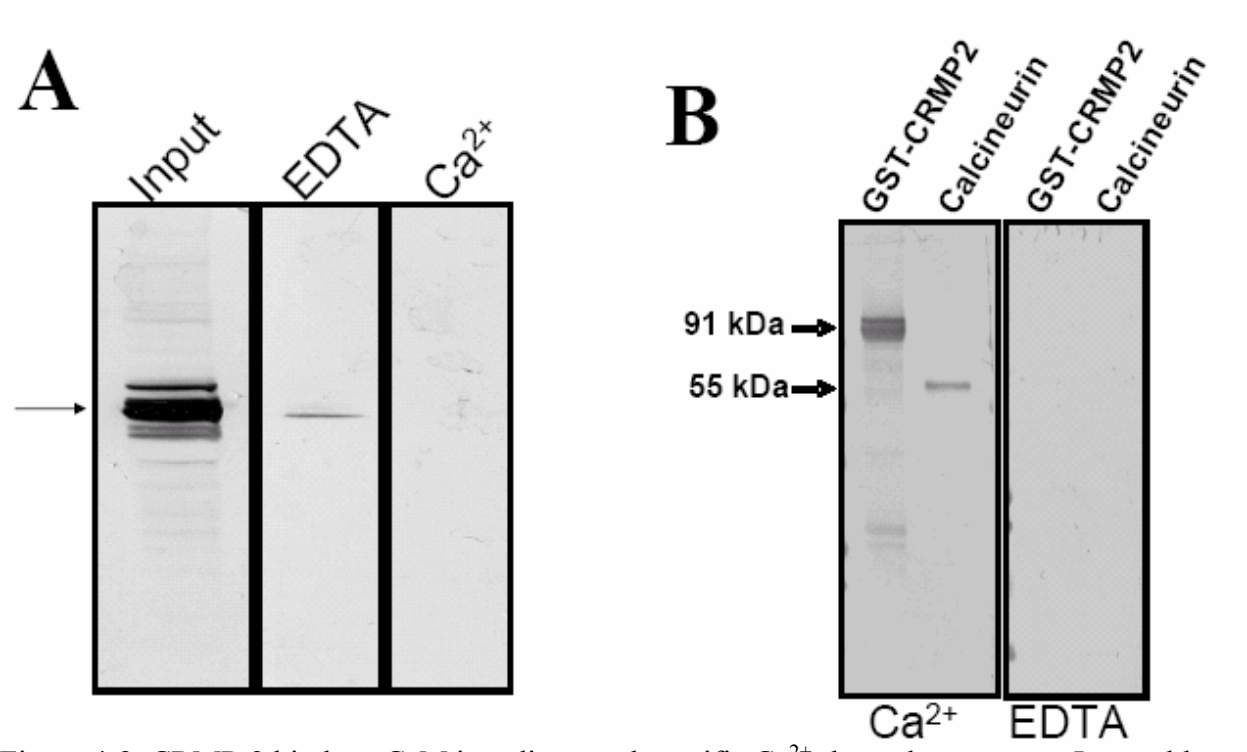

Figure 4-2. CRMP-2 binds to CaM in a direct and specific Ca^{2+}-dependent manner. Immuoblot of CRMP-2 as a putative CaMBP. Lysate before CaM-agarose purification, CaM-agarose-elution and flow through were separated by SDS-PAGE and analyzed by immunoblot for CRMP-2. (B) The purified GST-CRMP-2 and bovine brain calcineurin were subjected to overlay with 20 ng/ml biotinylated bovine CaM in the presence of 2 mM $CaCl_2$ or 2 mM EDTA. The PVDF membranes were further incubated for 1 h with avidin-conjugated alkaline phosphatase in the presence or absence of Ca^{2+} and detected using nitroblue tetrazolium and 5-bromo-4chloro-3-indolyl phosphate.

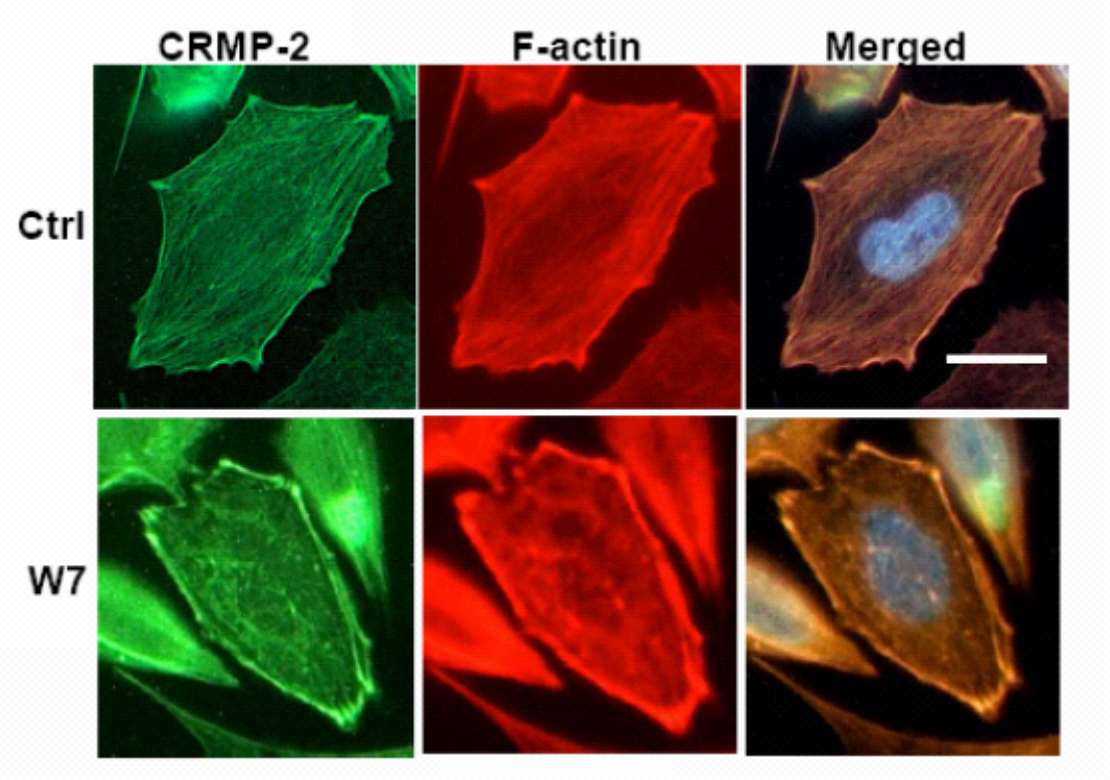

Figure 4-3. CRMP-2 co-localizes with F-actin and CaM antagonist W7 altered F-actin organization. PC-12 cells were culture in the presence of DMSO (upper panel) or 10 μM of W7 (lower panel). PC-12 cells were doubly staining with anti-CRMP-2 (green) and rhodamine F-actin (red). Yellow color in merge photographs corresponds to colocalization of CRMP-2 with F-actin. Blue is DAPI stained nuclei. Scale bar=10 μM

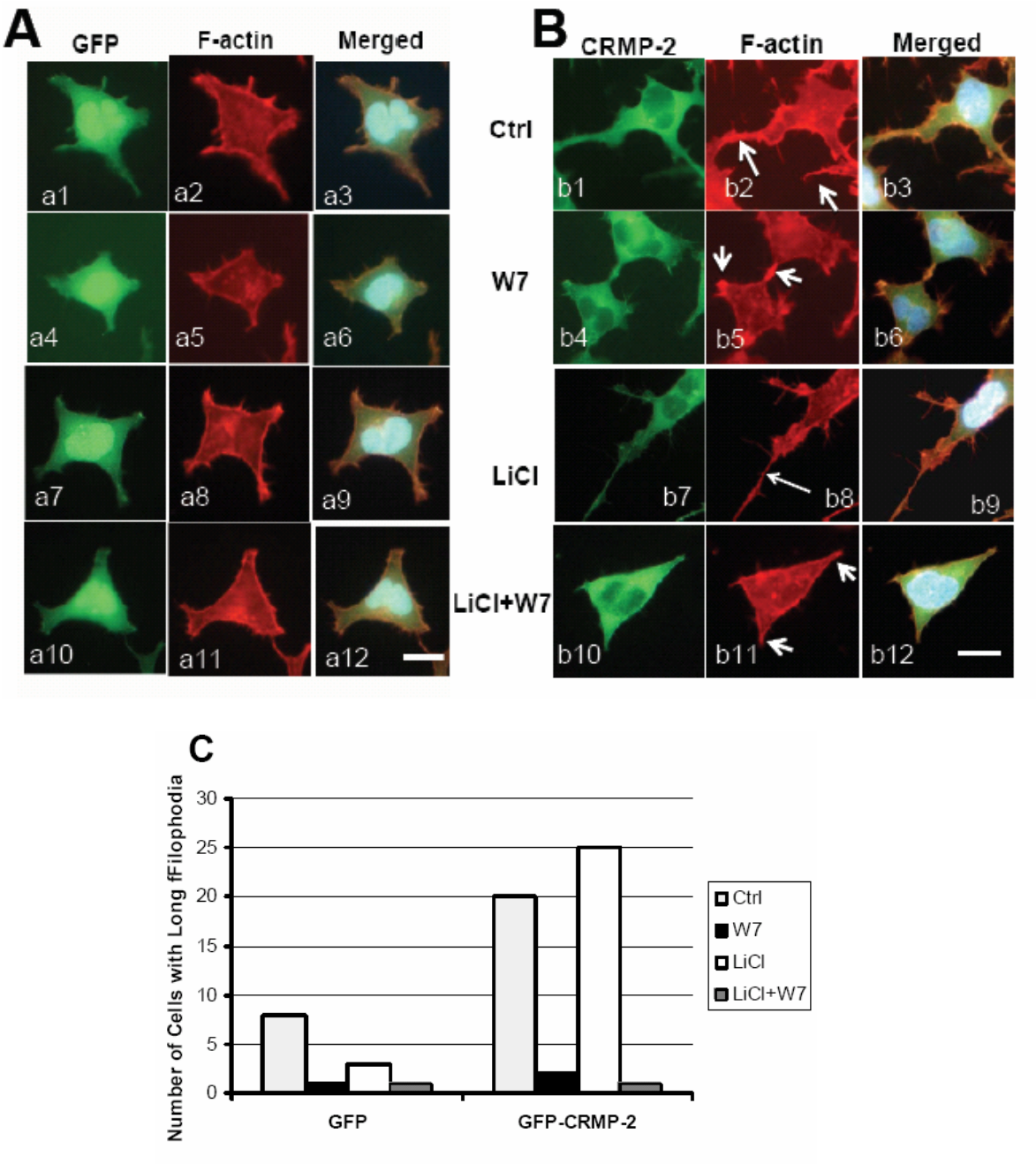

Figure 4-4. CaM antagonist W7 induces filopodia retraction in CRMP-2 overexpressing HEK293 cells. HEK293 cells with over-expressed GFP (A) or GFP-CRMP-2 (B) were treated with W7, LiCl or both. F-actin was stained by rhodamine-phalloidin. Yellow color in merged photographs corresponds to colocalization of CRMP-2 with F-actin. Typical Changes of filopodia are indicated by arrows. Blue is DAPI stained nuclei. Scale bar=10 μM. (C) Quantification of cells with at least one filopodia greater than half the diameter of the cell body following various treatments. For each experiment, at least 30 cells were randomly measured.

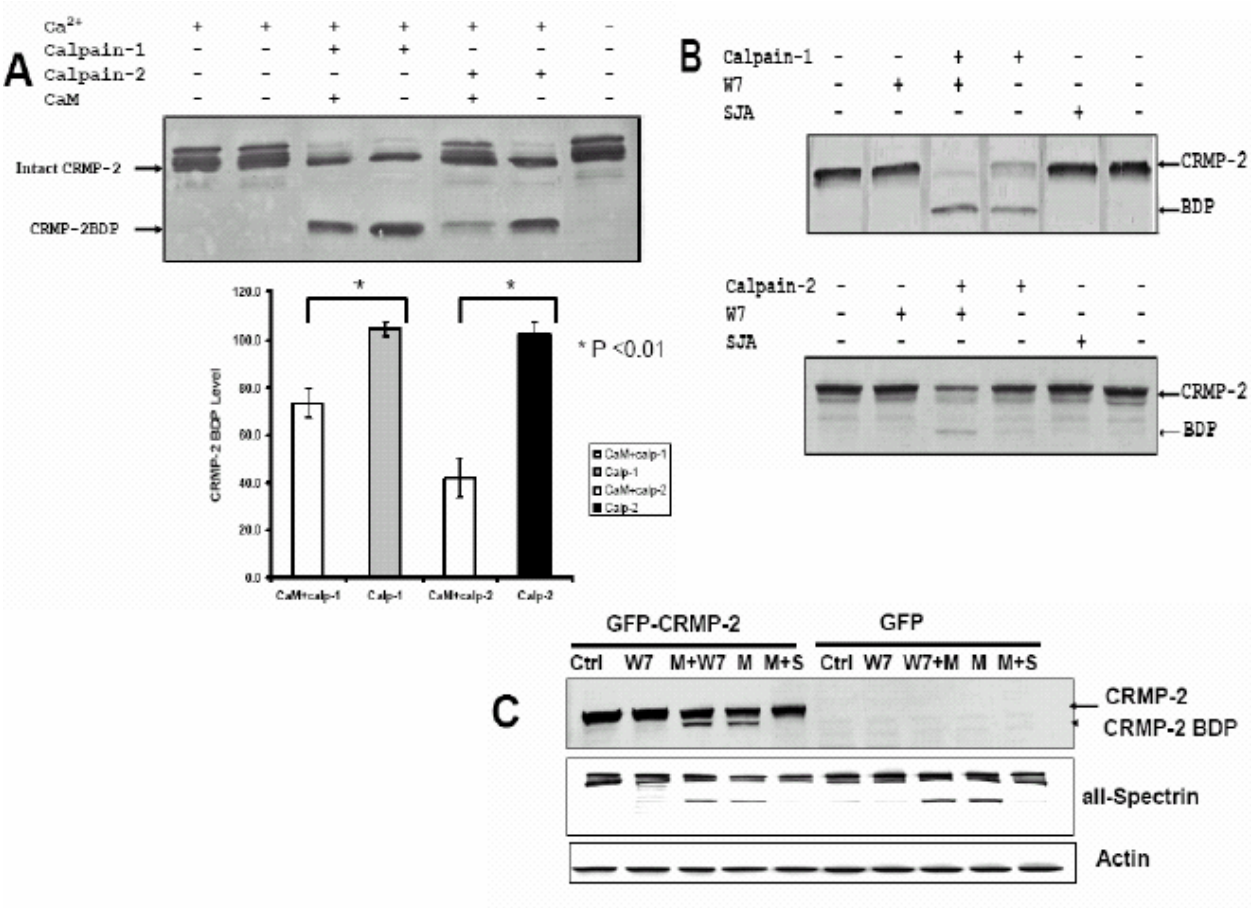

Figure 4-5. CaM modulates calpain-mediated CRMP-2 proteolysis *in vitro*. (A) Calpain mediated purified CRMP-2 proteolysis is retarded by CaM *in vitro*. Purified GST-CRMP-2 protein (1μg) was incubated with calpain-1/2 in the presence of calmodulin (10 μM) or Ca^{2+} (2 μM). (B) Calpain mediated CRMP-2 proteolysis in cell lysate is enhanced by CaM antagonist *in vitro*. Whole PC-12 cell lysates (20μg) were incubated with calpain-1/2 in the presence of CaM antagonist W7 (50 μM) or SJA (30 μM) (C) W7 application acts synergistically with MTX to induce CRMP-2 proteolysis. Therefore, CaM might regulate CRMP-2 proteolysis after intracellular Ca^{2+} elevation. HEK293 cells with over-expressed GFP or GFP-CRMP-2 were treated with MTX with or without W7 or calpain inhibitor SJA. Total proteins in the cell lysates were resolved by SDS-PAGE and immunoblotted with anti-CRMP-2 (C4G), aII-spectrin and actin.

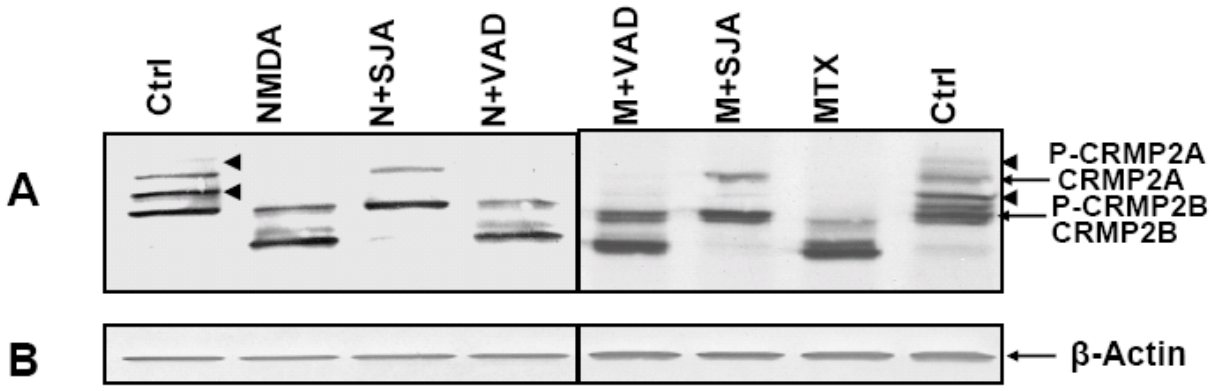

Figure 4-6. Elevation of intracellular Ca^{2+} results in CRMP-2 proteolysis and dephosphorylation. Primary cortical neurons were pretreated with or without calpain inhibitor (30 μM SJA6017) or caspase inhibitor Z-VAD for one hour, and then exposed to Ca^{2+} channel opener maitotoxin (MTX 3 nM) for 3 hours, and NMDA (200 μM) for 12 hours. Total proteins in the cell lysates were resolved by SDS-PAGE and immunoblotted with anti-CRMP-2 (C4G).

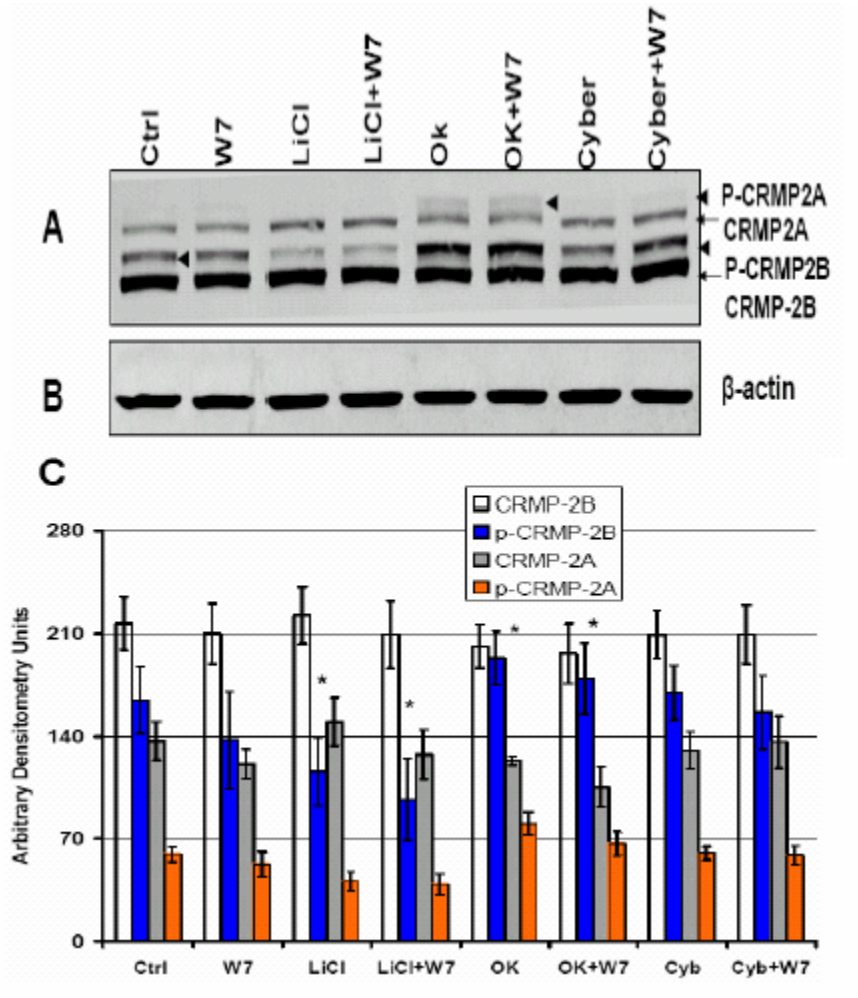

Figure 4-7. Okadaic acid enhances CMRP-2 phosphorylation but CaM does not affect the dynamics of CRMP-2 phosphorylation. Primary cortical neurons were pretreated with calmodulin antagonist (W7, 10 μM) for thirty minutes, and then exposed to LiCl (20mM), okadaic acid (50 nM) and cybermethrin (4 μM) for one hour. Total proteins in the cell lysates were resolved by SDS-PAGE and immunoblotted with anti-CRMP-2 (C4G) (A). β-actin (B) was used as a loading control. (C) Densitometric analyses of CRMP-2 and phospho-CRMP-2 immunoblots were performed. Values were means ± S.E.M. n = 4. Statistical significance of differences between the control and each treated group was determined by one-way ANOVA with Dunnett's multiple comparison tests. A difference was considered to be statistically significant when the *P* value was less than 0.05 (*$P < 0.05$).

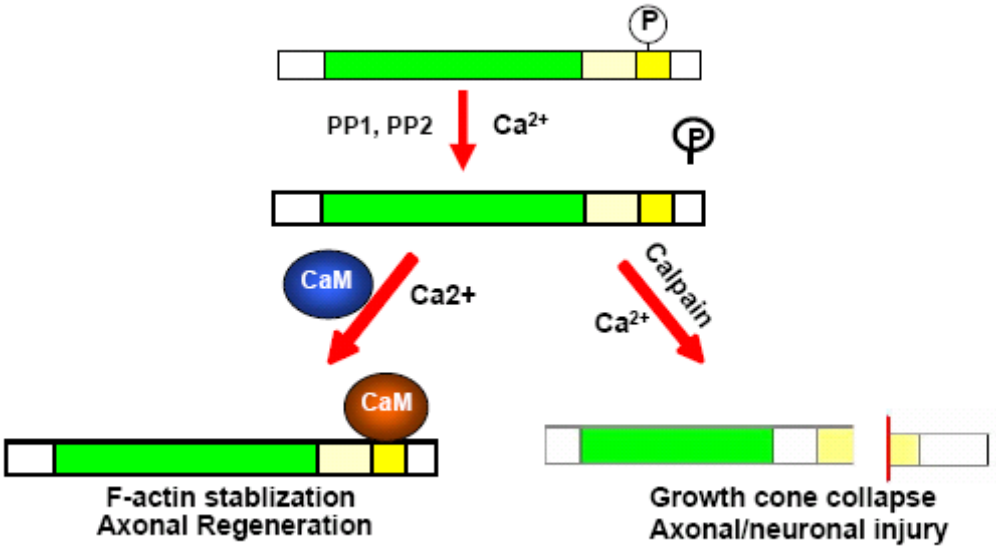

Figure 4-8. Proposed model of the role of calmodulin in CRMP-2 post-translation modification under pathological conditions. CRMP-2 is phosphorylated when in physiological state (Figures 4-6 and 4-7). Under pathological states with the elevated cytosolic Ca^{2+}, activation of calpain and protein phosphatases PP1 and PP2A induces CaM independent CRMP-2 dephosphorylation and proteolysis (Figure 4-7). With the sustained Ca^{2+} influx and calpain activation, CRMP-2 undergoes CaM independent proteolysis, which may contribute to growth cone collapse and axonal injury (Figure 4-6). Meanwhile, in our model, CaM undergoes conformational changes upon Ca^{2+} influx, binds to CRMP-2 and prevents CRMP-2 from calpain-mediated cleavage, thereby serving as a negative feedback as part of the cell's response after injury (Figure 4-5). In addition, CaM binding to CRMP-2 might play a role in F-actin bundling (Figure 4-3) and, in turn, maintains stable structure or enhancing axonal regeneration (Figure 4-4).

CHAPTER 5
DIRECT RHO-ASSOCIATED KINASE INHIBITION INDUCES COFILIN DEPHOSPHORYLATION AND NEURITE OUTGROWTH IN PC-12 CELLS

Introduction

Unlike in the peripheral nervous system, axons in the adult central nervous system (CNS) undergo little spontaneous regeneration. The lack of regeneration is due to a diverse class of neuritogenic inhibitors that prevail in the CNS. Some of these inhibitors have already been identified, such as Nogo-A, myelin associated glycoprotein (MAG) (McKerracher et al., 1994), chondroitin sulfate proteoglycans (CSPGs) and oligodendrocyte myelin glycoprotein (OMgp) (Wang et al., 2002; McKerracher and David, 2004). Approaches targeting these molecules could promote axonal regeneration. A number of studies have demonstrated that inhibition of small Rho-GTPases and Rho kinase can promote axonal regeneration by overcoming the inhibitory effects of myelin, as well as Nogo-A, CSPG, and MAG (Lehmann et al., 1999; Yamashita et al., 2002; Fournier et al., 2003; Yamashita et al., 2005). In contrast, neurotrophic factors promote the growth and survival of neurons in the mature nervous system. They also play a significant role in influencing nerve fiber growth. In addition to nerve growth factor (NGF) (Bonini et al., 2003), several other molecules exhibit neurotrophic properties, including fibroblast growth factor (FGF), brain-derived neurotrophic factor (BDNF) and neurotrophin-3 (NT-3) (Ebadi et al., 1997; Petruska and Mendell, 2004). Also reported, NGF and NT-3 promote axonal outgrowth via the suppression of Rho-A activity (Ozdinler and Erzurumlu, 2001; Yamaguchi et al., 2001). Accumulating evidence has linked the Rho-A family with permissive as well as inhibitory pathways of neurite outgrowth.

ROCKs (also known as Rho kinases), a class of serine/threonine kinases, were the first downstream effectors of Rho to be discovered (Kwon et al., 2002). Numerous studies showed the ROCKs mediate a large proportion of the signals from Rho in regulating dynamic reorganization

of the cytoskeleton (Amano et al., 2000; Hall, 2005). Initially, activation of ROCKs was characterized by direct phosphorylation of myosin light chain (MLC) (Somlyo and Somlyo, 2000) and by indirect inhibition of MLC phosphatase (MLCP) (Kawano et al., 1999) in mediating Rho-A induced stress fibers and focal adhesions. ROCKs consist of an amino-terminal kinase domain and an autoinhibitory carboxy-terminal region, which includes the Rho-binding (RB) domain and the pleckstrin homology (PH) domain. Both the RB and PH domains can interact independently from the amino-terminal kinase domain and in turn inactivate the enzyme. Activated Rho interacts with the RB domain, and disrupts the negative regulated interaction between the kinase domain and the autoinhibitory region, thereby freeing kinase activity. Two ROCK isoforms have been identified: ROCK I (also known as ROKβ and P160ROCK) and ROCK II (ROKα). The kinase domains of ROCK I and ROCK II are 92% identical, and so far there is no evidence that they have different functions (Riento and Ridley, 2003).

Recently, the Rho-ROCK pathway has been demonstrated to play a prominent role in mediating neurite retraction, growth cone collapse and axonal growth through ROCK inhibition on dorsal root ganglion (DRG) on an inhibitory substrate (such as MAG) (Amano et al., 2000; Fournier et al., 2003). Strategies for promoting axonal regeneration in the CNS are therapeutically attractive for treatment of various diseases such as traumatic brain injury, stroke and Alzheimer's disease. The rat pheochromocytoma cell line, PC-12, has been widely used as an important model for neuronal differentiation. PC-12 cells differentiate into a neuronal phenotype in response to various neurotrophins. For instance, nerve growth factor (NGF) treated PC-12 cells exhibit proliferation arrest, neurite outgrowth (NOG) and electrical excitability (Greene and Tischler, 1976). In previous studies we also demonstrated that repeated amphetamine treatment induces NOG in PC-12 cells, similar to that found with known

neurotrophic factors (Park et al., 2003). Moreover, PC-12 cells elicit NOG via Rho inhibition by Clostridium b. C-3 exoenzyme treatment of PC-12 cells (Lehmann et al., 1999; Sebok et al., 1999) or DRG on inhibitory substrate (Fournier et al., 2003), making it an invaluable model system for studying potential Rho-ROCK downstream signal transduction pathways in NOG.

Cytoskeletal reorganization plays a striking role in NOG, such as through actin and microtubule remodeling. Thus, it is essential to understand the signaling pathways that control cytoskeleton dynamics (Tojima and Ito, 2004). Rho GTPase has been shown to influence actin cytoskeleton dynamics (Sebok et al., 1999; Dent and Gertler, 2003). ROCKs, also mediate signals to the actin cytoskeleton through various substrates, such as adducin and LIM kinase (LIMK) (Dent and Gertler, 2003). In turn, LIMK phosphorylates cofilin, an actin associated protein, which binds to actin and serves to enhance depolymerization of actin filaments. Once phosphorylated, cofilin is inactivated and loses its filament severing and monomer binding abilities (Maekawa et al., 1999; Ohashi et al., 2000). In addition, ROCKs phosphorylate other neurite intermediate filament or microtubule-associated proteins such as NF-L (Hashimoto et al., 1998), Tau and MAP2 (Amano et al., 2003).

A number of ROCK inhibitor compounds have been developed, including H-89, HA-1077, Y-27632 (Davies et al., 2000), H-1152 (Ikenoya et al., 2002) and Wf-536 (Nakajima et al., 2003). Among commercially available inhibitors, (R)-(+)-trans-N-(4-Pyridyl)-4-(1-aminoethyl)-cyclohexanecarboxamide (Y-27632), have shown high potency and selectivity for ROCK inhibition (Amano et al., 2000; Ishizaki et al., 2000). This selective inhibition of ROCKs makes Y-27632 very useful for evaluating ROCK functions in CNS since ROCKs are highly expressed in the brain.

In this study, the role of ROCK inhibitor (Y-27632 or H-1152) was systematically evaluated for promoting NOG in the well-defined PC-12 model. Dynamics in cell morphology and cytoskeleton components (actin, cofilin and βIII-tubulin) were characterized following treatment with ROCK inhibitor Y-27632. Results suggest ROCK inhibition might be a potential therapeutic avenue for promoting NOG after CNS injury.

Materials and Methods

Chemicals and Antibodies

Culture media and sera were obtained from Gibco Inc. (Rockville, MD). Y-27632, H-1152, Ro-32-0432, PD 98059, and H-89 were purchased from Calbiochem (San Diego, CA). The primary antibodies used include: polyclonal antibodies against phospho-cofilin and cofilin (Cell Signaling, Beverly, MA), monoclonal antibody against βIII-tubulin (Covance, Denver, PA) and FITC-conjugated phalloidin (Molecular Probes, Eugene, OR).

Cell Culture

PC-12 cells were maintained at 37ºC in Dulbeco's modified Eagle's medium (DMEM) supplied with 10% fetal bovine serum (FBS), 5% heat-inactivated horse serum, 100 μg/ml of streptomycin, 100 U/ml of penicillin and 1% Fungizone (Gibco, Rockville, MD) in a humidified 5% CO2 incubator. To induce neurite outgrowth, PC-12 cells were plated in the same medium with 25 μM Y-27632. Y-27632 was prepared as a 25 mM stock solution in dimethlsulfoxide (DMSO) and added directly into the medium. An equal amount of DMSO was added to control plates. Micrographs of cells were taken at 32x with an Axiocam digital camera using a Zeiss Axiovert 135 microscope. For the kinase inhibition study, PC-12 cells were treated with 25 μM Y-27632 for 2 hours, and then continued to be co-treated with 300 nM RO-32-0432 or 500 nM H-89 or 30 μM PD 98059 for 14 hours.

Quantification of Neurite Outgrowth

Cell processes were defined as neurites when longer than the diameter of the cell body. The percentage of neurite-bearing cells was calculated as the number of cells with one or more neurites divided by the total cell number (Park et al., 2003). Neurite length was evaluated by manually tracing the longest neurite per cell using the software ImageJ (version 1.29x, NIH, USA) and referenced to a known length. Each experiment was conducted in triplicate. Images were taken with 15 or more cells per field. For each experiment, at least 50 cells were randomly measured.

Immunoblotting

PC-12 cells were treated for various time periods, washed twice with phosphate-buffered saline (PBS), and solubilized with lysis buffer containing 20 mM Tris-HCl, pH 7.4, 150 mM NaCl, 5 mM EDTA, 5 mM EGTA, 1% Triton X-100, 1 mM NaF, 1 mM Na3VO4, and a protease inhibitor cocktail tablet (Roche, Indianapolis, IN). The cell lysates were briefly sonicated before clarification by centrifugation at 15,000 g for 10 minutes at 4ºC. Protein concentration of the supernatant was determined by a modified Lowry method (DC Protein Assay Kit, Bio-Rad, Hercules, CA). Samples (20 μg protein) were resolved by 10-20% sodium dodecyl sulfate-polyacrylamide gel electrophoresis (SDS-PAGE) and transferred onto a polyvinylidene difluoride (PVDF) membrane by the semi-dry method. Membranes were blocked with 5% non-fat milk in tris-buffered saline containing 0.1% tween-20 (TBST) and then incubated with the primary antibody in 5% non-fat milk in TBST at 4ºC overnight. Following washes with TBST, membranes were incubated for one hour at room temperature with a biotinylated secondary antibody. Following another series of washes, the membrane was incubated with avidin-conjugated alkaline phosphatase for 30 minutes. Proteins were visualized using nitroblue tetrazolium and 5-bromo-4chloro-3-indolyl phosphate. The membranes were

scanned, and the optical density of the bands was quantified with the software ImageJ (version 1.29x, NIH, USA).

Immunocytochemistry

PC-12 cells were seeded onto LabTek II chamber slides (Nunc, Naperville, IL) followed by overnight incubation. On the next day, the medium was replaced with or without 25 μM Y-27632. Twenty-four hours following treatment, PC-12 cells were fixed with 4% paraformaldehyde (PFA) in PBS for 10 minutes, washed with PBS and permeabilized with 0.1% triton X-100 in PBS for 5 minutes. F-actin was fluorescently labeled with 5 units/ml FITC-conjugated phalloidin for 20 minutes at room temperature. βIII-tubulin staining was performed, following a one-hour blocking step in 10% goat serum at room temperature. Then the cells were incubated overnight at 4ºC with monoclonal rabbit anti-βIII-tubulin at a dilution of 1:2000. Alexa 488-conjugated goat-anti-rabbit secondary antibody (Molecular Probes, Eugene, OR) was added at a dilution of 1:1000, followed by washing with PBS. The cells were mounted using medium with 4, 6-diamidine-2-phenylindole (DAPI) (Vector Laboratories, Burlingame, CA). Fluorescence images were captured with a 20x objective on the Zeiss Axioplan 2 Fluorescence Microscope with a CCD camera and combined using SPOT imaging software (Diagnostic Instruments, Sterling Heights, MI).

Results

Dose-Dependent Neurite Outgrowth Induced by ROCK Inhibition in PC-12 Cells

The effect of ROCK inhibitor Y-27632 on a low-density culture of PC-12 cells over multiple concentrations is shown in Figure 1. At the low dose of 0.01 μM, PC-12 cells appear similar with control cells that are slightly larger and rounder, but possess few visible neurites (Fig. 1 A, top panel). At higher Y-27632 doses, from 1 μM to 100 μM, an increasing number of PC-12 cells present multiple long branched neurites, compared to sparse growth in controls (Fig.

1 B-F, top panel). The qualified data shows that the percentage of neurite-bearing cells significantly increased in a dose-dependent manner, peaking between 25 and 100 μM with greater than 90% (Fig.1, bottom panel). However, at 100 μM, cell detachment from the substrate and neurite loss was noticed after 48 hours of exposure (data not shown).

Dynamics of Neurite Outgrowth in ROCK Inhibitor Treated PC-12 Cells

To further examine NOG dynamics after ROCK inhibition, we executed a time course analysis of NOG in PC-12 cells using 25 μM Y-27632. NOG was immediate initiated within 5 minutes, with small protrusion veils (lamellipodia) developing (Fig. 2B), and 10 minutes later with a few spikes (filopodia) forming (Fig. 2C). Prominent neurite elongation was visualized between 30 minutes and 10 hours. Robust and fully extended neurites were observed following 6 to 10 hours of treatment, which was sustained for 24 hours after Y-27632 stimulation (Fig. 2D-I). There was a rapid increase in neurite-bearing cells after Y-27632 exposure, with greater than 85% of the cells showing neurites within 6 hours (Fig. 2J), The lengthening of neurites appears biphasic, with a rapid increase within 6 hours, and a more gradual extension to maximal length by 24 hours (Fig. 2K).Since protein kinase inhibitory agents, including Y-27632, can cross-inhibit other protein kinase, we further tested another more specific ROCK inhibitor, H-1152 (Fig. 3). We observed that even at a very low concentration (1 μM), H-1152 produced very rapid cell shape changes, lamellipodia and filopodia developing within 5-30 minutes (Fig. 3B, C), followed by fully extended neurites by 24 hours (Fig. 3F). We also found that 10 μM of H-1152 produced the same NOG effect (Fig. 3H), while 0.1 μM also produced partial NOG by 24 hours (Fig. 3G).

Remodeling of Cytoskeletal Architecture in ROCK Inhibition Mediated Neurite Outgrowth

With the cytoskeleton considered a principal determinant of NOG, we examined cytoskeleton reorganization during Y-27632 treatment (Tojima and Ito, 2004). FITC-phalloidin F-actin immunostaining and neuronal specific βIII-tubulin immunostaining (green) were performed against DAPI staining (blue) of the nuclear DNA, respectively. Before treatment, PC-12 cells were round and F-actin was uniformly localized in the periphery of the soma (triangle in Fig. 4A), whereas βIII-tubulin was evenly distributed within the cell body (Fig. 4C). After 12 hours treatment, F-actin accumulated in growth cone-like structures (short arrow in Fig. 4B), newly formed neurites (long arrow in Fig. 4B) and lamellipodia (triangle in Fig. 4B). In comparison with F-actin, βIII-tubulin was preferentially concentrated along the nascent neurites (arrow in the Fig. 4D).

ROCK Inhibition Induces Transient Cofilin Dephosphorylation

The polymerization/depolymerization of actin was shown to be necessary for NOG (Dent and Gertler, 2003), thus we investigated the signaling pathways that involved actin dynamics. Cofilin is the most well characterized stimulus-responsive mediator of actin dynamics. Cofilin dissociates from F-actin when phosphorylated by LIMK. Since LIMK is a direct downstream effector of ROCK, ROCK inhibition decreases LIMK1 activity and dephosphorylates cofilin. In a series of experiments, we sought to identify the cytoskeleton signal transduction pathways through which Y-27632 mediated NOG in PC-12 cells. The morphology change of PC-12 cells in response to Y-27632 indicated that the initiation of NOG occurred within 5 minutes. Correlated with morphology change, more than 60% of cofilin underwent dephosphorylation within 5 minutes. Subsequent partial recovery of phospho-cofilin was noticed during the neurite elongation and maintenance periods (6 to 24 hr) (Fig. 5A and B). There was no change in the

total expression level of cofilin during ROCK inhibitor treatment (Fig. 5A). Thus, dephosphorylation-phosphorylation of cofilin appears to be involved in the initiation of NOG.

We were intrigued by the observation that cofilin underwent partial re-phosphorylation following the initial phase of dephosphorylation, despite the presence of a constant level of ROCK inhibitor (Y-27632, 25 μM) (Fig. 5). We hypothesized the involvement of additional protein kinases or protein kinase cross talk. Protein kinase-A, protein kinase C and MAPK have all been implicated in neurite outgrowth in PC-12 cells (Hundle et al., 1995; Obara et al., 2002; Christensen et al., 2003). PC-12 cells were first subjected to 25 μM of Y-27632 for the maxima cofilin dephosphorylation. Then various protein kinase inhibitors were introduced to see if they would suppress cofilin re-phosphorylation. However, attenuated rephosphorylation was not bserved with any of the kinase inhibitors (Fig. 6). To further confirm that cofilin dephosphorylation is ROCK mediated, we again employed a second specific ROCK inhibitor H-1152 (Fig. 7). Again a rapid dephosphorylation of cofilin was observed with a low concentration of H-1152 (1 μM) within 30 minutes. Interestingly, H-1152 differed from Y-27632 in that the P-cofilin reduction was sustained for up to 24 hours (Fig.7).

Discussion

Although ROCK inhibitor (Y-27632) induced NOG in PC-12 cells had been briefly mentioned in previous studies (Birkenfeld et al., 2001; Fujita et al., 2001; Kishida et al., 2004), there has been no comprehensive biochemical analysis of this important phenomenon to define the role of ROCK inhibition to date. For example, Birkenfeld et al. (Birkenfeld et al., 2001) only described briefly the effects of Y-27632 on NOG without detailed biochemical studies. In addition, they only used the less selective ROCK inhibitor Y-27632, but we now for the first time use H-1152 to complement the use of the less selective Y-27632 (Fig. 1-3). In our studies, both Y-27632 and H-1152 rapidly initiated NOG within 5 to 30 minutes with the formation of

small protrusions (neurite initiation) followed by neurite extension in 6 to 10 hours (elongation) (Fig. 2). Importantly, both ROCK inhibitors produce rapid cofilin-dephosphorylation.

Since NGF-induced NOG in PC-12 cells by activating protein kinase C (PKC) (Christensen et al., 2003), it is possible that Y-27632 might exert its effects on PKC. However, this possibility was ruled out as PKC was not inhibited at all at 10 μM of Y-27632, yet 1-5 μMY-27632 already produced NOG effects (Fig. 1). Y-27632 is also known to inhibit MAP kinase activated protein kinase-1b (MAPAP-K1b) (IC50 19 μM) but at a higher concentration than ROCK (IC50 800 nM) in vitro (Ishizaki et al., 2000). Under our cell treatment conditions, Y-27632 even as low as 1-5 μM already produced NOG effects, so it is unlikely that it was attributable to MAPAP-K1b inhibition. Furthermore, a more selective ROCK inhibitor H-1152 (Ikenoya et al., 2002; Sasaki et al., 2002) produced the same NOG effects at a concentration as low as 1 μM (Fig. 3).

Neuronal differentiation processes were mediated by cytoskeletal reorganization, as observed with F-actin and microtubules. Two major F-actin networks were observed in the filopodia and lamellipodia of the neuronal growth cones (Tojima and Ito, 2004). Neuron-specific βIII-tubulin usually is expressed in cell bodies and neurites and highly concentrated in neurites of mature neurons (Braun et al., 2002). In our study, F-actin accumulated in growth cone-like structures, lamellipodia and neurites (Fig. 4B), whereas βIII-tubulin was preferentially enriched along the nascent neurites of PC-12 cells following ROCK inhibition (Fig. 4D). Similar to NGF-induced NOG, ROCK inhibition induced PC-12 cell differentiation into a neuronal phenotype as indicated by neuronal specific βIII-tubulin antibody staining and morphological changes (Fig. 4D). Thus, differentiated PC-12 cells are representative of neurons and can be used to further explore the downstream ROCK pathways in NOG.

Interestingly, ROCK inhibitor induced a rapid decrease and then subsequent gradual increase in phosphorylation of cofilin, which correlated with the initiation and elongation of neurites (Fig. 5). It is important to point out that Maekawa et al. had previously established that ROCK inhibition causes cofilin dephosphorylation through LIMK-1 (Maekawa et al., 1999). However, they did not study the relationship between ROCK-cofilin dephosphorylation and neurite outgrowth in model cell system such as PC-12 cells. Tojima and Ito recently proposed a signal transduction cascade that involves ROCK inhibition decreasing LIMK1 activity and dephosphorylating cofilin, thus inhibiting neuritogenesis (Tojima and Ito, 2004). Yet, based on our studies, instead of inhibiting neuritogenesis, our results showed that cofilin dephosphorylation coincided with NOG initiation (5 to 30 minutes), while cofilin re-phosphorylation occurred during elongation and maintenance phase (6 to 24 hours) of NOG (Fig. 5A). Our results were consistent with the previous work of Aizawa et al, where a sequential cofilin phosphorylation-dephophorylation cycling occured during semaphoring 3A (Sema-3A) treatment on DRG cells on inhibitory substrate (Aizawa et al., 2001). Sema-3A, a chemorepulsive axonal guidance molecule, induces growth cone collapse via the LIMK-cofilin pathway regulating actin filament dynamics. The dynamic cofilin dephosphorylation-phosphorylation found in our work indicates that in addition to LIMK, other signaling pathways may also be involved in the mechanism of regulating the cofilin cycling in NOG of PC-12 cells. Upon ROCK inhibition LIM kinases are inactivated leading to dephosphorylation of cofilin and resulting in massive new barbed ends for initiation neurites. We attempted to elucidate the mechanism of cofilin re-phosphorylation shown during longer Y-27632 treatments (6 h to 24 h) (Fig. 5). Since protein kinase A, C and MAPK have all been implicated at NOG previously in PC-12 cells (Hundle et al., 1995; Obara et al., 2002; Christensen et al., 2003); we tested the

potential effects of pharmacological inhibitors of these kinases on post-Y-27632 cofilin rephosphorylation. However, protein kinase A, protein kinase C and MAPK inhibition all failed to prevent cofilin re-phosphorylation (Fig. 6). Other signaling pathways, such as inhibition of the Slingshot phosphatase (Niwa et al., 2002) or type 1 and type 2A serine/threonine phosphatases (Ambach et al., 2000), may be involved in the re-phosphorylation of cofilin, which in turn leads to actin polymerization, and subsequently contributes to the elongation and maintenance of neurites. This mechanism may also apply to the formation and/or stability of essential actin-based structures in growth cones and postsynaptic densities (Revenu et al., 2004). In addition to inhibiting ROCKs, Y-27632 also inhibits protein kinase C-related kinase (PRK)2 in vitro, which may contribute to the dephosphorylation-phosphorylation dynamics of cofilin (Davies et al., 2000). We thus tested a more specific ROCK inhibitor (H-1152) (Ikenoya et al., 2002; Sasaki et al., 2002). It is of interest to note that, when PC-12 cells treated with H-1152, cofilin dephosphorylation was sustained for 24 hours without notable rephosphorylation (Fig. 7). Further work is needed to understand crosstalk between signaling cascades in ROCK inhibition mediated NOG. Understanding the signaling mechanisms of ROCK inhibition mediated NOG opens up the possibility for developing novel strategies to promote axon regeneration in vivo. Clinically, the use of a ROCK inhibitor may be useful for developing therapies in CNS following damage by Alzheimer's disease (Zhou et al., 2003), spinal cord injury (Ellezam et al., 2002), traumatic brain injury (Brabeck et al., 2004) and stroke (Brabeck et al., 2003).

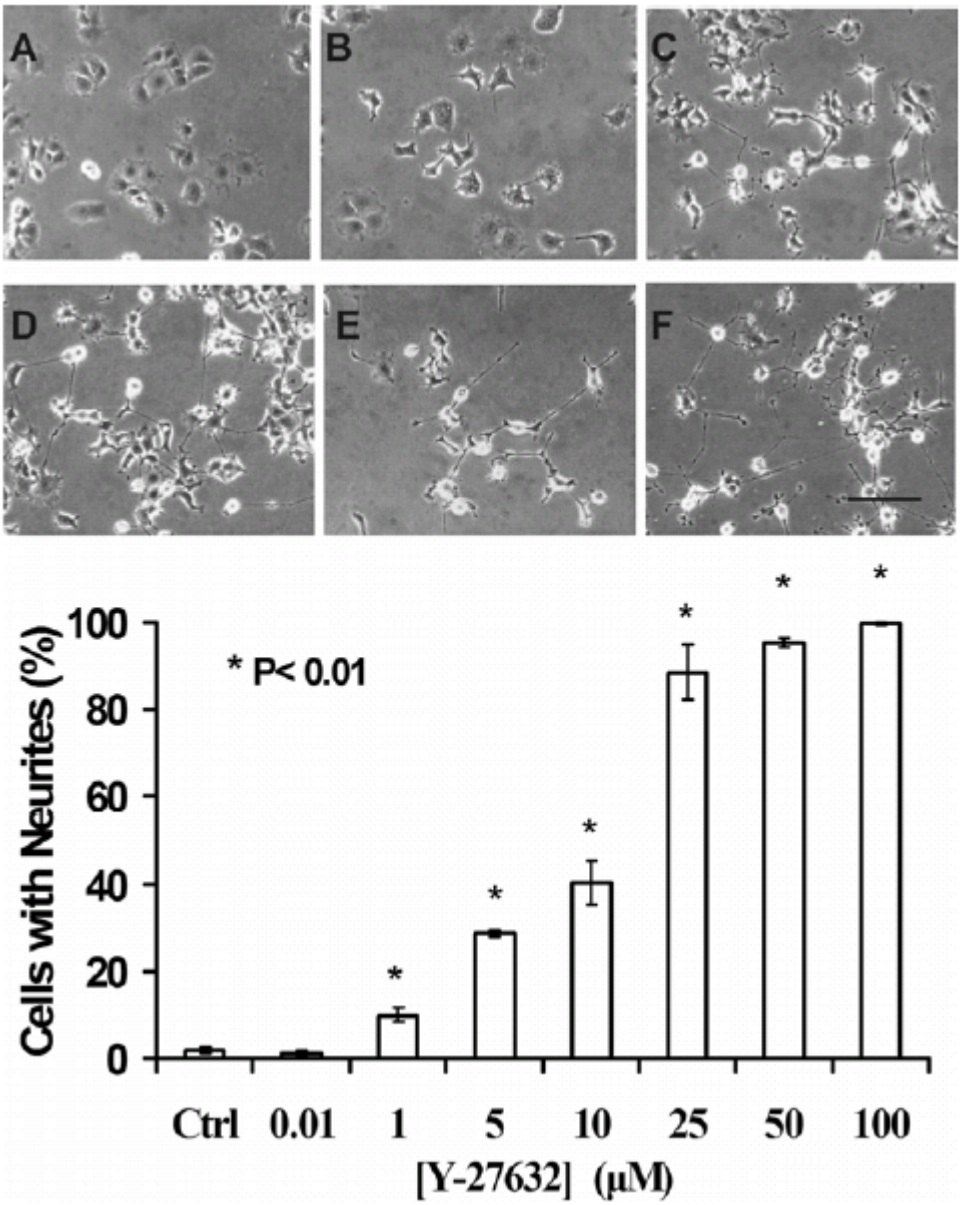

Figure 5-1. Neurite outgrowth of PC-12 cells in response to ROCK inhibitor Y-27632 in a dose-dependent manner. *Top panel*: A through F are phase-contrast images of PC-12 cells following treatment by different concentration of Y-27632 for 24 hours. (A) 0.01 μM; (B) 1 μM; (C) 5 μM; (D) 10 μM; (E) 25 μM; and (F) 100 μM of Y-27632. Scale bar represents 50 μm. *Bottom Panel*: Quantification of neurite outgrowth following Y-27632 treatment for 24 hours. Cells with at least one neurite greater than the diameter of the cell body were counted and expressed as a percentage of the total number of cells in a field. For each experiment, at least 50 cells were randomly measured. Data shown are mean values ± S.E.M, n = 3. Statistical significance of differences (P <0.01) between the control and each treated group was determined by one-way ANOVA with Dunnett's multiple comparison tests.

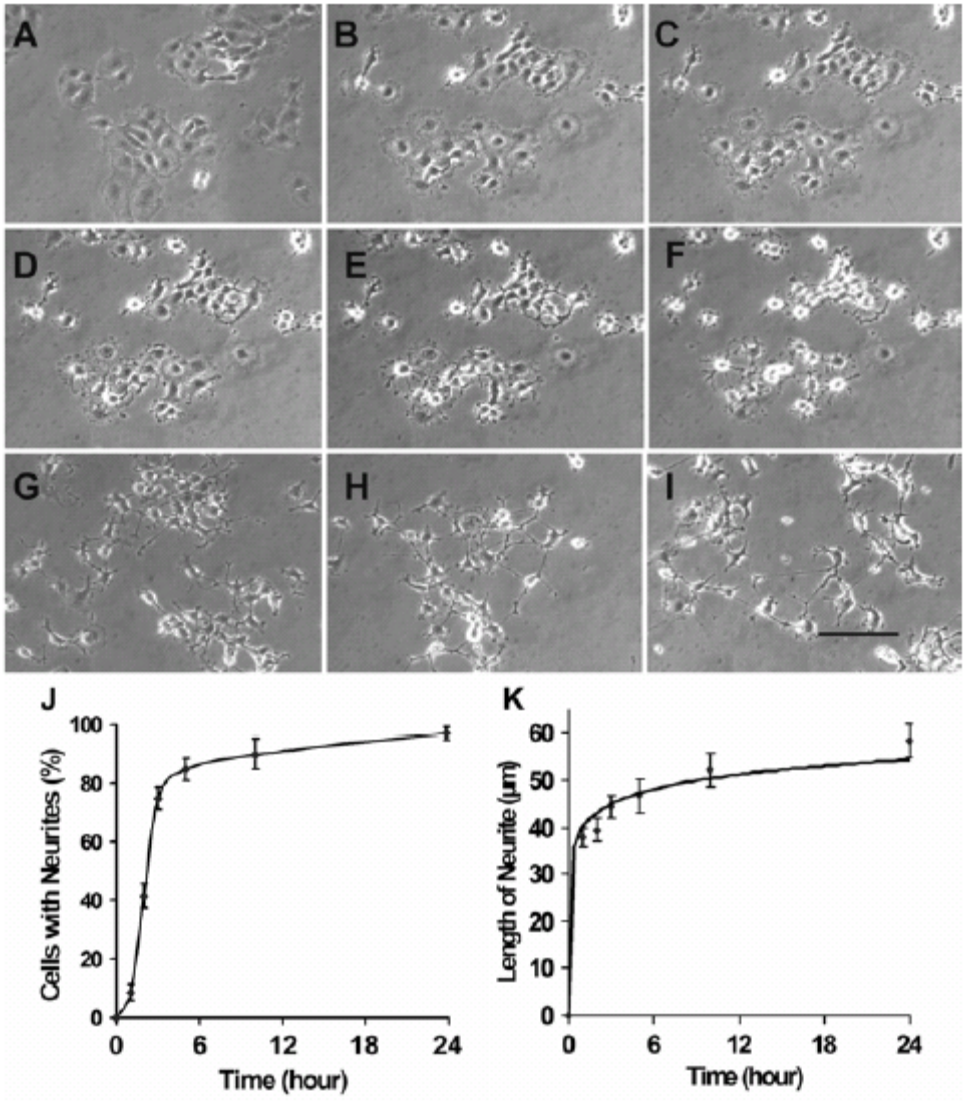

Figure 5-2. ROCK inhibitor Y-27632 induced neurite outgrowth in PC-12 cells in a time-dependent manner. Panels A through I are phase-contrast images of PC-12 cells following 25 μM Y-27632 treatment for different time points: **A**) Control **B**) 5 min; **C**) 10 min; **D**) 30 min; **E**) 1 hr; **F**) 3 hr; **G**) 6 hr; **H**) 10 hr; and **I**) 24 hr. Arrows indicate examples of typical neurite outgrowth in PC-12 cells over time. Cells were plated onto 6-well plates at a cell density of 4 x $10^3/cm^2$. Scale bar represents 50 μm.

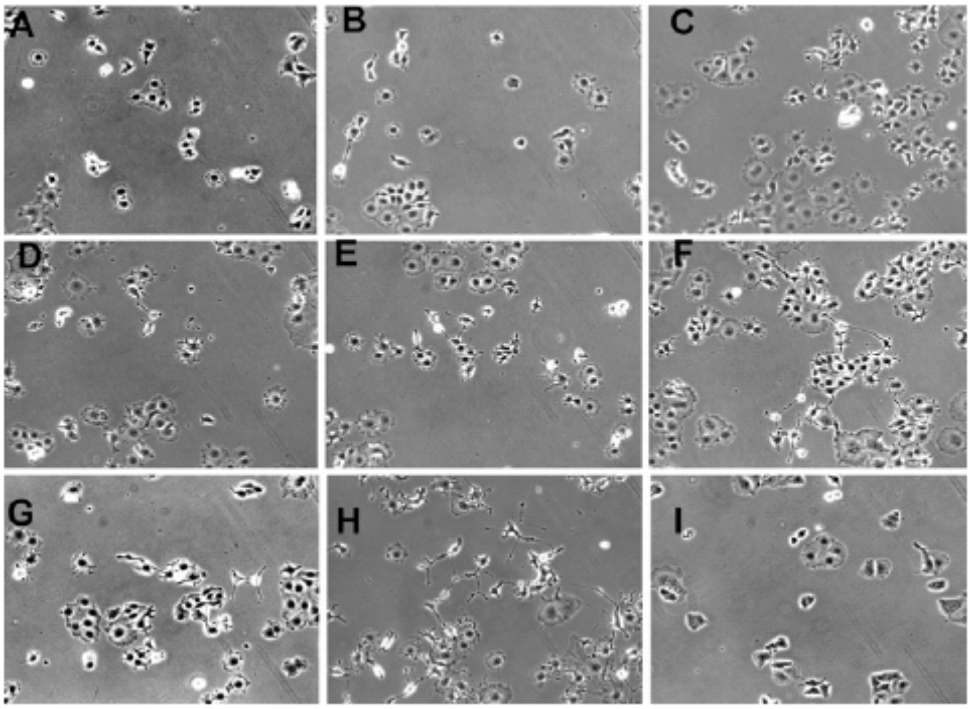

Figure 5-3. Quantification of neurite outgrowth post Y-27632 treatment in PC-12 cells. Quantification of cells with neurites **A**) and neurite lengths **B**) were performed after PC-12 cells were treated with 25 μM Y-27632 at various time points. The length of the longest neurite was counted for cells with at least one identified neurite. Neurite length was determined by manually tracing the length of the longest neurite per cell. For each experiment, at least 50 cells were randomly measured. Values represent means ± S.E.M. n = 4.

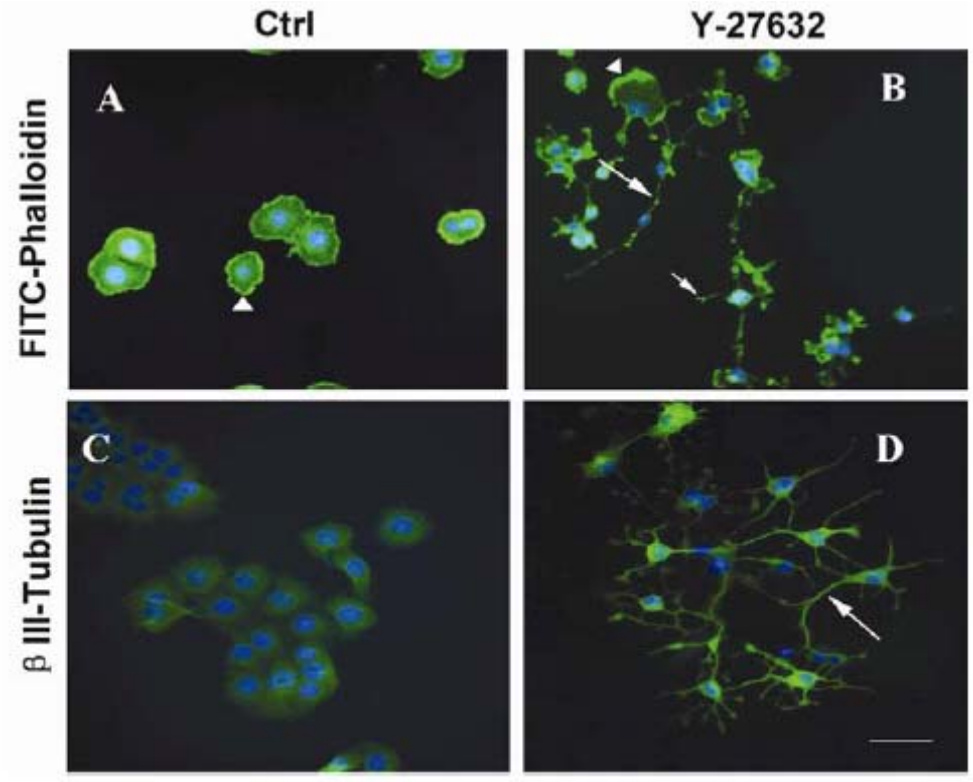

Figure 5-4. Reorganization of cytoskeletal architecture in ROCK inhibition mediated neurite outgrowth. PC-12 cell nuclei were visualized with DAPI-DNA staining (blue). Panel A and B were FITC-phalloidin F-actin-staining (green) following treatment with Y-27632. Before treatment, F-actin is uniformly localized in the periphery of the soma (triangle in panel A). After 12-hour treatment, F-actin became highly accumulated in growth cone-like structures (short arrow in **panel A**), the neurites (long arrow in **panel C)** and lamellipodia (triangle in **panel B**). Panels C through D were Alexa 488-conjugated neuronal specific βIII-tubulin immunostaining (green). Most βIII-tubulin is concentrated in nascent neurites (arrow in **panel D**). Cells were treated by DMSO as a control (A, C) or 25 μM Y-27632 (B, D) for 12 hours prior to fixation. Scale bar represents 50 μm.

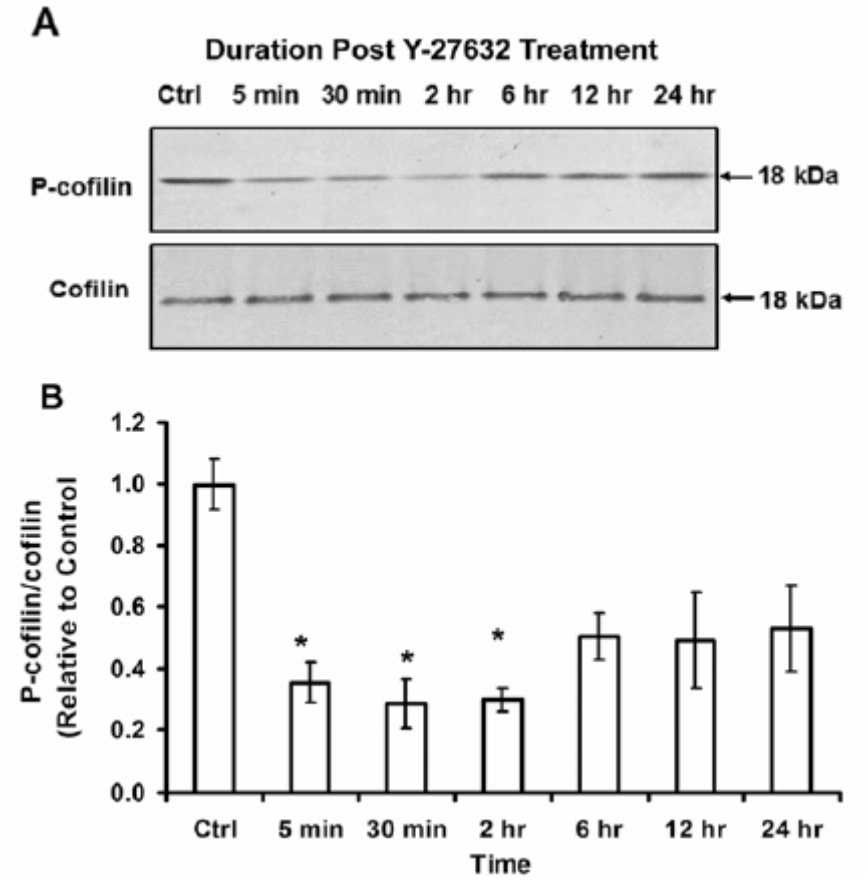

Figure 5-5. Immunoblot analysis of cofilin phosphorylation following Y-27632 treatment. **A**) PC-12 cells were treated with ROCK inhibitor (Y-27632; 25 μM) for various time points. Total protein lysate were extracted for immunoblotting analysis with phospho-cofilin (P-cofilin) and total cofilin antibodies. Representative blots were shown here. **B**) Densitometric analyses of cofilin immunoblots were performed. The optical densities of phospho-cofilin were normalized to the corresponding values for total cofilin. Values represent means ± S.E.M. n = 4. Statistical significance of differences between the control and each treated group was determined by one-way ANOVA with Dunnett's multiple comparison tests. A difference was considered to be statistically significant when the *P* value was less than 0.01 (**P* < 0.01).

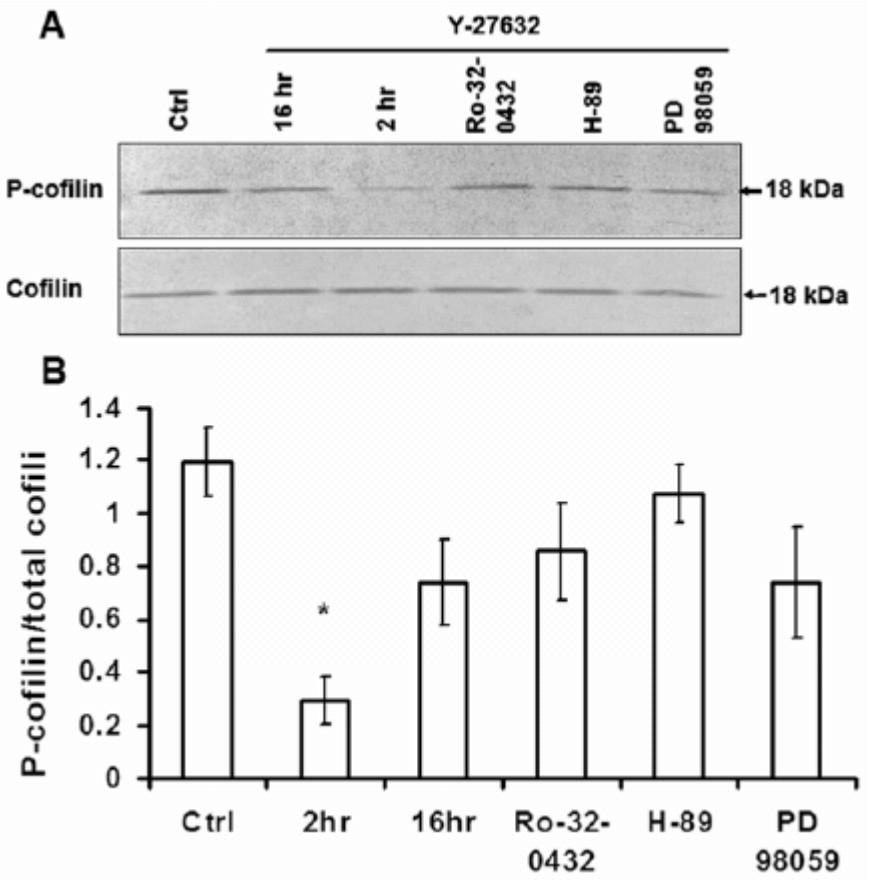

Figure 5-6. Effect of various protein kinase inhibitiors on cofilin rephosphorylation in the presence of Y-27632. (A) PC-12 cells were treated with ROCK inhibitor (Y-27632; 25 μM) for 2 h. For the same conditions, protein protein kinase-A (H-89; 500 nM), protein kinase-C (Ro-32-0432, 300 nM) or MAPK (PD98059, 30 μM) attenuated cofilin rephosphoryaltion. The cells were further incubated to 16 hour before cell lysate was collected for immunoblotting analysis with phospho-cofilin (P-cofilin) and total cofilin antibodies. (B) Densitometric analyses of cofilin immunoblots were performed. The optical densities of phospho-cofilin were normalized to the corresponding values for total cofilin. Values represent average from two experiments (*$P < 0.01$).

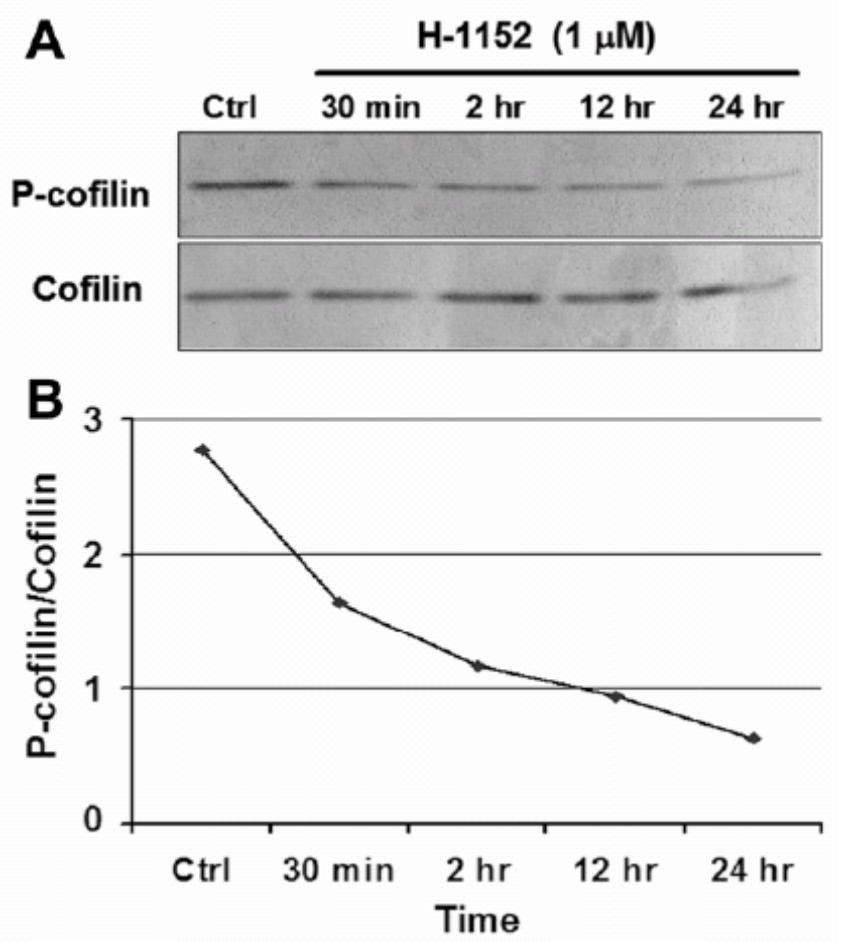

Figure 5-7. Persistent cofilin phosphorylation following ROCK inhibitor H-1152 treatment. (A) PC-12 cells were treated with ROCK inhibitor (H-1152; 1 μM) for various time points (30 min, 2 h, 12 h and 24 h). Total protein lysate were extracted for immnuoblotting analysis with phosphor-cofilin (P-cofilin) and total cofilin antibodies. Representative blots were shown here. (B) Densitometric analyses of cofilin immunoblots were performed. The optical densities of P-cofilin were normalized to the corresponding values for total cofilin. Values represent means from two separate experiments.

CHAPTER 6
SYSTEMS BIOLOGY APPROACH TO DECIPHER NEURITOGENESIS: ROCK PATHWAYS IN MEDIATING NEURITE OUTGROWTH IN PC-12 CELLS

Introduction

Traumatic brain injury (TBI) is a major cause of death and disability in young people less than 24 years old (www.cdc.gov). The pathogenesis of TBI involves two components: the initial mechanical injury and the subsequent secondary events, which further increase the brain damage. The secondary injury results in a massive enlargement of the initial small primary lesion, typically characterized by disrupted axons, a cystic cavity encased within a glial scar, and a variable amount of intact tissue (Hayes et al., 1998; Denslow et al., 2003; Wang et al., 2004). The clinical challenge is to promote compensatory sprouting from neurons with intact axons or the re-growth of axons across the injury site. Unlike the peripheral nervous system, axons in the adult central nervous system (CNS) rarely undergo spontaneous regeneration after injury. This lack of regeneration appears to be due to inhibitory elements within the CNS environment, such as myelin and the glial scar. Over the past two decades, Nogo-A, myelin-associated glycoprotein (MAG), and oligodendrocyte myelin glycoprotein (OMgp) have been well-characterized as CNS/myelin-associated inhibitors (Yamashita et al., 2005). Other neurite growth inhibitors have also been found directly at the lesion site or glial scar tissue. These inhibitors include chondroitin sulfate proteoglycans (CSPG), semaphorins, ephrins, and other repulsive guidance molecules (McKerracher et al., 1994; Kwon et al., 2002; McKerracher and David, 2004). Interestingly, recent studies indicate that Rho-Rho kinase (ROCK) is at the convergent point of those multiple neurite growth inhibitory pathways. A number of studies have demonstrated that inhibition of small Rho-GTPases by bacterial toxin Clostridium botulinum exoenzyme C3 transferase (C3) and Rho kinase (a downstream effecter of RhoA) by Y-27632 can promote axonal regeneration by overcoming the inhibitory effects of CSPG, as well as those of semaphorin 4A, ephrins A5

and other repulsive guidance molecules (Wahl et al., 2000; Monnier et al., 2003a; Yukawa et al., 2005). More specifically, Nogo, MAG, OMgp through downstream receptor NgR, p75 and LINGO-1 complex, activate the RhoA-ROCK pathway to execute the neurite growth inhibition (Selzer, 2003; Tang, 2003; Yamashita et al., 2005).

Most importantly, a variety of evidences indicate that TBI or spinal cord injury (SPI) induces activation of RhoA and RhoB at the lesion site in human brains (Brabeck et al., 2003; Brabeck et al., 2004) and of ROCKI and ROCKII in rats (Aimone et al., 2004). Intriguingly, the observed upregulation of RhoA and RhoB is still detectable months after TBI in humans (Brabeck et al., 2004) and at least for a period of 4 weeks after spinal cord injury (SCI) in rats (Conrad et al., 2005). Due to the persistent activation of Rho-ROCK pathway around the lesion site, makes Rho-ROCK inhibition an attractive site for therapy intervention not only for acute and sub-acute treatments, but also for delayed interventions after CNS injury.

Fortunately, a number of specific ROCK inhibiting compounds have been developed, including H-89, HA-1077, Y-27632 (Davies et al., 2000), wf-536 (Nakajima et al., 2003), and H-1152 (Ikenoya et al., 2002) . The selective inhibition of ROCK makes Y-27632 very useful for evaluating ROCK functions in CNS since ROCK is highly expressed in the brain. Taken together, targeting the ROCK pathway offers the advantage of antagonizing multiple neurite growth inhibitors. However, the Rho-ROCK pathway is also involved in a number of ubiquitous cell functions unrelated to neurite genesis including ruffling, motility, cytokinesis, and cell spreading (Schwartz, 2004; Hall, 2005). Therefore, it is reasonable to assume a subgroup of downstream targets from ROCKare directly involved in neurite growth while the rest are involved in other ROCK-mediated cell functions.

In this study, a system biological approach for studying the PC-12 cells neurite outgrowth model *in vitro* was applied to identify the molecular players in the ROCK pathways linked to neurite genesis. Here, we conducted gene regulatory networks, protein networks, and relationships between genomic and proteomic levels with neurite morphological changes that might be linked with the axon regeneration. This new research generated a massive data set, from which emerged the junction of two different fields, biomedicine and data analysis. One of the pioneering interdisciplinary fields that has enormous potential for making the most of the information such as in the above data sets is systems biology. Systems biology is a latest addtion to biology that aims at system-level understanding of complex biological processes. The scope of systems biology combines multiple advanced research areas, such as biosciences, data mining, control theory and a number of different engineering fields (Kitano, 2002). The novelty of the present study is in combining advanced data mining methods with the novel application of systems biology to study neurite outgrowth and axonal regeneration. Specifically, we applied correspondence analysis and DTAselect to the data sets produced by sophisticated biological experiments that were carried out to study the underlying mechanisms at the gene and protein levels (Oda et al., 2005). This study will help significantly in increasing our understanding of the mechanisms involved in axonal regeneration and will help in developing strategies to manipulate axonal regeneration in various CNS pathologies such as TBI, stroke and Alzheimer's disease.

Experimental and Computational Methods

Cell Culture

PC-12 cells were maintained at 37ºC in Dulbeco's modified Eagle's medium (DMEM) supplied with 10% fetal bovine serum (FBS), 5% heat-inactivated horse serum, 100 μg/ml of streptomycin, 100 U/ml of penicillin and 1% Fungizone (Gibco, Rockville, MD) in a humidified 5% CO_2 incubator. To induce neurite outgrowth, PC-12 cells were plated in the same medium

with 25 μM Y-27632 (Calbiochem, San Diego, CA). An equal amount of DMSO was added to control plates. Micrographs of cells were taken at 32 x with an Axiocam digital camera using a Zeiss Axiovert 135 microscope.

RNA Isolation

Total RNA from control and Y-27632 treated PC12 cells were isolated using the RNeasy Mini Kit (Qiagen, Maryland USA) according to the manufacturer's instructions. The amount and quality of RNA was determined using the Agilent 2100 system before performing the microchip arrays. Two independent pairs of samples were performed.

Affymetrix GeneChip

Differential gene expression analysis was performed on Affymetrix GeneChip® Rat genome 230 2.0 (Santa Clara, CA). Briefly, a T7 promoter-dT primer was used to generate cDNA with SuperScript II reverse transcriptase (Invitrogen, Carlsbad, CA) and amplified by *in vitro* transcription using T7 RNA polymerase. A second round of cDNA synthesis was performed using random hexamers as primers, and a final *in vitro* transcription using biotin-labeled nucleotides (Bioarray High Yield RNA; Enzo Life Sciences, Farmingdale, NY) yielded labeled cRNA for microarray hybridization. Fragmentation of the cRNA, hybridization, staining, and scanning of the microarray were performed according to the GeneChip Expression Analysis Manual provided by Affymetrix.

Sample Preparation for Protein Differential Analysis

Control and ROCK inhibitor treated PC-12 cells were solubilized in 0.1% SDS, 150mM NaCl, 3 mM EDTA, 2 mM EGTA, 1% IGEPAL, 1 mM Na_3VO_4 and a protease inhibitor cocktail tablet (Roche, Indianapolis, IN). 1mg samples of each were prepared for protein sepression. A Bio-Rad (Hercules, CA) Biologic DuoFlow system with QuadTec UV detector and BioFrac fraction collector was used with Uno series SCX (S1) and SAX (Q1) serially placed ion

exchange columns. Ice cold 20 mM Tris-HCl buffers (pH 7.5) were used (mobile phase A) with 1 M NaCl (Fisher Scientific, crystalline 99.8% certified) as the elution buffer (mobile phase B). Thirty-one 1ml fractions were automatically collected. Differential analysis between control and treatment groups were performed by pairing fractions for loading side by side on Bio-Rad Criterion 10-20% gradient sodium dodecyl sulfate-polyacrylamide gel electrophoresis (SDS-PAGE).

In-Gel Digestion

Bands (4 x 1 mm) with differential protein expression were excised and washed with HPLC water, then 50% 100 mM ammonium bicarbonate/ 50% acetonitrile. Pieces were dehydrated with 100% acetonitrile followed by speed vac. Cubes were rehydrated with 10 mM dithiothreitol for 30 min at 56° C. Dithiothreitol was replaced by 50ul of 55mM ammonium bicarbonate and incubated for 30 minutes in the dark at room temperature. This was followed by washing step followed with 100% acetonitrile, 15 ul of a 12.5 ng/ul trypsin solution for 30 minutes at 4° C, then 20 ul of 50 mM ammonium bicarbonate was added overnight at 37°C. The peptide extract was dried and resuspended in mobile phase.

Capillary RPLC-MSMS Based Protein Identification

Capillary reversed phase liquid chromatography tandem mass spectrometry protein identification was performed as described previously. Briefly, sample digests (2 μL) were loaded via an autosampler onto a 100 μm x 5 cm c-18 reversed phase capillary column at 1.5 μl/min. Peptide elution was performed by linear gradient: 5% to 60% methanol in 0.4% acetic acid over 30 minutes at 200 nL/min. Tandem mass spectra were collected in data-dependant mode (3-most intense peaks) on a Thermo Electron LCQ Deca XP plus ion trap mass spectrometer. Tandem mass spectra were searched against a NCBI rat indexed RefSeq protein database using Sequest. Filtering and sorting was performed with DTAselect software by

peptide number and Sequest cross correlation values (Xcorr values of 1.8, 2.5, 3.5 for +1, +2, +3 charge states(Tabb et al., 2002). Peptides filtered and sorted by DTAselect were assigned to specific protein accession numbers (National Center for Biotechnology Information [NCBI]).

Feature Selection

Two related statistical techniques are used in this study. The first technique is implemented using the two-sample t-test given that the normality assumption holds for the data. The other technique is based on the Wilcoxon rank-sum test, which is a non-parametric alternative to the t-test, allowing us to avoid the above assumption.

Results

Correpsondence Analysis for the Microarray Data of ROCKi Induced Neurite Outgrowth

We performed a numerical analysis of the data set describing the gene expression levels that were obtained in the microarray experiments. By using correspondence analysis, all samples and data points of a given data set can be mapped onto one low-dimensional space visualized as either as a biplot (2-D) or as a 3-D diagram (Fellenberg et al., 2001). Each axis of such a plot or diagram has the remarkable tendency for providing an insightful characterization of the data set. Furthermore, the samples/data points with a high degree of similarity with respect to such characterization also have very similar coordinates on the correspondent axis. A data set can be conveniently described by a rectangular matrix $A = (aij)m\times n$ of n samples (columns of the matrix) and m data points (rows of A). When working with the microarray data, genes are represented by rows, so that the value aij specifies the expression level of gene i in sample j. Given that we handle both columns and rows of the data matrix in a unified manner. This is in addition to the fact that we are always able to use the transpose of the data matrix without making any changes in the algorithm, it follows that, without loss of generality, we can assume

that m > n. In order to perform corresponding analysis, we first construct the correspondence matrix P = (pij)m×n by computing

$$p_{ij} = \frac{a_{ij}}{\sum_{i=1}^{m}\sum_{j=1}^{n} a_{ij}}$$

To some extent, the correspondence matrix is similar to a two-dimensional probability distribution table, where the sum of the elements equals 1. Next we calculate masses of rows and columns as follows:

$$r_i = \frac{\sum_{j=1}^{n} a_{ij}}{\sum_{i=1}^{m}\sum_{j=1}^{n} a_{ij}}$$

$$c_j = \frac{\sum_{i=1}^{m} a_{ij}}{\sum_{i=1}^{m}\sum_{j=1}^{n} a_{ij}}$$

Notice that the masses of columns or rows are also comparable to the marginal probability densities. Subsequently, we build the matrix S = (sij)m×n, to which SVD is later applied

$$s_{ij} = \frac{\left(p_{ij} - r_i c_j\right)}{\sqrt{r_i c_j}}$$

By means of the SVD the matrix S is represented as a product of three matrices as follows: S = U^V T , where matrices U and V are unitary, and D is a diagonal matrix. In particular, columns of the matrix U = (uij)m×n are orthonormal vectors spanning the columns of S, while columns of the matrix V = (vij)n×n are orthonormal vectors spanning the rows of S. One can easily show that in order to describe the optimal low-dimensional subspace (where the columns of S are to be projected) where the information loss would be minimum, it is enough to consider a suitable number of first columns of U. Likewise, the optimal low-dimensional subspace for projecting the rows of S can be constructed using an equal number of first columns of V. In

addition, as a consequence of the aforementioned properties of the matrix S, the columns and rows of the original data set, matrix A, may be represented in one low-dimensional space of dimensionality K < n in the following manner:

$$f_{ik} = \frac{\lambda_k u_{ik}}{\sqrt{r_i}}, \quad k = 1, 2, ..., K$$

gives the k-th coordinate of the row I, and

$$g_{jk} = \frac{\lambda_k v_{jk}}{\sqrt{c_j}}, \quad k = 1, 2, ..., K$$

gives the k-th coordinate of the j-th column in the new space. Clearly, by choosing K = 2, we obtain a bi-plot, while taking K = 3 gives us a 3-D diagram of the analyzed data set. All genes shaving at least one absent call in the data set were discarded. The resulting data array had 4 samples and 11,419 features (genes). Next, a statistical analysis was performed to select the informative genes by means of the Wilcoxon rank-sum test. The feature selection algorithm based on the Wilcoxon test selected a total of 4,002 relevant features out of the analyzed 11,419 features. With a high probability we assumed that the selected relevant features represent the genes that are involved in regulation of the processes underlying neurogenesis and axonal regeneration. To observe the up-regulated genes from the down-regulated genes we further obtained a two-dimensional projection of the data using correspondence analysis. The resulting projection onto the plain is shown in Figure 6-1.

From the biplot of the data in Figure 6-1, we can see that the first (horizontal) axis discriminates all the active (up-regulated) genes against all the genes that need to be suppressed for a neuritogenesis in a PC-12 cell to take place (i.e. down-regulated). Particularly, the points of the biplot with the most positive coordinates on this axis correspond to the up-regulated genes, whereas the points having the most negative coordinates represent the genes that are down-regulated.

Identification of ROCKi-induced Neurite Outgrowth Transcriptome

The list of genes whose biplot projection points have the most positive first coordinates gives the up-regulated genes upon ROCK inhibition induced neurite outgrowth, shown in Table 6-1 below. Next, we also selected points with the most negative first coordinate. The resulting down-regulated genes are summarized in Table 6-2. All genes with perturbation were searched against the Gene Ontology Consortium (http://www.geneontology.org (Harris et al., 2004)) and grouped into categories that define their biological and molecular functions, as indicated in Tables 1 and 2. Many of those genes were found to be functionally unclassified. The rest of the groups of up-regulated genes are involved in transcription, cell signaling, cell cycle regulation, cytoskeleton/motility protein, cell adhesion receptor, trafficking proteins, cell receptors and metabolism et al. Some of the up-regulated genes include rhoB, drebrin, neuritin, S-100 calcium binding protein, olfactomedin 1, Per1 interacting protein, protein kinase C, BCL-2 and bone morphogenetic protein 2 (BMP2). neurexophilin 3, prostaglandin E synthase, bone morphogenetic protein 7, histone deacetylase 10, and Nogo-66 receptor (NgR).

Identification of Differentially Expressed Proteins by RPLC-MSMS

Differential protein expression analysis was accomplished by multi-dimensional separations involving biphasic ion-exchange chromatography in tandem followed by LC-MS/MS protein identification. Thirty-two fractions collected from each CAX experiment were paired (i.e., fraction 1of control with fraction 1 of ROCK inhibitor treatment) and loaded side-by-side onto 1D-PAGE for the second dimension protein separation. The gels were visualized with Coomassie blue stain for differential band analysis. Thirty-five bands with an observed difference in densitometry were selected and excised for proteomic analysis as boxed and labeled in Figure 6-2. In all, more than 20 proteins were confirmed to be differentially expressed between control and Y-27632 treated PC-12 cells as shown in Table 6-3. Those proteins are

presented here with their respective GI numbers along with the calculated mass spectrometry sequence coverage along with the SDS-PAGE apparent molecular mass. The identified proteins were grouped into upregulated or downregulated abundance in Table 6-4. The proteins that upregulated upon ROCK inhibitor treatment include cytoskeleton associated proteins (talin, 14-3-3 protein and filamin), S-100 calcium binding protein, heat shock protein, ubiquitin carboxyl extension protein 80 and programmed cell death 6 interacting protein and others. Among the downreuglated proteins are annexin II, cerebellar postnatal development protein 1, proliferation related acidic leucine rich protein PAL31 and heat shock protein 70K.

Discussion

In this paper we employed an innovative methodology for applying the systems biology approach to the complex biological system underlying neurite outgrowth and axonal regeneration. We presented an integrated approach to data mining of microarray data that incorporates feature selection based on statistical analysis with the dimensionality reduction by means of projection methods (Fellenberg et al., 2001). In particular, the relevant features were selected from the obtained gene expression data using the Wilcoxon rank-sum test, and then the selected data was projected onto a two-dimensional space using the correspondence analysis algorithm. Utilizing statistical procedures to perform feature selection significantly aids in reducing the number of features in a data set. In addition, the Wilcoxon test is a non-parametric procedure, and hence does not require any assumptions about the distribution of data to hold. Also application of correspondence analysis allows us to obtain an informative projection of high-dimensional data onto a low-dimensional space, and then visually explore the data. In addition, correspondence analysis offers some additional advantages. First, this technique does not require any prior information about classification of samples or features of the data set. Second, unlike many other data mining procedures, correspondence analysis is very

computationally efficient. To summarize, application of data mining techniques to the study of systems biology of PC-12 cells proves to be especially useful as it allows us to answer the key questions about the processes underlying neurogenesis at the gene level. Furthermore, such approach can be applied to many others biomedical studies based on analysis of the microarray data that can be naturally subdivided into some classes.

Of those differentially expressed genes, some of them are particularly interesting and need to be further studied. It has been reported that application of the selective ROCK inhibitor, Y-27632 preferentially lowered brain levels of Abeta42 in a transgenic mouse model of Alzheimer's disease (AD) (Zhou et al., 2003). However, the mechanism underlying the ROCK inhibition contribution to AD is still unknown. Our data suggests that Y-27632 induces up-regulation of drebrin and down-regulation of prostaglandin E synthase. Drebrin, an acitn-binding protein, is localized in postsynaptic terminals of adult brains and regulates synaptic plasticity. A remarkable reduction of drebrin was found in Alzheimer's disease brains (Harigaya et al., 1996; Counts et al., 2006). In another case, Prostaglandin E (PGE) synthase highly influences the synthesis of the inflammatory factor PGE. Thus, Y-27632 may alleviate the pathogenesis and memory loss of AD by inhibiting prostaglandin E synthase and stimulating the expression of drebrin.

Interestingly, several apoptosis related genes have also been implicated in relation to the ROCK inhibitor induced neurite outgrowth model, such as Bcl-2 and Annexin II. The role of Bcl-2 family members on axonal regeneration has thus far been controversial. Delivering recombinant, or over-expressed Bcl-2, into retinal tissue stimulates axonal initiation but not axonal elongation after crush injury to retinal explants, which is independent of its anti-apoptotic role. The subsequent activation of ERK and CREB may underlie the ability of Bcl-2 to promote

axon regeneration (Chen et al., 1997; Jiao et al., 2005; Dietz et al., 2006). ROCK inhibition might lead to increased levels of Bcl-2, thereby contributing to the axon regeneration after brain injury.

It has been shown that MAG, NogoA and OMgp can bind to NgR, Lingo and p75 or TROY to form trimeric receptor complexes, and thus activate Rho-ROCK pathway leading to its inhibitory effects on axons (Yamashita et al., 2005). Consistent with previous studies, ROCK inhibition reduces NgR expression, thereby enhancing neurite outgrowth. Neuexophilin 3 is highly expressed in the brain (Beglopoulos et al., 2005; Dudanova et al., 2006; Craig and Kang, 2007). A group of bone morphogenetic proteins also have been changed with Y-27632 treatment. The exact influence of ROCK on those proteins is still unknown. Further genetic studies are needed to explore their functions.

There were 35 pairs of bands were cut in our proteomic study. Eighteen proteins were identified as being up-regulated and four proteins were found to be down-regulated after ROCKi treatment. Of these identified proteins, only one protein, S-100 calcium binding protein, was shown to be differentially regulated at the mRNA level using microarray analysis. The lack of correlation between mRNA and protein levels may be due to several reasons. In terms of the transcriptome, microarrays provide a abundance measurement for a finite set of targets, while a typical proteome analysis does not. The current technical challenges, such as the presence of splice isoforms in the transcriptome, the incomplete protein index database and sensitivity limitations of mass spectrometry in proteome analyses affect the data sets generated. In addition, instead of being static, mRNAs and proteins are highly dynamic, they change in numerical, spatial and temporal patterns. Typical transcriptomic and proteomic profiles are snapshots of a specific time point. There is not enough resolving power to distinguish newly-synthesized

transcripts or proteins from those accumulated over time. Dynamic and high-throughput quantitative assays might be needed to determine the proteome. Finally, the proteomes we examined at a specific point in time isnot a replica of the underlying transcriptomes. After transcription from DNA to RNA, the gene transcript can be spliced in different ways prior to its translation into a specific protein. Following translation, most proteins are chemically altered through post-translational modifications. As a consequence, the information from a single gene may encode many different proteins. There are already compelling data suggesting that proteomics is a complement or alternative to mRNA based measurements. Those quantitative data sets will give us insight into how cells responsed to a given stimuli and allow us to construct a systems biology.

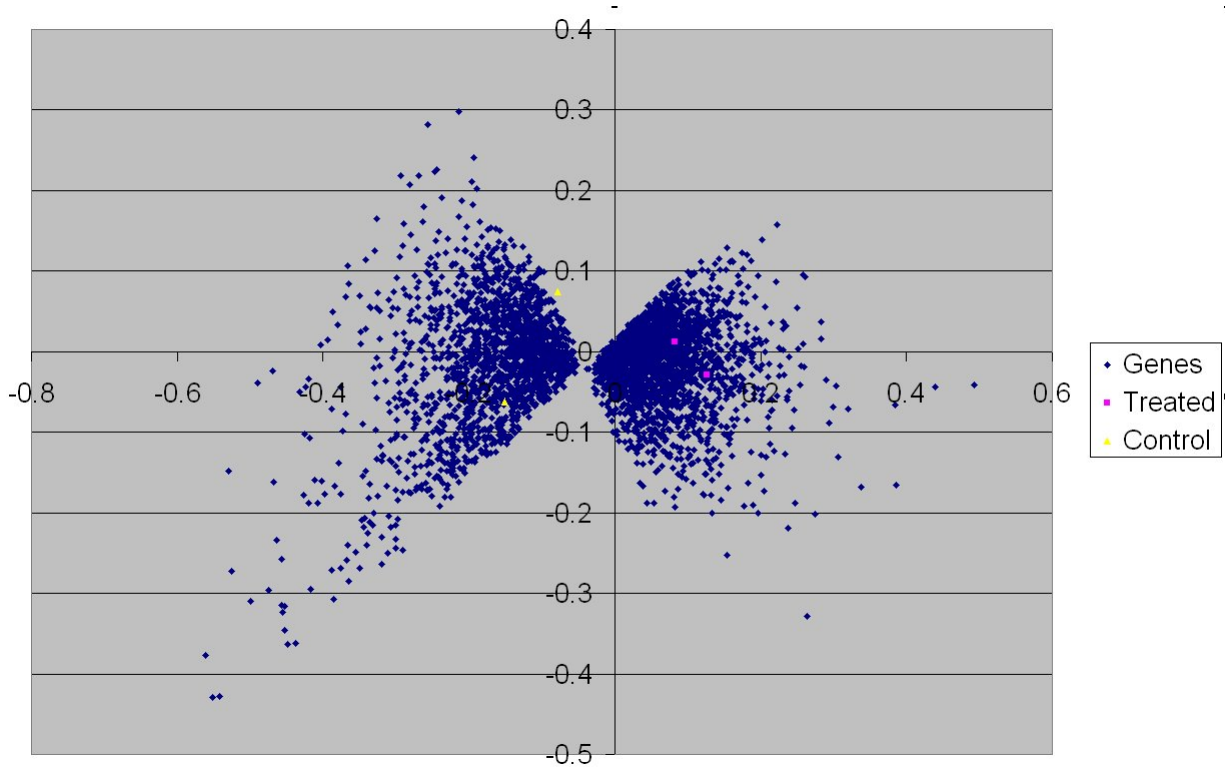

Figure 6-1. Correspondence analysis bipot for PC-12 microarray dataset

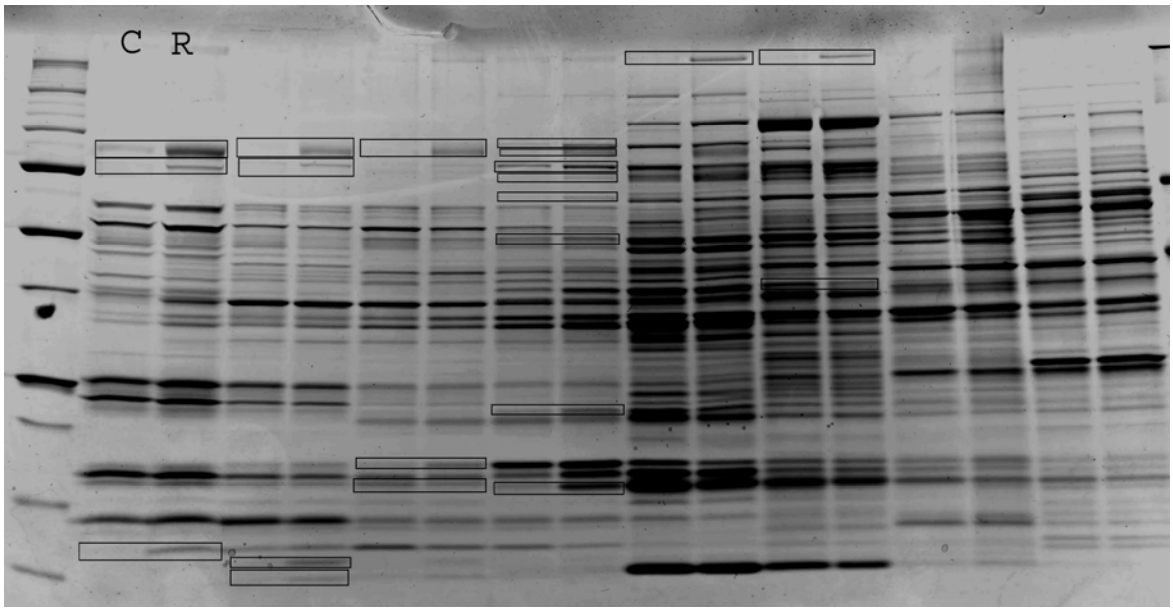

Figure 6-2. One representative proteome of ROCK inhibition induced neurite outgrowth visualized on 1D-PAGE following CAX Fractionation. One milligram of PC-12 lysate was divided into 32 CAX fractions resolved on 1D-polyacrylamide gel electrophoresis and gels were stained with Coomassie Blue staining. Control and treatment samples were run side by side.

Table 6-1. The up-regulated genes upon Y-27632 treatment

Functional group	%
Transcription	4.2
Cell cycle	1.4
Oncogenes and tumor suppressors	6.9
Membrane channels and transporters	1.4
Trafficking/targeting proteins	1.4
Metabolism	5.6
Post-translational modification/protein folding	2.8
Apoptosis associated proteins	1.4
Cell receptors	4.2
Cell signaling, extracellular communication proteins	2.8
Intracellular transducers/effectors/modulators	5.6
Cytoskeleton/motility proteins	2.8
DNA synthesis, recombination, and repair	1.4
Unclassified	56.9

Table 6-2. The down-regulated genes upon Y-27632 treatment

Functional group	%
Transcription	5.6
Cell cycle	1.1
Cell adhesion receptors/protein	1.1
Oncogenes and tumor suppressors	1.1
Stress response proteins	2.2
Membrane channels and transporters	1.1
Trafficking/targeting proteins	3.3
Metabolism	3.3
Translation	1.1
Cell receptors	5.6
Cell signaling, extracellular communication proteins	2.2
Unclassified	72.2

Table 6-3. Proteins with Increased Abundance post Y-27632 treatment

Protein Name	GI Number	MW of Protein(kDa)	MW from gel(kDa)	Matched peptides in Control	Sequence Coverage in Control (%)	Matched peptides in ROCKi	Sequence Coverage in ROCKi (%)
Aconitase 2, mitochondrial	gi|18079339	85.5	82	1	1.2	13	18.2
Fibroblast growth factor receptor 4	gi|6679789	89.8	90	0	0	1	1.4
Aconitase 2, mitochondrial [Mus musculus	gi|18079339	85.5	82	1	1.7	8	12.6
S100 calcium-binding protein A	gi|4506761	11.2	11	0	0	1	7.2
Ubiquitin carboxyl extension protein 80	gi|4506713	18	10	2	16	4	25.6
Programmed cell death 6 interacting protein	gi|6755002	96	95	1	1.2	12	13.3
Transketolase	gi|6678359	67	65	0	0	4	2.7
Eukaryotic translation elongation factor 2	gi|33859482	95	90	0	0	8	10.8
Gamma filamin	gi|4557597	288	280	3	1.6	12	5.1
Heat shock 90kDa protein 1	gi|2014594	84	85	1	1	3	3.2
Laminin receptor 1	gi|31560560	33	38	3	11.9	6	20.3
L4-3-3 protein, zeta polypeptide	gi|6756041	27.7	28	1	4.9	2	10.6
L4-3-3 protein tau	gi|5803227	27.7	28	1	6.5	2	12.2
Talin 1	gi|16753233	270	270	0	0	9	4.1
Alpha 2 macroglobulin precursor	gi|4557225	163	180	0	0	2	1.4
SET translocation	gi|13591862	33	35	0	0	1	3.5

Table 6-4. Proteins with decreased Abundance post Y-27632 treatment

Protein Name	GI Number	MW of Protein(kDa)	MW from gel(kDa)	Matched peptides in Control	Sequence Coverage in Control (%)	Matched peptides in ROCKi	Sequence Coverage in ROCKi (%)
Heat shock protein 70k	gi|31981690	70.8	71	1	12.2	7	14.1
Annexin II	gi|4757756	38.6	35	6	20.4	0	0
Proliferation related acidic leucine rich protein PAL31	gi|18777770	31	31	1	5.1	0	0
Cerebellar postnatal development protein 1	gi|31542131	29.6	30	1	5.4	0	0

CHAPTER 7
CONCLUSIONS AND FUTURE DIRECTIONS

Many significant advances have been made recently to sharpen our understanding of important molecular mechanisms involving in axon/neuronal injury. Given one of the key mediator of axonal injury is Ca2+ "dyshomeostasis", calmodulin binding proteins (CaMBPs) are particularly vulnerable to two abnormal processes: (i) over-activation by calcium bound calmodulin (CaM), and (ii) proteolytic processing by calpains and caspases. Thus, it is imperious to study the calmodulin signal pathway in a systematic manner after traumatic injury. In chapter 2, we developed a novel CaM-affinity capture method coupled with reversed-phase liquid chromatography tandem mass spectrometry (RPLC-MSMS) to identify the calcium-dependent CaM-binding proteome in rat brain and its vulnerability to calpain and caspase. Our results suggested that this is a simple and efficient way to explore the CaM-binding proteome and its vulnerability to proteolysis. A comprehensive protein-protein interaction map was constructed to facilitate understanding how brain cells respond in terms of initiating proteases to Ca2+ stimuli. In this map, brain enriched CRMP-2 is of most interest to further study. CRMP-2 plays a crucial role in neurite outgrowth and axon formation. As described in chapter 3, it is the first time we demonstrated the degradation of CRMP-2 after acute neuronal injuries by in vivo TBI and in vitro glutamate excitotoxicity. Furthermore, calpain-2 was identified as the possible proteolytic mediator of CRMP-2 following excitotoxic injury and TBI which appears to correlate well with neuronal cell injury and neurite damage. CaM binds to CRMP-2 in a calcium dependent manner, thereby preventing proteolysis of CRMP-2 both in vivo and in vitro. Meanwhile, CaM binding to CRMP-2 might play a role in F-actin bundling, and in turn maintain a stable structure or enhance axonal regeneration.

Although it is excited to construct a Ca2+/CaM interactions map, the mechanisms of axonal injury in CNS is enormously complex. Axons fail to regenerate in the adult central nervous system (CNS) after injury. Fortunately, both inhibitory and permissive pathways converge at the Rho/ROCK (Rho-associated kinase) pathway. Thus, Rho-ROCK is an emerging target to promote axonal regeneration and functionary recovery. However, inhibition of ROCK pathway in vivo is a complex process, with numerous specific downstream effectors that may or may not involve in axonal regeneration. This is further complicated by the temporal and spatial nature of many of these effects. As a result, it is critical to evaluate the entire cellular system from the neuritogenesis perspective to include differential expression of transcriptome, proteome and even phosphor-proteome. In chapter 5, we found that ROCK inhibitor can induce robust neurite outgrowth in PC-12 cells and it initiated neuritis through dephosphorylation of cofilin. Next, differential gene transcriptome and protein expression influenced by ROCK inhibition were identified by affymetrix Mciroarray and proteomic studies in a systems biology approach. More than 200 genes and 20 proteins, many of which are known to be associated with neuritogenesis or cell growth, were potentially involved in ROCK inhibition induced neurite outgrowth in PC-12 cells. Post translation modification might contribute to the lack of correlation between mRNA and protein level.

Thus a comprehensive picture emerged after applying ROCK inhibition from not only one single downstream effecter but whole cell response. Studies such as these can ultimately be used to understand the molecular events that accompany neuritogenesis, and therefore to develop more specific therapeutic targets and assess the cell response after applying the medicine. Further investigation is underway be exploring the role of these genes or proteins in injury animal model by a combination of biochemistry, cell biology and molecular biology.

Taken together, data from our studies provide clues regarding the perturbation factors that are important in the axonal injury/regeneration. We will further investigate the role of these proteins in pathophysilogical significance. Clinically, this systemic biological approach to decipher signal pathways may provide promising potential in finding novel biomarkers and therapeutic targets after axonal injury.

LIST OF REFERENCES

Adamec E, Beermann ML, Nixon RA (1998) Calpain I activation in rat hippocampal neurons in culture is NMDA receptor selective and not essential for excitotoxic cell death. Brain Res Mol Brain Res 54:35-48.

Aguayo AJ, David S, Bray GM (1981) Influences of the glial environment on the elongation of axons after injury: transplantation studies in adult rodents. J Exp Biol 95:231-240.

Aimone JB, Leasure JL, Perreau VM, Thallmair M (2004) Spatial and temporal gene expression profiling of the contused rat spinal cord. Exp Neurol 189:204-221.

Aizawa H, Wakatsuki S, Ishii A, Moriyama K, Sasaki Y, Ohashi K, Sekine-Aizawa Y, Sehara-Fujisawa A, Mizuno K, Goshima Y, Yahara I (2001) Phosphorylation of cofilin by LIM-kinase is necessary for semaphorin 3A-induced growth cone collapse. Nat Neurosci 4:367-373.

Amano M, Fukata Y, Kaibuchi K (2000) Regulation and functions of Rho-associated kinase. Exp Cell Res 261:44-51.

Amano M, Kaneko T, Maeda A, Nakayama M, Ito M, Yamauchi T, Goto H, Fukata Y, Oshiro N, Shinohara A, Iwamatsu A, Kaibuchi K (2003) Identification of Tau and MAP2 as novel substrates of Rho-kinase and myosin phosphatase. J Neurochem 87:780-790.

Ambach A, Saunus J, Konstandin M, Wesselborg S, Meuer SC, Samstag Y (2000) The serine phosphatases PP1 and PP2A associate with and activate the actin-binding protein cofilin in human T lymphocytes. Eur J Immunol 30:3422-3431.

Araujo IM, Verdasca MJ, Leal EC, Bahr BA, Ambrosio AF, Carvalho AP, Carvalho CM (2004) Early calpain-mediated proteolysis following AMPA receptor activation compromises neuronal survival in cultured hippocampal neurons. J Neurochem 91:1322-1331.

Arimura N, Inagaki N, Chihara K, Menager C, Nakamura N, Amano M, Iwamatsu A, Goshima Y, Kaibuchi K (2000) Phosphorylation of collapsin response mediator protein-2 by Rho-kinase. Evidence for two separate signaling pathways for growth cone collapse. J Biol Chem 275:23973-23980.

Arimura N, Menager C, Fukata Y, Kaibuchi K (2004) Role of CRMP-2 in neuronal polarity. J Neurobiol 58:34-47.

Arimura N, Menager C, Kawano Y, Yoshimura T, Kawabata S, Hattori A, Fukata Y, Amano M, Goshima Y, Inagaki M, Morone N, Usukura J, Kaibuchi K (2005) Phosphorylation by Rho Kinase Regulates CRMP-2 Activity in Growth Cones. Mol Cell Biol 25:9973-9984.

Arundine M, Tymianski M (2003) Molecular mechanisms of calcium-dependent neurodegeneration in excitotoxicity. Cell Calcium 34:325-337.

Babcock DF, Herrington J, Goodwin PC, Park YB, Hille B (1997) Mitochondrial participation in the intracellular Ca2+ network. J Cell Biol 136:833-844.

Barnes JA, Gomes AV (1995) PEST sequences in calmodulin-binding proteins. Mol Cell Biochem 149-150:17-27.

Barzilai A, Zilkha-Falb R, Daily D, Stern N, Offen D, Ziv I, Melamed E, Shirvan A (2000) The molecular mechanism of dopamine-induced apoptosis: identification and characterization of genes that mediate dopamine toxicity. J Neural Transm Suppl:59-76.

Beglopoulos V, Montag-Sallaz M, Rohlmann A, Piechotta K, Ahmad M, Montag D, Missler M (2005) Neurexophilin 3 is highly localized in cortical and cerebellar regions and is functionally important for sensorimotor gating and motor coordination. Mol Cell Biol 25:7278-7288.

Benaim G, Villalobo A (2002) Phosphorylation of calmodulin. Functional implications. Eur J Biochem 269:3619-3631.

Berglund A, Backman L, Shanbhag VP (1986) The 240-kDa subunit of human erythrocyte spectrin binds calmodulin at micromolar calcium concentrations. FEBS Lett 201:306-310.

Bignone PA, Baines AJ (2003) Spectrin alpha II and beta II isoforms interact with high affinity at the tetramerization site. Biochem J 374:613-624.

Birkenfeld J, Betz H, Roth D (2001) Inhibition of neurite extension by overexpression of individual domains of LIM kinase 1. J Neurochem 78:924-927.

Blesch A, Grill RJ, Tuszynski MH (1998) Neurotrophin gene therapy in CNS models of trauma and degeneration. Prog Brain Res 117:473-484.

Blesch A, Tuszynski MH (2007) Transient growth factor delivery sustains regenerated axons after spinal cord injury. J Neurosci 27:10535-10545.

Boivin P, Galand C (1984) Is spectrin a calmodulin-binding protein? Biochem Int 8:231-236.

Bonini S, Rasi G, Bracci-Laudiero ML, Procoli A, Aloe L (2003) Nerve growth factor: neurotrophin or cytokine? Int Arch Allergy Immunol 131:80-84.

Bouche N, Yellin A, Snedden WA, Fromm H (2004) Plant-Specific Calmodulin-Binding Proteins. Annu Rev Plant Biol.

Brabeck C, Beschorner R, Conrad S, Mittelbronn M, Bekure K, Meyermann R, Schluesener HJ, Schwab JM (2004) Lesional expression of RhoA and RhoB following traumatic brain injury in humans. J Neurotrauma 21:697-706.

Brabeck C, Mittelbronn M, Bekure K, Meyermann R, Schluesener HJ, Schwab JM (2003) Effect of focal cerebral infarctions on lesional RhoA and RhoB expression. Arch Neurol 60:1245-1249.

Braun H, Schafer K, Hollt V (2002) BetaIII tubulin-expressing neurons reveal enhanced neurogenesis in hippocampal and cortical structures after a contusion trauma in rats. J Neurotrauma 19:975-983.

Bretin S, Reibel S, Charrier E, Maus-Moatti M, Auvergnon N, Thevenoux A, Glowinski J, Rogemond V, Premont J, Honnorat J, Gauchy C (2005) Differential expression of CRMP1, CRMP2A, CRMP2B, and CRMP5 in axons or dendrites of distinct neurons in the mouse brain. J Comp Neurol 486:1-17.

Bretin S, Rogemond V, Marin P, Maus M, Torrens Y, Honnorat J, Glowinski J, Premont J, Gauchy C (2006) Calpain product of WT-CRMP2 reduces the amount of surface NR2B NMDA receptor subunit. J Neurochem.

Buki A, Okonkwo DO, Wang KK, Povlishock JT (2000) Cytochrome c release and caspase activation in traumatic axonal injury. J Neurosci 20:2825-2834.

Buki A, Povlishock JT (2006) All roads lead to disconnection?--Traumatic axonal injury revisited. Acta Neurochir (Wien) 148:181-193; discussion 193-184.

Butterfield DA, Boyd-Kimball D, Castegna A (2003) Proteomics in Alzheimer's disease: insights into potential mechanisms of neurodegeneration. J Neurochem 86:1313-1327.

Cai D, Deng K, Mellado W, Lee J, Ratan RR, Filbin MT (2002) Arginase I and polyamines act downstream from cyclic AMP in overcoming inhibition of axonal growth MAG and myelin in vitro. Neuron 35:711-719.

Carafoli E (2003) Historical review: mitochondria and calcium: ups and downs of an unusual relationship. Trends Biochem Sci 28:175-181.

Chan CC, Khodarahmi K, Liu J, Sutherland D, Oschipok LW, Steeves JD, Tetzlaff W (2005) Dose-dependent beneficial and detrimental effects of ROCK inhibitor Y27632 on axonal sprouting and functional recovery after rat spinal cord injury. Exp Neurol.

Charrier E, Reibel S, Rogemond V, Aguera M, Thomasset N, Honnorat J (2003) Collapsin response mediator proteins (CRMPs): involvement in nervous system development and adult neurodegenerative disorders. Mol Neurobiol 28:51-64.

Chen DF, Schneider GE, Martinou JC, Tonegawa S (1997) Bcl-2 promotes regeneration of severed axons in mammalian CNS. Nature 385:434-439.

Chiesa R, Angeretti N, Del Bo R, Lucca E, Munna E, Forloni G (1998) Extracellular calcium deprivation in astrocytes: regulation of mRNA expression and apoptosis. J Neurochem 70:1474-1483.

Christensen AE, Selheim F, de Rooij J, Dremier S, Schwede F, Dao KK, Martinez A, Maenhaut C, Bos JL, Genieser HG, Doskeland SO (2003) cAMP analog mapping of Epac1 and cAMP kinase. Discriminating analogs demonstrate that Epac and cAMP kinase act synergistically to promote PC-12 cell neurite extension. J Biol Chem 278:35394-35402.

Chung MA, Lee JE, Lee JY, Ko MJ, Lee ST, Kim HJ (2005) Alteration of collapsin response mediator protein-2 expression in focal ischemic rat brain. Neuroreport 16:1647-1653.

Cole AR, Knebel A, Morrice NA, Robertson LA, Irving AJ, Connolly CN, Sutherland C (2004) GSK-3 phosphorylation of the Alzheimer epitope within collapsin response mediator proteins regulates axon elongation in primary neurons. J Biol Chem 279:50176-50180.

Conrad S, Schluesener HJ, Trautmann K, Joannin N, Meyermann R, Schwab JM (2005) Prolonged lesional expression of RhoA and RhoB following spinal cord injury. J Comp Neurol 487:166-175.

Counts SE, Nadeem M, Lad SP, Wuu J, Mufson EJ (2006) Differential expression of synaptic proteins in the frontal and temporal cortex of elderly subjects with mild cognitive impairment. J Neuropathol Exp Neurol 65:592-601.

Cousin MA (2000) Synaptic vesicle endocytosis: calcium works overtime in the nerve terminal. Mol Neurobiol 22:115-128.

Craig AM, Kang Y (2007) Neurexin-neuroligin signaling in synapse development. Curr Opin Neurobiol 17:43-52.

Croall DE, Chacko S, Wang Z (1996) Cleavage of caldesmon and calponin by calpain: substrate recognition is not dependent on calmodulin binding domains. Biochim Biophys Acta 1298:276-284.

Czech T, Yang JW, Csaszar E, Kappler J, Baumgartner C, Lubec G (2004) Reduction of hippocampal collapsin response mediated protein-2 in patients with mesial temporal lobe epilepsy. Neurochem Res 29:2189-2196.

Czogalla A, Sikorski AF (2005) Spectrin and calpain: a 'target' and a 'sniper' in the pathology of neuronal cells. Cell Mol Life Sci 62:1913-1924.

Dasgupta M, Honeycutt T, Blumenthal DK (1989) The gamma-subunit of skeletal muscle phosphorylase kinase contains two noncontiguous domains that act in concert to bind calmodulin. J Biol Chem 264:17156-17163.

Davies SJ, Fitch MT, Memberg SP, Hall AK, Raisman G, Silver J (1997) Regeneration of adult axons in white matter tracts of the central nervous system. Nature 390:680-683.

Davies SJ, Silver J (1998) Adult axon regeneration in adult CNS white matter. Trends Neurosci 21:515.

Davies SP, Reddy H, Caivano M, Cohen P (2000) Specificity and mechanism of action of some commonly used protein kinase inhibitors. Biochem J 351:95-105.

Del Rio JA, Soriano E (2007) Overcoming chondroitin sulphate proteoglycan inhibition of axon growth in the injured brain: lessons from chondroitinase ABC. Curr Pharm Des 13:2485-2492.

Denslow N, Michel ME, Temple MD, Hsu CY, Saatman K, Hayes RL (2003) Application of proteomics technology to the field of neurotrauma. J Neurotrauma 20:401-407.

Dent EW, Gertler FB (2003) Cytoskeletal dynamics and transport in growth cone motility and axon guidance. Neuron 40:209-227.

Dergham P, Ellezam B, Essagian C, Avedissian H, Lubell WD, McKerracher L (2002) Rho signaling pathway targeted to promote spinal cord repair. J Neurosci 22:6570-6577.

Dietz GP, Dietz B, Bahr M (2006) Bcl-x(L) increases axonal numbers but not axonal elongation from rat retinal explants. Brain Res Bull 70:117-123.

Dixon CE, Clifton GL, Lighthall JW, Yaghmai AA, Hayes RL (1991) A controlled cortical impact model of traumatic brain injury in the rat. J Neurosci Methods 39:253-262.

Dudanova I, Sedej S, Ahmad M, Masius H, Sargsyan V, Zhang W, Riedel D, Angenstein F, Schild D, Rupnik M, Missler M (2006) Important contribution of alpha-neurexins to Ca2+-triggered exocytosis of secretory granules. J Neurosci 26:10599-10613.

Dutta S, Chiu YC, Probert AW, Wang KK (2002) Selective release of calpain produced alphaII-spectrin (alpha-fodrin) breakdown products by acute neuronal cell death. Biol Chem 383:785-791.

Ebadi M, Bashir RM, Heidrick ML, Hamada FM, Refaey HE, Hamed A, Helal G, Baxi MD, Cerutis DR, Lassi NK (1997) Neurotrophins and their receptors in nerve injury and repair. Neurochem Int 30:347-374.

Ellezam B, Dubreuil C, Winton M, Loy L, Dergham P, Selles-Navarro I, McKerracher L (2002) Inactivation of intracellular Rho to stimulate axon growth and regeneration. Prog Brain Res 137:371-380.

Farkas O, Povlishock JT (2007) Cellular and subcellular change evoked by diffuse traumatic brain injury: a complex web of change extending far beyond focal damage. Prog Brain Res 161:43-59.

Fellenberg K, Hauser NC, Brors B, Neutzner A, Hoheisel JD, Vingron M (2001) Correspondence analysis applied to microarray data. Proc Natl Acad Sci U S A 98:10781-10786.

Fournier AE, Takizawa BT, Strittmatter SM (2003) Rho kinase inhibition enhances axonal regeneration in the injured CNS. J Neurosci 23:1416-1423.

Fujita A, Hattori Y, Takeuchi T, Kamata Y, Hata F (2001) NGF induces neurite outgrowth via a decrease in phosphorylation of myosin light chain in PC12 cells. Neuroreport 12:3599-3602.

Fukada M, Watakabe I, Yuasa-Kawada J, Kawachi H, Kuroiwa A, Matsuda Y, Noda M (2000) Molecular characterization of CRMP5, a novel member of the collapsin response mediator protein family. J Biol Chem 275:37957-37965.

Fukata Y, Kimura T, Kaibuchi K (2002a) Axon specification in hippocampal neurons. Neurosci Res 43:305-315.

Fukata Y, Itoh TJ, Kimura T, Menager C, Nishimura T, Shiromizu T, Watanabe H, Inagaki N, Iwamatsu A, Hotani H, Kaibuchi K (2002b) CRMP-2 binds to tubulin heterodimers to promote microtubule assembly. Nat Cell Biol 4:583-591.

Fukiage C, Azuma M, Nakamura Y, Tamada Y, Nakamura M, Shearer TR (1997) SJA6017, a newly synthesized peptide aldehyde inhibitor of calpain: amelioration of cataract in cultured rat lenses. Biochim Biophys Acta 1361:304-312.

Gallagher CN, Hutchinson PJ, Pickard JD (2007) Neuroimaging in trauma. Curr Opin Neurol 20:403-409.

Geddes JF, Whitwell HL, Graham DI (2000) Traumatic axonal injury: practical issues for diagnosis in medicolegal cases. Neuropathol Appl Neurobiol 26:105-116.

Gerendasy D (1999) Homeostatic tuning of Ca2+ signal transduction by members of the calpacitin protein family. J Neurosci Res 58:107-119.

Glenney JR, Jr., Weber K (1985) Separation of fodrin subunits by affinity chromatography on calmodulin-Sepharose. Anal Biochem 150:364-368.

Gold L (2001) mRNA display: diversity matters during in vitro selection. Proc Natl Acad Sci U S A 98:4825-4826.

Goshima Y, Nakamura F, Strittmatter P, Strittmatter SM (1995) Collapsin-induced growth cone collapse mediated by an intracellular protein related to UNC-33. Nature 376:509-514.

Goto H, Kosako H, Tanabe K, Yanagida M, Sakurai M, Amano M, Kaibuchi K, Inagaki M (1998) Phosphorylation of vimentin by Rho-associated kinase at a unique amino-terminal site that is specifically phosphorylated during cytokinesis. J Biol Chem 273:11728-11736.

Greene LA, Tischler AS (1976) Establishment of a noradrenergic clonal line of rat adrenal pheochromocytoma cells which respond to nerve growth factor. Proc Natl Acad Sci 73:2424-2428.

Gu Y, Hamajima N, Ihara Y (2000) Neurofibrillary tangle-associated collapsin response mediator protein-2 (CRMP-2) is highly phosphorylated on Thr-509, Ser-518, and Ser-522. Biochemistry 39:4267-4275.

Gu Y, Ihara Y (2000) Evidence that collapsin response mediator protein-2 is involved in the dynamics of microtubules. J Biol Chem 275:17917-17920.

Gungabissoon RA, Bamburg JR (2003) Regulation of growth cone actin dynamics by ADF/cofilin. J Histochem Cytochem 51:411-420.

Haeseleer F, Palczewski K (2002) Calmodulin and Ca2+-binding proteins (CaBPs): variations on a theme. Adv Exp Med Biol 514:303-317.

Hall A (2005) Rho GTPases and the control of cell behaviour. Biochem Soc Trans 33:891-895.

Hannila SS, Filbin MT (2007) The role of cyclic AMP signaling in promoting axonal regeneration after spinal cord injury. Exp Neurol.

Harigaya Y, Shoji M, Shirao T, Hirai S (1996) Disappearance of actin-binding protein, drebrin, from hippocampal synapses in Alzheimer's disease. J Neurosci Res 43:87-92.

Harris MA, Clark J, Ireland A, Lomax J, Ashburner M, Foulger R, Eilbeck K, Lewis S, Marshall B, Mungall C, Richter J, Rubin GM, Blake JA, Bult C, Dolan M, Drabkin H, Eppig JT, Hill DP, Ni L, Ringwald M, Balakrishnan R, Cherry JM, Christie KR, Costanzo MC, Dwight SS, Engel S, Fisk DG, Hirschman JE, Hong EL, Nash RS, Sethuraman A, Theesfeld CL, Botstein D, Dolinski K, Feierbach B, Berardini T, Mundodi S, Rhee SY, Apweiler R, Barrell D, Camon E, Dimmer E, Lee V, Chisholm R, Gaudet P, Kibbe W, Kishore R, Schwarz EM, Sternberg P, Gwinn M, Hannick L, Wortman J, Berriman M, Wood V, de la Cruz N, Tonellato P, Jaiswal P, Seigfried T, White R (2004) The Gene Ontology (GO) database and informatics resource. Nucleic Acids Res 32:D258-261.

Harris AS, Croall DE, Morrow JS (1989) Calmodulin regulates fodrin susceptibility to cleavage by calcium-dependent protease I. J Biol Chem 264:17401-17408.

Hashimoto R, Nakamura Y, Goto H, Wada Y, Sakoda S, Kaibuchi K, Inagaki M, Takeda M (1998) Domain- and site-specific phosphorylation of bovine NF-L by Rho-associated kinase. Biochem Biophys Res Commun 245:407-411.

Hashimoto R, Nakamura Y, Komai S, Kashiwagi Y, Tamura K, Goto T, Aimoto S, Kaibuchi K, Shiosaka S, Takeda M (2000) Site-specific phosphorylation of neurofilament-L is mediated by calcium/calmodulin-dependent protein kinase II in the apical dendrites during long-term potentiation. J Neurochem 75:373-382.

Hata K, Kubo T, Yamaguchi A, Yamashita T (2006) Signaling mechanisms of axon growth inhibition. Drug News Perspect 19:541-547.

Hayes RL, Wang KK, Kampfl A, Posmantur RM, Newcomb JK, Clifton GL (1998) Potential contribution of proteases to neuronal damage. Drug News Perspect 11:215-222.

Hergan K, Schaefer PW, Sorensen AG, Gonzalez RG, Huisman TA (2002) Diffusion-weighted MRI in diffuse axonal injury of the brain. Eur Radiol 12:2536-2541.

Hill JJ, Callaghan DA, Ding W, Kelly JF, Chakravarthy BR (2006) Identification of okadaic acid-induced phosphorylation events by a mass spectrometry approach. Biochem Biophys Res Commun 342:791-799.

Hou ST, Jiang SX, Desbois A, Huang D, Kelly J, Tessier L, Karchewski L, Kappler J (2006) Calpain-cleaved collapsin response mediator protein-3 induces neuronal death after glutamate toxicity and cerebral ischemia. J Neurosci 26:2241-2249.

Hundle B, McMahon T, Dadgar J, Messing RO (1995) Overexpression of epsilon-protein kinase C enhances nerve growth factor-induced phosphorylation of mitogen-activated protein kinases and neurite outgrowth. J Biol Chem 270:30134-30140.

Ikenoya M, Hidaka H, Hosoya T, Suzuki M, Yamamoto N, Sasaki Y (2002) Inhibition of rho-kinase-induced myristoylated alanine-rich C kinase substrate (MARCKS) phosphorylation in human neuronal cells by H-1152, a novel and specific Rho-kinase inhibitor. J Neurochem 81:9-16.

Inagaki N, Chihara K, Arimura N, Menager C, Kawano Y, Matsuo N, Nishimura T, Amano M, Kaibuchi K (2001) CRMP-2 induces axons in cultured hippocampal neurons. Nat Neurosci 4:781-782.

Ishizaki T, Uehata M, Tamechika I, Keel J, Nonomura K, Maekawa M, Narumiya S (2000) Pharmacological properties of Y-27632, a specific inhibitor of rho-associated kinases. Mol Pharmacol 57:976-983.

Itano T, Matsui H, Doi A, Ohmura Y, Hatase O (1986) Identification of calmodulin-binding proteins in pure mitochondria by photoaffinity labeling. Biochem Int 13:787-792.

Ito T, Kagoshima M, Sasaki Y, Li C, Udaka N, Kitsukawa T, Fujisawa H, Taniguchi M, Yagi T, Kitamura H, Goshima Y (2000) Repulsive axon guidance molecule Sema3A inhibits branching morphogenesis of fetal mouse lung. Mech Dev 97:35-45.

Jiang SX, Kappler J, Zurakowski B, Desbois A, Aylsworth A, Hou ST (2007) Calpain cleavage of collapsin response mediator proteins in ischemic mouse brain. Eur J Neurosci 26:801-809.

Jiao J, Huang X, Feit-Leithman RA, Neve RL, Snider W, Dartt DA, Chen DF (2005) Bcl-2 enhances Ca(2+) signaling to support the intrinsic regenerative capacity of CNS axons. Embo J 24:1068-1078.

Jin J, Smith FD, Stark C, Wells CD, Fawcett JP, Kulkarni S, Metalnikov P, O'Donnell P, Taylor P, Taylor L, Zougman A, Woodgett JR, Langeberg LK, Scott JD, Pawson T (2004) Proteomic, functional, and domain-based analysis of in vivo 14-3-3 binding proteins involved in cytoskeletal regulation and cellular organization. Curr Biol 14:1436-1450.

Johnson GV, Greenwood JA, Costello AC, Troncoso JC (1991) The regulatory role of calmodulin in the proteolysis of individual neurofilament proteins by calpain. Neurochem Res 16:869-873.

Johnston MV (2005) Excitotoxicity in perinatal brain injury. Brain Pathol 15:234-240.

Johnston-Wilson NL, Sims CD, Hofmann JP, Anderson L, Shore AD, Torrey EF, Yolken RH (2000) Disease-specific alterations in frontal cortex brain proteins in schizophrenia, bipolar disorder, and major depressive disorder. The Stanley Neuropathology Consortium. Mol Psychiatry 5:142-149.

Kawano Y, Fukata Y, Oshiro N, Amano M, Nakamura T, Ito M, Matsumura F, Inagaki M, Kaibuchi K (1999) Phosphorylation of myosin-binding subunit (MBS) of myosin phosphatase by Rho-kinase in vivo. J Cell Biol 147:1023-1038.

Kawano Y, Yoshimura T, Tsuboi D, Kawabata S, Kaneko-Kawano T, Shirataki H, Takenawa T, Kaibuchi K (2005) CRMP-2 is involved in kinesin-1-dependent transport of the Sra-1/WAVE1 complex and axon formation. Mol Cell Biol 25:9920-9935.

Khawaja X, Xu J, Liang JJ, Barrett JE (2004) Proteomic analysis of protein changes developing in rat hippocampus after chronic antidepressant treatment: Implications for depressive disorders and future therapies. J Neurosci Res 75:451-460.

Kimura T, Watanabe H, Iwamatsu A, Kaibuchi K (2005) Tubulin and CRMP-2 complex is transported via Kinesin-1. J Neurochem 93:1371-1382.

Kishida S, Yamamoto H, Kikuchi A (2004) Wnt-3a and Dvl induce neurite retraction by activating Rho-associated kinase. Mol Cell Biol 24:4487-4501.

Kitano H (2002) Systems biology: a brief overview. Science 295:1662-1664.

Kobeissy FH, Ottens AK, Zhang Z, Liu MC, Denslow ND, Dave JR, Tortella FC, Hayes RL, Wang KK (2006) Novel differential neuroproteomics analysis of traumatic brain injury in rats. Mol Cell Proteomics 5:1887-1898.

Kosaki G, Tsujinaka T, Kambayashi J, Morimoto K, Yamamoto K, Yamagami K, Sobue K, Kakiuchi S (1983) Specific cleavage of calmodulin-binding proteins by low Ca2+-requiring form of Ca2+-activated neutral protease in human platelets. Biochem Int 6:767-775.

Kosako H, Amano M, Yanagida M, Tanabe K, Nishi Y, Kaibuchi K, Inagaki M (1997) Phosphorylation of glial fibrillary acidic protein at the same sites by cleavage furrow kinase and Rho-associated kinase. J Biol Chem 272:10333-10336.

Kowara R, Chen Q, Milliken M, Chakravarthy B (2005) Calpain-mediated truncation of dihydropyrimidinase-like 3 protein (DPYSL3) in response to NMDA and H2O2 toxicity. J Neurochem 95:466-474.

Krucker T, Siggins GR, McNamara RK, Lindsley KA, Dao A, Allison DW, De Lecea L, Lovenberg TW, Sutcliffe JG, Gerendasy DD (2002) Targeted disruption of RC3 reveals a calmodulin-based mechanism for regulating metaplasticity in the hippocampus. J Neurosci 22:5525-5535.

Kupina NC, Nath R, Bernath EE, Inoue J, Mitsuyoshi A, Yuen PW, Wang KK, Hall ED (2001) The novel calpain inhibitor SJA6017 improves functional outcome after delayed administration in a mouse model of diffuse brain injury. J Neurotrauma 18:1229-1240.

Kurz JE, Parsons JT, Rana A, Gibson CJ, Hamm RJ, Churn SB (2005) A significant increase in both basal and maximal calcineurin activity following fluid percussion injury in the rat. J Neurotrauma 22:476-490.

Kwon BK, Borisoff JF, Tetzlaff W (2002) Molecular targets for therapeutic intervention after spinal cord injury. Mol Intervent 2:244-258.

Lakshmikuttyamma A, Selvakumar P, Sharma AR, Anderson DH, Sharma RK (2004) In vitro proteolytic degradation of bovine brain calcineurin by m-calpain. Neurochem Res 29:1913-1921.

Lee S, Kim JH, Lee CS, Kim Y, Heo K, Ihara Y, Goshima Y, Suh PG, Ryu SH (2002) Collapsin response mediator protein-2 inhibits neuronal phospholipase D(2) activity by direct interaction. J Biol Chem 277:6542-6549.

Lehmann M, Fournier A, Selles-Navarro I, Dergham P, Sebok A, Leclerc N, Tigyi G, McKerracher L (1999) Inactivation of Rho signaling pathway promotes CNS axon regeneration. J Neurosci 19:7537-7547.

Lingor P, Teusch N, Schwarz K, Mueller R, Mack H, Bahr M, Mueller BK (2007) Inhibition of Rho kinase (ROCK) increases neurite outgrowth on chondroitin sulphate proteoglycan in vitro and axonal regeneration in the adult optic nerve in vivo. J Neurochem 103:181-189.

Liu F, Grundke-Iqbal I, Iqbal K, Oda Y, Tomizawa K, Gong CX (2005) Truncation and activation of calcineurin A by calpain I in Alzheimer disease brain. J Biol Chem 280:37755-37762.

Liu MC, Akle V, Zheng W, Kitlen J, O'steen B, Larner SF, Dave JR, Tortella FC, Hayes RL, Wang KK (2006) Extensive degradation of myelin basic protein isoforms by calpain following traumatic brain injury. J Neurochem 98:700-712.

Liu PC, Yang ZJ, Qiu MH, Zhang LM, Sun FY (2003) Induction of CRMP-4 in striatum of adult rat after transient brain ischemia. Acta Pharmacol Sin 24:1205-1211.

Llansola M, Monfort P, Felipo V (2000) Inhibitors of phospholipase C prevent glutamate neurotoxicity in primary cultures of cerebellar neurons. J Pharmacol Exp Ther 292:870-876.

Lopez-Otin C, Overall CM (2002) Protease degradomics: a new challenge for proteomics. Nat Rev Mol Cell Biol 3:509-519.

Lopez-Picon FR, Kukko-Lukjanov TK, Holopainen IE (2006) The calpain inhibitor MDL-28170 and the AMPA/KA receptor antagonist CNQX inhibit neurofilament degradation and enhance neuronal survival in kainic acid-treated hippocampal slice cultures. Eur J Neurosci 23:2686-2694.

Luk SC, Ngai SM, Tsui SK, Fung KP, Lee CY, Waye MM (1999) In vivo and in vitro association of 14-3-3 epsilon isoform with calmodulin: implication for signal transduction and cell proliferation. J Cell Biochem 73:31-35.

Maekawa M, Ishizaki T, Boku S, Watanabe N, Fujita A, Iwamatsu A, Obinata T, Ohashi K, Mizuno K, Narumiya S (1999) Signaling from Rho to the actin cytoskeleton through protein kinases ROCK and LIM-kinase. Science 285:895-898.

Markgraf CG, Velayo NL, Johnson MP, McCarty DR, Medhi S, Koehl JR, Chmielewski PA, Linnik MD (1998) Six-hour window of opportunity for calpain inhibition in focal cerebral ischemia in rats. Stroke 29:152-158.

Matsuzawa K, Kosako H, Azuma I, Inagaki N, Inagaki M (1998) Possible regulation of intermediate filament proteins by Rho-binding kinases. Subcell Biochem 31:423-435.

McGinnis KM, Wang KK, Gnegy ME (1999) Alterations of extracellular calcium elicit selective modes of cell death and protease activation in SH-SY5Y human neuroblastoma cells. J Neurochem 72:1853-1863.

McGinnis KM, Whitton MM, Gnegy ME, Wang KKW (1998) Calcium/calmodulin-dependent protein kinase IV is cleaved by caspase-3 and calpain in SH-SY5Y human neuroblastoma cells undergoing apoptosis. J Biol Chem 273:19993-20000.

McKerracher L, David S (2004) Easing the brakes on spinal cord repair. Nat Med 10:1052-1053.

McKerracher L, David S, Jackson DL, Kottis V, Dunn RJ, Braun PE (1994) Identification of myelin-associated glycoprotein as a major myelin-derived inhibitor of neurite growth. Neuron 13:805-811.

Medana IM, Esiri MM (2003) Axonal damage: a key predictor of outcome in human CNS diseases. Brain 126:515-530.

Mimura F, Yamagishi S, Arimura N, Fujitani M, Kubo T, Kaibuchi K, Yamashita T (2006) Myelin-associated glycoprotein inhibits microtubule assembly by a Rho-kinase-dependent mechanism. J Biol Chem 281:15970-15979.

Mizuno N, Yoshitomi H, Ishida H, Kuromi H, Kawaki J, Seino Y, Seino S (1998) Altered bcl-2 and bax expression and intracellular Ca2+ signaling in apoptosis of pancreatic cells and the impairment of glucose-induced insulin secretion. Endocrinology 139:1429-1439.

Monnier PP, Sierra A, Schwab JM, Henke-Fahle S, Mueller BK (2003a) The Rho/ROCK pathway mediates neurite growth-inhibitory activity associated with the chondroitin sulfate proteoglycans of the CNS glial scar. Mol Cell Neurosci 22:319-330.

Monnier PP, Sierra A, Schwab JM, Henke-Fahle S, Mueller BK (2003b) The Rho/ROCK pathway mediates neurite growth-inhibitory activity associated with the chondroitin sulfate proteoglycans of the CNS glial scar. Mol Cell Neurosci 22:319-330.

Mueller BK, Mack H, Teusch N (2005) Rho kinase, a promising drug target for neurological disorders. Nat Rev Drug Discov 4:387-398.

Mukerjee N, McGinnis KM, Gnegy ME, Wang KKW (2001) Caspase-mediated calcineurin activation contributes to IL-2 release during T cell activation. Biochem Biophys Res Commun 285:1192-1199.

Mukerjee N, McGinnis KM, Park YH, Gnegy ME, Wang KKW (2000) Caspase-mediated proteolytic activation of calcineurin in thapsigargin-mediated apoptosis in SH-SY5Y neuroblastoma cells. Arch Biochem Biophys 379:337-343.

Nakajima M, Hayashi K, Egi Y, Katayama K, Amano Y, Uehata M, Ohtsuki M, Fujii A, Oshita K, Kataoka H, Chiba K, Goto N, Kondo T (2003) Effect of Wf-536, a novel ROCK inhibitor, against metastasis of B16 melanoma. Cancer Chemother Pharmacol 52:319-324.

Nath R, Davis M, Probert AW, Kupina NC, Ren X, Schielke GP, Wang KK (2000a) Processing of cdk5 activator p35 to its truncated form (p25) by calpain in acutely injured neuronal cells. Biochem Biophys Res Commun 274:16-21.

Nath R, Huggins M, Glantz SB, Morrow JS, McGinnis K, Nadimpalli R, Wanga KK (2000b) Development and characterization of antibodies specific to caspase-3-produced alpha II-spectrin 120 kDa breakdown product: marker for neuronal apoptosis. Neurochem Int 37:351-361.

Newcombe VF, Williams GB, Nortje J, Bradley PG, Harding SG, Smielewski P, Coles JP, Maiya B, Gillard JH, Hutchinson PJ, Pickard JD, Carpenter TA, Menon DK (2007) Analysis of acute traumatic axonal injury using diffusion tensor imaging. Br J Neurosurg 21:340-348.

Ng J, Luo L (2004) Rho GTPases regulate axon growth through convergent and divergent signaling pathways. Neuron 44:779-793.

Nishimura T, Fukata Y, Kato K, Yamaguchi T, Matsuura Y, Kamiguchi H, Kaibuchi K (2003) CRMP-2 regulates polarized Numb-mediated endocytosis for axon growth. Nat Cell Biol 5:819-826.

Niwa R, Nagata-Ohashi K, Takeichi M, Mizuno K, Uemura T (2002) Control of actin reorganization by Slingshot, a family of phosphatases that dephosphorylate ADF/cofilin. Cell 108:233-246.

Obara Y, Aoki T, Kusano M, Ohizumi Y (2002) Beta-eudesmol induces neurite outgrowth in rat pheochromocytoma cells accompanied by an activation of mitogen-activated protein kinase. J Pharmacol Exp Ther 301:803-811.

Oda K, Matsuoka Y, Funahashi A, Kitano H (2005) A comprehensive pathway map of epidermal growth factor receptor signaling. Mol Syst Biol 1:2005 0010.

O'Day DH (2003) CaMBOT: profiling and characterizing calmodulin-binding proteins. Cell Signal 15:347-354.

O'Day DH, Myre MA (2004) Calmodulin-binding domains in Alzheimer's disease proteins: extending the calcium hypothesis. Biochem Biophys Res Commun 320:1051-1054.

Ohashi K, Nagata K, Maekawa M, Ishizaki T, Narumiya S, Mizuno K (2000) Rho-associated kinase ROCK activates LIM-kinase 1 by phosphorylation at threonine 508 within the activation loop. J Biol Chem 275:3577-3582.

Ottens AK, Kobeissy FH, Golden EC, Zhang Z, Haskins WE, Chen SS, Hayes RL, Wang KK, Denslow ND (2006) Neuroproteomics in neurotrauma. Mass Spectrom Rev 25:380-408.

Ottens AK, Kobeissy FH, Wolper RA, Haskins WE, Hayes RL, Denslow ND, Wang KKW (2005) A multidimensional differential proteomic platform using dual-phase ion-exchange chromatography - polyacrylamide gel electrophoresis/reversed-phase liquid chromatography tandem mass spectrometry. Anal Chem 77:4836-4845.

Ozdinler PH, Erzurumlu RS (2001) Regulation of neurotrophin-induced axonal responses via Rho GTPases. J Comp Neurol 438:377-387.

Park YH, Kantor L, Guptaroy B, Zhang M, Wang KK, Gnegy ME (2003) Repeated amphetamine treatment induces neurite outgrowth and enhanced amphetamine-stimulated dopamine release in rat pheochromocytoma cells (PC12 cells) via a protein kinase C- and mitogen activated protein kinase-dependent mechanism. J Neurochem 87:1546-1557.

Peri S, Navarro JD, Amanchy R, Kristiansen TZ, Jonnalagadda CK, Surendranath V, Niranjan V, Muthusamy B, Gandhi TK, Gronborg M, Ibarrola N, Deshpande N, Shanker K, Shivashankar HN, Rashmi BP, Ramya MA, Zhao Z, Chandrika KN, Padma N, Harsha HC, Yatish AJ, Kavitha MP, Menezes M, Choudhury DR, Suresh S, Ghosh N, Saravana R, Chandran S, Krishna S, Joy M, Anand SK, Madavan V, Joseph A, Wong GW, Schiemann WP, Constantinescu SN, Huang L, Khosravi-Far R, Steen H, Tewari M, Ghaffari S, Blobe GC, Dang CV, Garcia JG, Pevsner J, Jensen ON, Roepstorff P, Deshpande KS, Chinnaiyan AM, Hamosh A, Chakravarti A, Pandey A (2003) Development of human protein reference database as an initial platform for approaching systems biology in humans. Genome Res 13:2363-2371.

Peterson BZ, DeMaria CD, Adelman JP, Yue DT (1999) Calmodulin is the Ca2+ sensor for Ca2+ -dependent inactivation of L-type calcium channels. Neuron 22:549-558.

Petruska JC, Mendell LM (2004) The many functions of nerve growth factor: multiple actions on nociceptors. Neurosci Lett 361:168-171.

Pike BR, Flint J, Dutta S, Johnson E, Wang KKW, Hayes RL (2001) Accumulation of non-erythroid alpha II-spectrin and calpain-cleaved alpha II-spectrin breakdown products in cerebrospinal fluid after traumatic brain injury in rats. J Neurochem 78:1297-1306.

Pike BR, Zhao X, Newcomb JK, Posmantur RM, Wang KK, Hayes RL (1998) Regional calpain and caspase-3 proteolysis of alpha-spectrin after traumatic brain injury. Neuroreport 9:2437-2442.

Pike BR, Flint J, Dave JR, Lu XC, Wang KKW, Tortella FC, Hayes RL (2004) Accumulation of calpain and caspase-3 proteolytic fragments of brain-derived alphaII-spectrin in cerebral spinal fluid after middle cerebral artery occlusion in rats. J Cereb Blood Flow Metab 24:98-106.

Pineda JA, Wang KKW, Hayes RL (2004) Biomarkers of proteolytic damage following traumatic brain injury. Brain Pathol 14:202-209.

Pohorecki R, Becker GL, Reilly PJ, Landers DF (1990) Ischemic brain injury in vitro: protective effects of NMDA receptor antagonists and calmidazolium. Brain Res 528:133-137.

Povlishock JT, Buki A, Koiziumi H, Stone J, Okonkwo DO (1999) Initiating mechanisms involved in the pathobiology of traumatically induced axonal injury and interventions targeted at blunting their progression. Acta Neurochir Suppl 73:15-20.

Quach TT, Duchemin AM, Rogemond V, Aguera M, Honnorat J, Belin MF, Kolattukudy PE (2004) Involvement of collapsin response mediator proteins in the neurite extension induced by neurotrophins in dorsal root ganglion neurons. Mol Cell Neurosci 25:433-443.

Reddy VS, Ali GS, Reddy AS (2002) Genes encoding calmodulin-binding proteins in the Arabidopsis genome. J Biol Chem 277:9840-9852.

Revenu C, Athman R, Robine S, Louvard D (2004) The co-workers of actin filaments: from cell structures to signals. Nat Rev Mol Cell Biol 5:635-646.

Riento K, Ridley AJ (2003) Rocks: multifunctional kinases in cell behaviour. Nat Rev Mol Cell Biol 4:446-456.

Riss TL, Moravec RA (2004) Use of multiple assay endpoints to investigate the effects of incubation time, dose of toxin, and plating density in cell-based cytotoxicity assays. Assay Drug Dev Technol 2:51-62.

Ruben L, Goodman DB, Rasmussen H (1980) Identification of calmodulin in mitochondria from rat liver: a possible role in regulation of the oligomycin sensitive ATPase. Ann N Y Acad Sci 356:427-428.

Sahuquillo J, Poca MA, Amoros S (2001) Current aspects of pathophysiology and cell dysfunction after severe head injury. Curr Pharm Des 7:1475-1503.

Saris NE, Carafoli E (2005) A historical review of cellular calcium handling, with emphasis on mitochondria. Biochemistry (Mosc) 70:187-194.

Sasaki Y, Suzuki M, Hidaka H (2002) The novel and specific Rho-kinase inhibitor (S)-(+)-2-methyl-1-[(4-methyl-5-isoquinoline)sulfonyl]-homopiperazine as a probing molecule for Rho-kinase-involved pathway. Pharmacol Ther 93:225-232.

Schwartz M (2004) Rho signalling at a glance. J Cell Sci 117:5457-5458.

Schweitzer J, Becker CG, Schachner M, Becker T (2005) Expression of collapsin response mediator proteins in the nervous system of embryonic zebrafish. Gene Expr Patterns 5:809-816.

Sebok A, Nusser N, Debreceni B, Guo Z, Santos MF, Szeberenyi J, Tigyi G (1999) Different roles for RhoA during neurite initiation, elongation, and regeneration in PC12 cells. J Neurochem 73:949-960.

Selzer ME (2003) Promotion of axonal regeneration in the injured CNS. Lancet Neurol 2:157-166.

Shen X, Valencia CA, Szostak JW, Dong B, Liu R (2005) Scanning the human proteome for calmodulin-binding proteins. Proc Natl Acad Sci U S A 102:5969-5974.

Shevchenko A, Schaft D, Roguev A, Pijnappel WW, Stewart AF (2002) Deciphering protein complexes and protein interaction networks by tandem affinity purification and mass spectrometry: analytical perspective. Mol Cell Proteomics 1:204-212.

Shewan D, Dwivedy A, Anderson R, Holt CE (2002) Age-related changes underlie switch in netrin-1 responsiveness as growth cones advance along visual pathway. Nat Neurosci 5:955-962.

Smillie KJ, Cousin MA (2005) Dynamin I phosphorylation and the control of synaptic vesicle endocytosis. Biochem Soc Symp:87-97.

Smith DH, Meaney DF, Shull WH (2003) Diffuse axonal injury in head trauma. J Head Trauma Rehabil 18:307-316.

Sola C, Barron S, Tusell JM, Serratosa J (1999) The Ca2+/calmodulin signaling system in the neural response to excitability. Involvement of neuronal and glial cells. Prog Neurobiol 58:207-232.

Somlyo AP, Somlyo AV (2000) Signal transduction by G-proteins, rho-kinase and protein phosphatase to smooth muscle and non-muscle myosin II. J Physiol 522 Pt 2:177-185.

Stenmark P, Ogg D, Flodin S, Flores A, Kotenyova T, Nyman T, Nordlund P, Kursula P (2007) The structure of human collapsin response mediator protein 2, a regulator of axonal growth. J Neurochem 101:906-917.

Tabb DL, McDonald WH, Yates JR, 3rd (2002) DTASelect and Contrast: tools for assembling and comparing protein identifications from shotgun proteomics. J Proteome Res 1:21-26.

Tahimic CG, Tomimatsu N, Nishigaki R, Fukuhara A, Toda T, Kaibuchi K, Shiota G, Oshimura M, Kurimasa A (2006) Evidence for a role of Collapsin response mediator protein-2 in signaling pathways that regulate the proliferation of non-neuronal cells. Biochem Biophys Res Commun 340:1244-1250.

Takahashi TT, Austin RJ, Roberts RW (2003) mRNA display: ligand discovery, interaction analysis and beyond. Trends Biochem Sci 28:159-165.

Takei K, Yoshida Y, Yamada H (2005) Regulatory mechanisms of dynamin-dependent endocytosis. J Biochem (Tokyo) 137:243-247.

Tang BL (2003) Inhibitors of neuronal regeneration: mediators and signaling mechanisms. Neurochem Int 42:189-203.

Thienpont LM, Van Uytfanghe K, Marriot J, Stokes P, Siekmann L, Kessler A, Bunk D, Tai S (2005) Metrologic traceability of total thyroxine measurements in human serum: efforts to establish a network of reference measurement laboratories. Clin Chem 51:161-168.

Tojima T, Ito E (2004) Signal transduction cascades underlying de novo protein synthesis required for neuronal morphogenesis in differentiating neurons. Prog Neurobiol 72:183-193.

Tompa P, Buzder-Lantos P, Tantos A, Farkas A, Szilagyi A, Banoczi Z, Hudecz F, Friedrich P (2004) On the sequential determinants of calpain cleavage. J Biol Chem 279:20775-20785.

Tsunekawa S, Takahashi K, Abe M, Hiwada K, Ozawa K, Murachi T (1989) Calpain proteolysis of free and bound forms of calponin, a troponin T-like protein in smooth muscle. FEBS Lett 250:493-496.

Uchida Y, Ohshima T, Sasaki Y, Suzuki H, Yanai S, Yamashita N, Nakamura F, Takei K, Ihara Y, Mikoshiba K, Kolattukudy P, Honnorat J, Goshima Y (2005) Semaphorin3A signalling is mediated via sequential Cdk5 and GSK3beta phosphorylation of CRMP2: implication of common phosphorylating mechanism underlying axon guidance and Alzheimer's disease. Genes Cells 10:165-179.

van Dalen JJ, Gerendasy DD, de Graan PN, Schrama LH, Gruol DL (2003) Calcium dynamics are altered in cortical neurons lacking the calmodulin-binding protein RC3. Eur J Neurosci 18:13-22.

Verma DP, Hong Z (2005) The ins and outs in membrane dynamics: tubulation and vesiculation. Trends Plant Sci 10:159-165.

Wahl S, Barth H, Ciossek T, Aktories K, Mueller BK (2000) Ephrin-A5 induces collapse of growth cones by activating Rho and Rho kinase. J Cell Biol 149:263-270.

Walmsley AR, Mir AK (2007) Targeting the Nogo-A signalling pathway to promote recovery following acute CNS injury. Curr Pharm Des 13:2470-2484.

Wang KC, Koprivica V, Kim JA, Sivasankaran R, Guo Y, Neve RL, He Z (2002) Oligodendrocyte-myelin glycoprotein is a Nogo receptor ligand that inhibits neurite outgrowth. Nature 417:941-944.

Wang KK (2000a) Calpain and caspase: can you tell the difference? Trends Neurosci 23:20-26.

Wang KK, Nath R, Raser KJ, Hajimohammadreza I (1996) Maitotoxin induces calpain activation in SH-SY5Y neuroblastoma cells and cerebrocortical cultures. Arch Biochem Biophys 331:208-214.

Wang KK, Ottens A, Haskins W, Liu MC, Kobeissy F, Denslow N, Chen S, Hayes RL (2004) Proteomics studies of traumatic brain injury. Int Rev Neurobiol 61:215-240.

Wang KK, Villalobo A, Roufogalis BD (1989a) Calmodulin-binding proteins as calpain substrates. Biochem J 262:693-706.

Wang KKW (2000b) Calpain and caspase: can you tell the difference? Trends Neurosci 23:20-26.

Wang KKW, Villalobo A, Roufogalis BD (1989b) Calmodulin-binding proteins as calpain substrates. Biochem J 262:693-706.

Wang LH, Strittmatter SM (1996) A family of rat CRMP genes is differentially expressed in the nervous system. J Neurosci 16:6197-6207.

Wang LH, Strittmatter SM (1997) Brain CRMP forms heterotetramers similar to liver dihydropyrimidinase. J Neurochem 69:2261-2269.

Waterhouse N, Kumar S, Song Q, Strike P, Sparrow L, Dreyfuss G, Alnemri ES, Litwack G, Lavin M, Watters D (1996) Heteronuclear ribonucleoproteins C1 and C2, components of the spliceosome, are specific targets of interleukin 1beta-converting enzyme-like proteases in apoptosis. J Biol Chem 271:29335-29341.

Weitzdoerfer R, Fountoulakis M, Lubec G (2001) Aberrant expression of dihydropyrimidinase related proteins-2,-3 and -4 in fetal Down syndrome brain. J Neural Transm Suppl:95-107.

Xia Z, Choi EJ, Wang F, Blazynski C, Storm DR (1993) Type I calmodulin-sensitive adenylyl cyclase is neural specific. J Neurochem 60:305-311.

Xia Z, Storm DR (2005) The role of calmodulin as a signal integrator for synaptic plasticity. Nat Rev Neurosci 6:267-276.

Xie F, Zheng B (2007) White matter inhibitors in CNS axon regeneration failure. Exp Neurol.

Yamaguchi Y, Katoh H, Yasui H, Mori K, Negishi M (2001) RhoA inhibits the nerve growth factor-induced Rac1 activation through Rho-associated kinase-dependent pathway. J Biol Chem 276:18977-18983.

Yamamoto H, Fukunaga K, Goto S, Tanaka E, Miyamoto E (1985) Ca2+, calmodulin-dependent regulation of microtubule formation via phosphorylation of microtubule-associated protein 2, tau factor, and tubulin, and comparison with the cyclic AMP-dependent phosphorylation. J Neurochem 44:759-768.

Yamashima T (2004) Ca2+-dependent proteases in ischemic neuronal death: a conserved 'calpain-cathepsin cascade' from nematodes to primates. Cell Calcium 36:285-293.

Yamashita T, Fujitani M, Yamagishi S, Hata K, Mimura F (2005) Multiple signals regulate axon regeneration through the nogo receptor complex. Mol Neurobiol 32:105-112.

Yamashita T, Higuchi H, Tohyama M (2002) The p75 receptor transduces the signal from myelin-associated glycoprotein to Rho. J Cell Biol 157:565-570.

Yap KL, Kim J, Truong K, Sherman M, Yuan T, Ikura M (2000) Calmodulin target database. J Struct Funct Genomics 1:8-14.

Ybe JA, Brodsky FM, Hofmann K, Lin K, Liu SH, Chen L, Earnest TN, Fletterick RJ, Hwang PK (1999) Clathrin self-assembly is mediated by a tandemly repeated superhelix. Nature 399:371-375.

Yoshida H, Watanabe A, Ihara Y (1998) Collapsin response mediator protein-2 is associated with neurofibrillary tangles in Alzheimer's disease. J Biol Chem 273:9761-9768.

Yoshimura T, Kawano Y, Arimura N, Kawabata S, Kikuchi A, Kaibuchi K (2005) GSK-3beta regulates phosphorylation of CRMP-2 and neuronal polarity. Cell 120:137-149.

Yuasa-Kawada J, Suzuki R, Kano F, Ohkawara T, Murata M, Noda M (2003) Axonal morphogenesis controlled by antagonistic roles of two CRMP subtypes in microtubule organization. Eur J Neurosci 17:2329-2343.

Yukawa K, Tanaka T, Bai T, Ueyama T, Owada-Makabe K, Tsubota Y, Maeda M, Suzuki K, Kikutani H, Kumanogoh A (2005) Semaphorin 4A induces growth cone collapse of hippocampal neurons in a Rho/Rho-kinase-dependent manner. Int J Mol Med 16:115-118.

Zhang S, Ehlers MD, Bernhardt JP, Su CT, Huganir RL (1998) Calmodulin mediates calcium-dependent inactivation of N-methyl-D-aspartate receptors. Neuron 21:443-453.

Zhang Z, Ottens AK, Golden EC, Hayes RL, Wang KK (2006a) Using Calmodulin-Affinity Capture to Study the Rat Brain Calmodulin Binding Proteome and Its Vulnerability to Calpain and Caspase Proteolysis. J Neurotrauma 1:125-129.

Zhang Z, Ottens AK, Larner SF, Kobeissy FH, Williams ML, Hayes RL, Wang KK (2006b) Direct Rho-associated kinase inhibiton induces cofilin dephosphorylation and neurite outgrowth in PC-12 cells. Cell Mol Biol Lett 11:12-29.

Zhang Z, Ottens AK, Sadasivan S, Kobeissy FH, Fang T, Hayes RL, Wang KK (2007) Calpain-mediated collapsin response mediator protein-1, -2, and -4 proteolysis after neurotoxic and traumatic brain injury. J Neurotrauma 24:460-472.

Zhao XH, Jin WL, Ju G (2007) An in vitro study on the involvement of LINGO-1 and Rho GTPases in Nogo-A regulated differentiation of oligodendrocyte precursor cells. Mol Cell Neurosci 36:260-269.

Zheng B, Ho C, Li S, Keirstead H, Steward O, Tessier-Lavigne M (2003) Lack of enhanced spinal regeneration in Nogo-deficient mice. Neuron 38:213-224.

Zheng B, Lee JK, Xie F (2006) Genetic mouse models for studying inhibitors of spinal axon regeneration. Trends Neurosci 29:640-646.

Zhou Y, Su Y, Li B, Liu F, Ryder JW, Wu X, Gonzalez-DeWhitt PA, Gelfanova V, Hale JE, May PC, Paul SM, Ni B (2003) Nonsteroidal anti-inflammatory drugs can lower amyloidogenic Abeta42 by inhibiting Rho. Science 302:1215-1217.

Zhu H, Bilgin M, Bangham R, Hall D, Casamayor A, Bertone P, Lan N, Jansen R, Bidlingmaier S, Houfek T, Mitchell T, Miller P, Dean RA, Gerstein M, Snyder M (2001) Global analysis of protein activities using proteome chips. Science 293:2101-2105.

BIOGRAPHICAL SKETCH

Zhiqun Zhang was born in 1975 in Linxiang, mid-southern of China. She received a Bachelor of Science degree in medicine from Nanjing University (Nanjing, China) in 1997. In 1999 she received a Master of Science degree in medicine from the same university. After graduation, she moved to Suzhou and became a physician in the Department of Nephrology at SuZhou Medical School Hospital. In 2003, she joined the Interdisciplinary Program in Biomedical Sciences at the UF College of Medicine. From 2004, she began her doctoral study under the guidance of Dr. Kevin K. W. Wang in the Departments of Psychiatry and Neuroscience. Under the guidance of her mentor Dr. Kevin K. W. Wang, Zhiqun earned a number of research honors including the Outstanding Research Award from the College of Medicine, and the Bryan W. Robinson Neurological Foundation Hornable Mention Achievement Award (2006). She also presented her research work at the National Institute of Mental Health Research Festival in 2006. During her research studies, she was the first author of four published journal articles, one of which was featured in an editorial commentary in the journal Calcium Binding Proteins.